Advanced Drug Delivery Reviews 201 (2023) 115049

Contents lists available at ScienceDirect

Advanced Drug Delivery Reviews

journal homepage: www.elsevier.com/locate/adr

Biosafety of mesoporous silica nanoparticles; towards clinical translation

Araceli Lérida-Viso [a,b,c,d,1], Alejandra Estepa-Fernández [b,c,d,1], Alba García-Fernández [b,c,d,*], Vicente Martí-Centelles [b,d], Ramón Martínez-Máñez [a,b,c,d,*]

[a] Unidad Mixta de Investigación en Nanomedicina y Sensores. Universitat Politècnica de València, IIS La Fe. Av. Fernando Abril Martorell, 106 Torre A 7ª planta. 46026, Valencia, Spain
[b] Instituto Interuniversitario de Investigación de Reconocimiento Molecular y Desarrollo Tecnológico (IDM) Universitat Politècnica de València, Universitat de València. Camino de Vera, s/n. 46022, Valencia, Spain
[c] Unidad Mixta UPV-CIPF de Investigación en Mecanismos de Enfermedades y Nanomedicina, Universitat Politècnica de València, Centro de Investigación Príncipe Felipe, C/ Eduardo Primo Yúfera 3. 46012, Valencia, Spain
[d] CIBER de Bioingeniería, Biomateriales y Nanomedicina, Instituto de Salud Carlos III, Spain

GRAPHICAL ABSTRACT

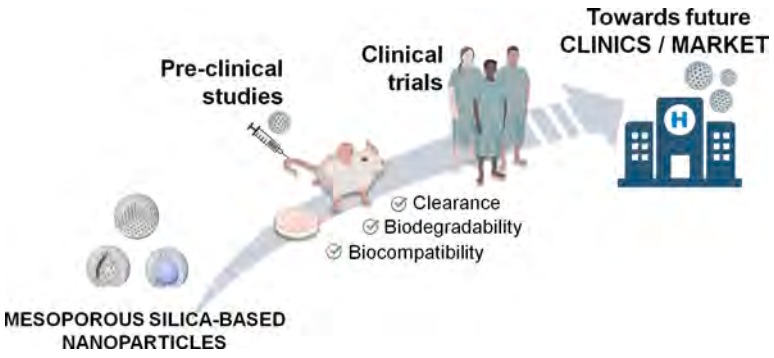

ARTICLE INFO

Keywords:
mesoporous silica nanoparticles (MSNs)
Biodistribution
Biocompatibility
Biodegradation
Clearance
Clinical application

ABSTRACT

Mesoporous silica nanoparticles (MSNs) have attracted the attention of chemists, who have developed numerous systems for the encapsulation of a plethora of molecules, allowing the use of mesoporous silica nanoparticles for biomedical applications. MSNs have been extensively studied for their use in nanomedicine, in applications such as drug delivery, diagnosis, and bioimaging, demonstrating significant *in vivo* efficacy in different preclinical models. Nevertheless, for the transition of MSNs into clinical trials, it is imperative to understand the characteristics that make MSNs effective and safe. The biosafety properties of MSNs *in vivo* are greatly influenced by their physicochemical characteristics such as particle shape, size, surface modification, and silica framework. In this review, we compile the most relevant and recent progress in the literature up to the present by analyzing the contributions on biodistribution, biodegradability, and clearance of MSNs. Furthermore, the ongoing clinical trials and the potential challenges related to the administration of silica materials for advanced therapeutics are

* Corresponding authors.
E-mail addresses: algarfe4@etsia.upv.es (A. García-Fernández), rmaez@qim.upv.es (R. Martínez-Máñez).
[1] This author contributes equally to this work.

https://doi.org/10.1016/j.addr.2023.115049
Received 12 January 2023; Received in revised form 14 July 2023; Accepted 4 August 2023
Available online 12 August 2023

discussed. This approach aims to provide a solid overview of the state-of-the-art in this field and to encourage the translation of MSNs to the clinic.

1. Introduction

The application of nanoparticles as a promising technology in the biomedical field, referred to as nanomedicine, has attracted the attention of chemists in the last decades. [1] Particularly, mesoporous silica nanoparticles (MSNs) have gained attention since their first synthesis in the early 1990 s[2] and their first use in drug delivery in 2001 reported by Vallet-Regi at al.[3] MSNs have unique properties such as a confined space to encapsulate therapeutic compounds and attracted the attention of numerous groups that developed drug delivery systems based on MSNs.[4–6] Besides, MSNs have remarkable characteristics such as adjustable porous structures, tunable and narrow pore size distributions, high pore volumes, high loading capacity, and high silanol density that allows easy dual-functionalization (exterior and interior).[7–9] Further report in the 2000 s of the first gated MSNs[10] and the possibility to develop gated MSNs operative in aqueous solution[11] fueled the development of numerous materials containing molecular gates (also known as gatekeepers or nanovalves) sensitive to different stimuli. These molecular gates are grafted onto the external surface of the MSN blocking cargo transport from the pores to the solution, that is released on-command in response to a certain stimulus (chemical, biochemical or physical) that usually breaks apart the molecular gate, opening the pore for cargo release.[7,12,13] As a result, the functionalization of MSNs with gatekeepers allows obtaining efficient drug delivery carriers improving the biocompatibility, cell membrane penetration, and site-specific delivery and controlled release of drugs and therapeutic agents.[7,14–17].

Gated MSNs have demonstrated a wide range of biomedical applications, including encapsulation and delivery of drugs, proteins, or genes for *in vivo* biological imaging, and therapies such as photothermal therapy, photodynamic therapy, radiotherapy, ultrasound therapy, antibacterial applications, and tissue engineering.[18] Moreover, gated materials have also been used in sensing and communication applications.[19–22] Gated MSNs for drug delivery have been used successfully in *in vivo* models, resulting in an improvement of the solubility of the encapsulated drugs and in a reduction of undesired side effects. [23–28] From a chemical point of view, nanomaterials present several properties that can be tailored to achieve specific applications. Consequently, many MSNs-based nanoparticles with different compositions, structures, morphologies, and functionalizations have been synthesized with excellent results in terms of cytotoxicity, therapeutic effect, and compatibilities. An exhaustive revision of synthetic protocols of MSNs has been published by Croissant and coworkers.[29].

Although the application of MSNs to clinical medicine seems feasible based on many promising *in vitro* results obtained to date, the *in vivo* translation remains challenging as the administration may exhibit different results under physiological environments and might have adverse effects leading to long-term safety issues. In addition, the effect of opsonization, enhanced permeability, and retention (EPR) effect, or the transportation in the blood stream are difficult to replicate in *in vitro* systems. Moreover, the cytotoxicity of MSNs captured by the reticulo-endothelial system (RES) organs is rarely studied in *in vivo* models. Therefore, this field raises many new questions regarding the pharmacokinetic and safety behavior of nanoparticles within living systems.

Compared to the number of preclinical studies, only a few silica-based nanomaterials have been FDA authorized for clinical trials. To reach clinical permission, the application of nanotechnology requires synthesizing nanoparticles with optimal *in vivo* features, not only for therapeutics outcomes but also for bio-safety concerns. Nevertheless, the literature around the biocompatibility, biodistribution, and biodegradation of MSNs is inconsistent, revealing an important gap in the complex knowledge of nanomedicine. Besides, the biological outcome of MSNs depends significantly on the nanoparticles' physicochemical properties as it also happens with other nanoparticles.[30,31].

Despite many excellent articles and reviews have been previously published related to MSNs in biomedical applications,[32–38] the lack of evidence in the literature regarding safety issues of MSNs during *in vivo* studies has emerged as the most critical barrier to clinical translation. In this review, we have compiled selected examples in the literature up to the present, with an emphasis on the biodistribution, biodegradability, and clearance of MSNs showing the potential and challenges related to the administration of MSNs for advanced therapeutics. Along the review, we also evaluate the main factors influencing the MSNs fate when administered in living organisms and highlight the strategies to reduce potential toxicities from MSNs administration. [30,31] This approach aims to provide a general conceptual view of this field and aims to help researchers to develop MSNs to reach the clinical application.

2. Preparation and types of mesoporous silica nanoparticles

Porous materials have received much attention in the last decade because of their physicochemical features, which makes them particularly versatile for a wide range of applications. The International Union of Pure and Applied Chemistry (IUPAC) classified the porous material according to the pore size as microporous (pore size < 2 nm), mesoporous (2–50 nm), and macroporous (greater than50 nm) materials. [39].

In 1992, researchers from Mobile Oil Company developed the synthesis of mesoporous silica materials (also known as M41S) using a self-assembled surfactant as the organic template: MCM-41 with a hexagonal arrangement of mesopores, MCM-48 with a cubic arrangement of mesopores, and MCM-50 with a lamellar structure.[40–42] These materials have pores with diameters ranging from 2 to10 nm and surface areas larger than 1000 m^2/g [43]. In addition, in 1998 researchers from Santa Barbara University reported the SBA-15 material, another class of hexagonal mesoporous materials, with pores sizes in the 5–30 nm intervals. [44,45] Since the breakthrough discovery of MCM-41, numerous synthetic methods for the preparation of MSNs have been developed.[45] Overall, these methods provide a range of options for synthesizing MSNs with different sizes, shapes, and pore structures, enabling the development of tailored materials for specific applications. The developed methods include the template-directed method,[46] the sol–gel method, [47] the chemical etching,[48] and microwave-assisted protocols.[49] For example, in the sol–gel method, alkoxysilanes are hydrolyzed and polymerized in the presence of a template that can be a surfactant or a block copolymer to direct the mesopore formation [50–53]. In this method, once the material is prepared, the template is removed from the mesopores. Of note is that certain procedures use surfactants that can be highly toxic, and an incomplete removal result in high toxicity in *in intro* and *in vivo*. Therefore, it is crucial to ensure complete removal of surfactants from MSNs specially for drug delivery applications.[53].

Among all possible types of MSNs, the MCM-41 phase has attracted considerable attention and it is perhaps the most studied. The synthesis of MCM-41 materials involves the use of cetyltrimethylammonium bromide as surfactant (CTAB) and tetraethyl orthosilicate (TEOS) at basic pH obtained by the addition of NaOH. The reaction is performed at 80 °C for 2 h and the product of the reaction is isolated by centrifugation or filtration yielding a material with hexagonal pores of 2 to 3 nm. The surfactant is removed from the pores of the MCM-41 structure by extraction under reflux conditions in acidic media or by calcination with heating at temperatures around 550 °C in a muffle furnace for several

hours.[54] A uniform particle size distribution can be obtained using a low concentration of surfactants[55].

MSNs are formed by a 3D framework of $(SiO_2)_x$ where silicon atoms have tetrahedral coordination with oxygen atoms (SiO_4). In particular, SiO_4 moieties are interconnected by bridge oxygen atoms (see Q4 structure in Fig. 1) and isolated silanol groups, which are mostly present at the surface of the structure exposed to the solvent (see Q3 and Q2 structures in Fig. 1). If the network connectivity is low (i.e. if the ratio (Q2 + Q3)/Q4 is high), the dissolution and biodegradation rates are higher.[56] Moreover, the chemical composition of the MSNs, the size, shape, and porosity of the nanoparticle are key parameters that define the dissolution and biodegradation rates.

Besides the MCM-41 type structures, various types of silica nanoparticles such as nonporous, hollow, core–shell or rod MSNs, etc., have been developed for biomedical applications (see representations in Fig. 2).[57] Additionally, more complex geometries can also be obtained, as for example, dendritic mesoporous silica nanoparticles, [58–60] or virus like mesoporous silica nanoparticles.[61–63].

One of the key challenges in developing MSNs for biological applications is achieving a homogeneous solution or dispersion. MSNs, as other nanoparticles, tend to aggregate and form clumps, which can lead to inaccurate dosing, inconsistent biological interactions, and potential toxicity.[64,65] Therefore, it is critical to ensure that the particles are dispersed to minimize the risk of toxicity, maximize their therapeutic potential and avoid problems such as having an actual number of circulating particles being much less than the number of particles in the injected dose. However, achieving this dispersion is not straightforward, and various strategies, such as coatings and sonication, are required.[66] In this regard, it is essential to assess the monodispersity of the samples to ensure that the nanoparticles do not form aggregates or multiple nanoparticles. Besides, it is of importance to measure the bulk monodispersity of the sample to accurately determine the dose of nanoparticles injected in *in vivo* studies. However, such important issue is not fully addressed in many publications.

3. Safety and biocompatibility

Even though silica-based nanosystems are widely regarded as very bio-safe *in vivo*, indicating that they could be used for controlled release, drug delivery, or diagnosis, the possibility of long-term retention in the body remains a potential concern and one of the crucial issues for clinical translation. In this section, we review how the safety of MSNs is influenced by the intrinsic physicochemical properties of the nanoparticles as well as the route of administration and describe different studies that assess MSN biocompatibility and biodegradability to ensure clinical translation.

3.1. Nanotoxicity of MSNs

The dose, exposure, route of administration, as well as the particle size shape and composition play a key role in the assessment of nanoparticles' toxicity. Regarding the dose and exposure time, there are frequently differences between the toxicity shown after a single dose, which typically results in short-term toxicity, compared with a repeated exposure. On its part, the toxicity is classified as acute (observed<24 h after single administration), subacute (observed<1 month after repeated exposure), subchronic (observed 1–3 months after repeated exposure), and chronic (observed 3 months after repeated exposure).[67] Nanotoxicology studies usually evaluate similarly acute and subacute toxicity by monitoring during the study different parameters, such as: immediate hematological, cardiac and neuronal responses, weight change, clinical observation of effects on cardiovascular, respiratory, locomotor, gastrointestinal function and effects on skin and fur, mortality, macroscopic necropsy and histopathological evaluation in selected organs.[68].

In the case of inorganic nanoparticles (including MSNs), acute toxicities have frequently been studied, however, there is a significant lack of information regarding long-term toxicity.[69] Besides, the differences between published studies about dose levels, frequency and delivery routes make it difficult to compare the toxicity of inorganic nanoparticles. In addition, the specific characteristics of each nanoparticle may also contribute to toxicity through unique mechanisms. For example, some toxicological mechanisms appear to be shared by all inorganic materials during chronic exposure: inflammation, generation of oxidative stress, impaired clearance, and fibrosis. Nevertheless, the toxicological mechanisms appear to be type specific. The chronic toxicity of different inorganic nanoparticles (gold, iron oxide, silver, zinc oxide and silica nanoparticles) has been shown to correlate with different factors such as particle composition, physicochemical properties, dose, duration, frequency, animal age, strain, and sex as well as the route of administration, as it has been extensively reviewed by the group of Ghandehari.[67] Following the purpose of this review, we focus

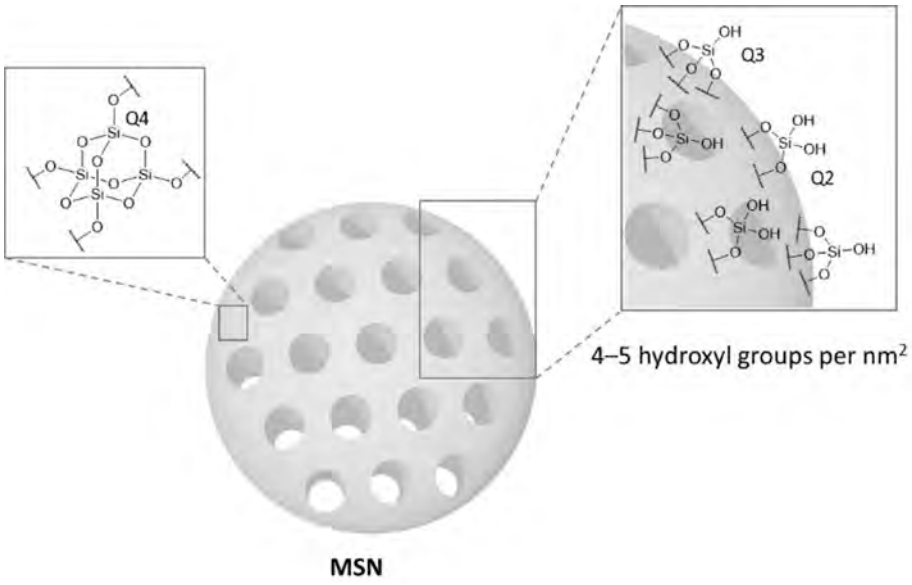

Fig. 1. The framework and surface chemistry of MSNs.

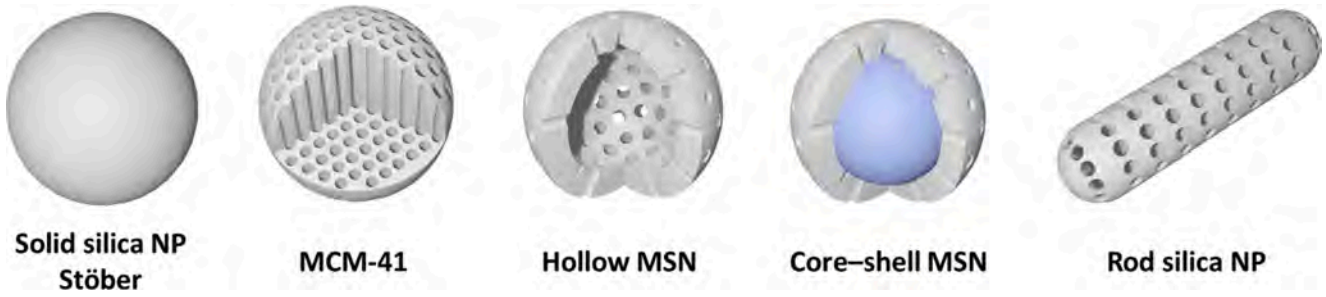

Fig. 2. Selected examples of the different types of silica nanoparticles.

below on the literature that specifically refers to the toxicity of silica nanoparticles (including MSNs) and evaluate their safety after administration by various routes.

3.1.1. *Intravenous administration (I.V.)*

The main safety concern in the use of inorganic nanoparticles is the potential to saturate the mononuclear phagocytic system (MPS) after their direct administration in the bloodstream, which might diminish the response to pathogens. However, a two-month FDA study reported that repeated intravenous administration (I.V.) to mice for up to 8 weeks of silica (10 nm) nanoparticles (5 mg/kg) did not saturate the MPS in the liver or spleen. Nevertheless, some changes in histopathology and in serum were noticed after week 3.[70] In addition, it has also been found that the toxicity produced by silica-based nanomaterials vary significantly depending on changes in porosity.[71].

Following the role of surface characteristics and porosity in toxicity, Ghandehari and co-workers evaluated acute toxicity of different silica nanoparticles with similar size (ca.120 nm) *in vivo* in Female CD-1 immune-competent mice after intravenous injection. According to the results, unmodified or amine-modified nonporous SiO_2 exhibited the lowest systemic toxicity and the highest maximum tolerated doses (MTDs) (450 mg/kg). On the other hand, regardless of geometrical aspects, MSNs caused significant systemic toxicity, with MTDs ranging from 30 to 65 mg/kg. However, when MSNs was amine-modified, the toxicity was reduced, and MTDs increased to 100–150 mg/kg. The adverse reactions were mainly associated with vasculature obstruction due to the hydrodynamic size of the nanoparticles upon protein exposure in serum, as the larger the hydrodynamic size, the lower the MTD. The lung and kidney were most susceptible to nanoparticle obstruction in vasculature above MTDs as a result of their abundant blood supply and special anatomic structures.[72].

A more recent and extensive study reported the influence of silica nanoparticle size, porosity, animal sex, and time on *in vivo* acute (10-day) and subchronic (60-day and 180-day) toxicity and inflammation profiles of nonporous silica nanoparticles (SNPs) of 50 nm (Stöber SNPs50) and 500 nm in diameter (Stöber SNPs500), and MSNs of approximately 500 nm in diameter (MSNs500) after single-dose intravenous administration in male and female BALB/c mice up to 180 days.[73] While nonporous Stöber silica nanoparticles of 50 nm (SNPs50) and mesoporous silica nanoparticles of 500 nm (MSNs500) showed to be more toxic under acute conditions, these nanoparticles showed less toxicity on days 60 and 180 at the MTDs in comparison to SNPs500. Importantly, it was found that male BALB/c mice appear to be more sensitive to MSNs500 at 10 days of survival evaluation, with MTD from 40 ± 2 mg/kg to 95 ± 2 mg/kg for male and female mice, respectively. However, this sex-related effect was not observed at 60 and 180 days. Toxicity was influenced by the porosity of the nanoparticles as Stöber silica nanoparticles with the same size did not show the same effect. Attending to tissue toxicity, the histological examination also showed size-, porosity- and time-dependent tissue toxicity. The Stöber SNPs500 caused major toxic effects in different organs as lung, heart, brain, kidneys and liver. However, the most affected tissue by both spherical Stöber and MSNs was the liver, which showed a higher accumulation after 10 days post-injection. Nevertheless, higher inflammatory responses occurred in the subchronic studies at day 60 and day 180. Despite the relatively high doses, none of the SNPs caused severe subchronic toxicity at day 180 after a single-dose intravenous injection and most of the lesions observed during the 60- and 180-day periods of the study are related to the recovery and clearance processes of the body following blood obstructions.[73] These observations correlate with previous work showing that the liver and spleen were the major organs for the toxicity of nonporous SNPs (70 nm diameter) at 4 weeks in male BALB/c mice chronically administered intravenously.[74].

In addition, the biocompatibility of MSNs in the long-term has been recently evaluated by the group of Ghandehari.[75] The authors determined one-year chronic toxicity of non-surface modified silica nanoparticles with different sizes and porosity (Stöber silica NPs 46 ± 4.9 nm diameter, Stöber silica NPs 432.0 ± 18.7 nm diameter, and MSNs 466.0 ± 86.0 diameter) after a single intravenous administration in both male and female BALB/c mice. Clinical observation showed no significant changes in body weight or hematology markers such as cell blood count or plasma biomarker indices. Post-necropsy examination of internal organs confirmed the biocompatibility of these silica nanoparticles. Nevertheless, a few animals showed microscopic lesions in the liver, kidney, spleen, or lungs which might indicate an ongoing or resolving injury that is caused by the rapid and long accumulation of nanoparticles in these organs upon I.V. administration. Importantly, the pathologic lesions were observed mainly when large, non-porous silica nanoparticles were administered, and no significant toxicity was found for small non-porous, and mesoporous nanoparticles. Furthermore, *ex vivo* evaluation with human blood and plasma revealed no hemolysis or activation of the complement pathway after incubation with the silica nanoparticles. This work is a long evaluation supporting the biosafety of silica nanoparticles for biomedical applications. [75].

3.1.2. *Oral gavage administration (O.G.)*

In the case of oral administration, there is only a report by Zande et al in which the long-term toxicity of different silica-based materials was evaluated after oral administration. Zande and coworkers demonstrated that oral gavage of 25 nm nanostructured silica to rats resulted in pathological effects on liver tissue after 84 days of exposure, whereas exposure to 7 nm synthetic amorphous silica nanoparticles did not. The histopathological analysis and the expression of fibrosis-related genes in liver samples confirmed increased fibrosis.[76].

3.1.3. *Intraperitoneal administration (I.P.)*

Both MSNs and colloidal silica NPs, having the same spherical morphology (approximately 100 nm in diameter), were intraperitoneally administered in female mice BALB/c for 4 weeks at different doses (2, 20, and 50 mg/kg/day) to evaluate clinical toxicity. MSNs seemed to increase the liver and spleen weight and splenocyte proliferation. Mice treated with MSNs showed altered lymphocyte populations in the spleen, increased serum IgG and IgM levels, and spleen histological changes but no systemic dysregulation was found with the colloidal NPs.

These results contradicted those obtained *in vitro*, emphasizing the importance of evaluating nanomaterials through both *in vitro* and *in vivo* experiments.[77].

Different reported studies with various inorganic nanoparticles identified hepatotoxicity and spleen alteration as the main subchronic toxic effects to be taken into account in safety analyses regardless of the route of administration.[67] Different studies analyzed here show that these data also apply specifically to silica-based nanoparticles, including MSNs. However, the few data collected, the observed effects and the difference between studies makes it difficult to draw meaningful conclusions in this regard.

3.2. Hemotoxicity and immune response

After administration, MSNs may interact with components in the bloodstream, therefore it is important to investigate the hemotoxicity properties of these materials for potential intravenous applications.[78] Indeed, amorphous silica compounds have been shown to cause hemolysis in mammalian red blood cells (RBCs), raising major bio-safety concerns.[79] Slowing et al. observed that the hemolytic activity of silica is related to the presence of silanol groups on the surface. The authors suggested that the presence of negatively charged silanols on the surface of bare MSNs (ca. 100 nm diameter) might react with the

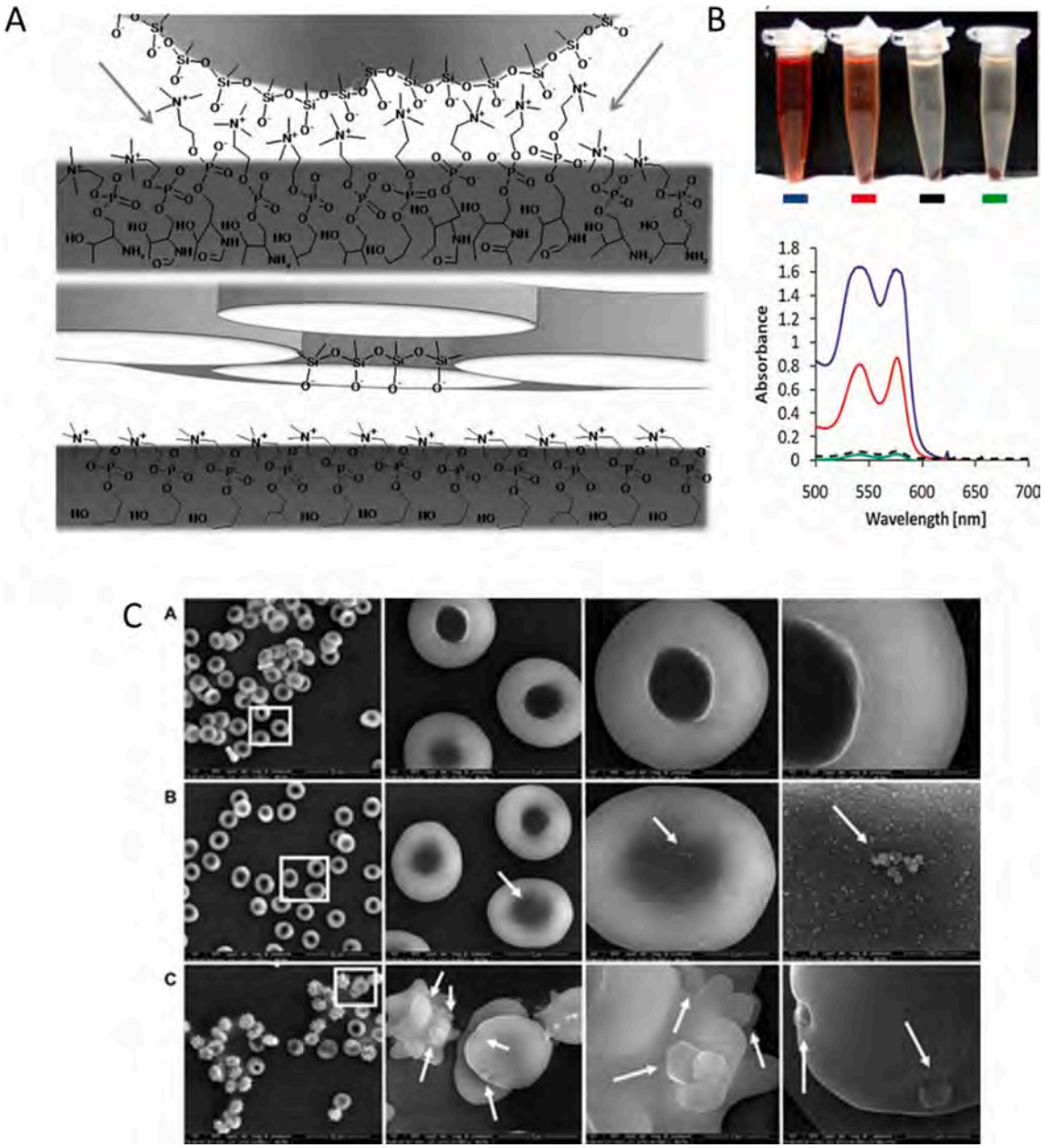

Fig. 3. (A) Representation of the interaction of (upper) amorphous silica nanoparticles, and (bottom) MSNs with the red blood cells (RBC) membrane (rectangular surfaces). (B) Hemolysis assay for amorphous silica (red lines) and MSN (green lines), at 100 mg/mL, using water as a positive control (blue lines) and PBS as a negative control (dashed black lines). The presence of hemoglobin (red) in the supernatant visually (up) and by absorption at 541 nm (bottom). Adapted with permission from Small 2009, 5: 57–62. Copyright © 2009 Wiley-VCH Verlag GmbH & Co. KGaA, Weinheim. (C) Scanning electron images of RBCs incubated for 2 h at room temperature with (a) PBS as control, (b) 100 μg/mL of MCM-41-type MSN, and (c) 100 μg/mL of SBA-15-type MSN. MCM-41-type MSNs were found to adsorb on the surface of RBC without modifying the normal biconcave shape compared to control RBCs. SBA-15-type MSN attached to RBC membranes induced a strong local membrane deformation, which resulted in particle encapsulation by RBCs, leading to the destruction of these cells. Reprinted with permission from ACS Nano 2011, 5, 2, 1366–1375. Copyright © 2011, American Chemical Society.

positively charged trimethylammonium groups of the lipid RBCs, causing hemolysis[79] (Fig. 3A). When compared to their non-porous counterparts, (commercial amorphous with two size distributions centered at 459 and 1720 nm) MCM-41-type MSNs had a lower hemolytic impact at doses suitable for pharmacological applications, suggesting that this material was innocuous[79] (Fig. 3B). To forward clarify this mechanism, a comprehensive study evaluated the interaction between MSNs possessing different surface functional groups (ionic, polar, neutral, and hydrophobic) with different blood components, in terms of their hemolytic activity, thrombogenicity, and adsorption of blood proteins on their surfaces. The authors demonstrated that surface functionalization can significantly diminish or even prevent the hemolytic activity of bare MSNs (up to 1 mg/ml MSNs concentration). Besides, none of the MSNs used had significant thrombogenic activity. Finally, the authors used human serum albumin (HSA) and gamma globulins (gGs) to study non-specific protein adsorption on MSN surfaces (particle diameter around 80 nm) and observed that surface functionalization with ionic groups can considerably reduce protein adsorption.[80] Further research confirmed that the hemocompatibility of MSNs depends on the size of the nanoparticles, and the hemolytic activity of nonporous silica nanoparticles on RBCs is reduced when mesoporous silica particles of similar size are used (particle sizes from ~25 to ~250 nm diameter).[81] A different study compared the size-dependent hemocompatibility of two types of MSNs materials (MCM-41 and SBA-15), and it was found that MCM-41 MSNs (~100 nm diameter) did not disturb the membrane or morphology of RBCs. In contrast, adsorption of large SBA-15-type MSNs (~600 nm diameter) caused strong local membrane deformation leading to spiculation of RBCs, and eventual hemolysis, suggesting that smaller nanoparticles may be considered safe candidates for intravascular drug delivery[82] (Fig. 3C). Furthermore, nanoparticle-induced hemolysis can be avoided by modifying the silanol surface with a poly(ethylene glycol) coating. In addition, PEGylation might be a critical step for the systemic administration of MSNs (particle sizes from ~25 to ~250 nm diameter) since it reduced particle aggregation in presence of serum, which may obstruct vessels.[81] As an alternative to PEGylation, the group of Kuroda demonstrated that introducing ethenylene-bridge silsesquixane into the MSNs (diameter of ~20 nm) framework provided hemolytic protection due to the longer Si-Si distance and lower acidity of the silanol groups.[83].

Moreover, the interaction of nanoparticles with immune system components is one area of interest. Nanoparticles can be engineered to either avoid interaction or to specifically interact with the immune system. An interaction between a nanoparticle and the immune system is considered desirable when it led to beneficial medical applications, such as vaccines or therapeutics for inflammatory and autoimmune disorders. However, if the immune cells identify the nanoparticles as foreign, it could trigger an immunological reaction against them and ultimately cause toxicity in the host.[84] Amino-modified MSNs (160 nm diameter) were observed to induce a very low immune activation and non-toxic effect in primary murine leukocytes, determined by the release of inflammatory cytokines.[85] Even though, recently MSNs have been pointed out as good candidates for immunotherapy. MSNs can act as adjuvants to promote immune cell recruitment and enhance the immunostimulatory effect in cancer immunotherapy. Specific nanodevices can be designed to achieve a suitable immunogenic response by controlling nanoparticle shape, size, surface modification, etc. For example, cationic and small size (100–200 nm) nanoparticles have been developed as cancer vaccines due to their easy internalization by some types of antigens-presenting cells (APCs).[86] Additionally, the immune response has been found to play a significant role in biomaterial-mediated osteogenesis. By activating immune cells and increasing cytokine release, MSNs can regulate inflammation and create an immunological environment that is beneficial to bone regeneration at appropriate concentrations.[87].

3.3. Biodegradability

To exploit their use in clinical translation, MSNs should be degraded and excreted in a reasonable time after their biomedical mission in the organism, either diagnosis or drug delivery.[88] Thus, it is essential to evaluate the rate and mechanism of degradation of the inorganic support as it would determine the safety and biocompatibility of these materials.[29] Due to their nature, inorganic materials are more difficult to degrade, so there is still an assumption that silica nanoparticles are not metabolized and tend to accumulate in RES organs (e.g. liver and spleen), where clearance might take weeks or even months. Although silica and its degradation products have been “generally recognized as safe” (GRAF) by the FDA for the past 50 years, and silica nanoparticles are used in the food and pharmaceutical industries, the low degradability *in vivo* could lead to long-term toxicity in various tissues or cause diseases.[29,89,90] Although the degradation kinetics of these MSNs are critical, they have not been completely investigated, and the impacts of experimental conditions during synthesis are yet unclear.

The MSNs framework is obtained through siloxane bonds (Si-O-Si) with silanol groups (Si-OH) on the surface. The central Si atom in the tetrahedral SiO_4 network is susceptible to being breakable in aqueous media following hydration, hydrolysis, and ion-exchange steps (Fig. 4). First, the water molecules are absorbed into the silica framework, and then, the hydroxide molecules (OH^-) present in water cause a nucleophilic attack leading to a hydrolytic breakdown of the siloxane bond. MSNs decompose in soluble silicon species, such as silicic acid, which are soluble in water and can be excreted either through urine or absorbed by the human body, which even contributes to maintaining bone health,[91] with non-toxic effect leading to a reduction in unwanted side-effects by accumulation.[92–94].

The rate of degradation depends on the physical properties of the nanoparticles (e.g., surface area, pore size, shape, condensation degree, aggregation state, etc.), the surface coatings or surface modification, and alterations in the framework (e.g., ion-doping and hollowness). Furthermore, the physiological environment (e.g., pH, temperature, concentration, protein content, etc.) plays also a role in the degradation of MSNs. In this regard, the degradation rate in physiological fluids is an important factor to consider when evaluating cytotoxicity. Degradation can take place over a timescale of hours to days depending on the conditions.[95–97] Some studies show that simulated lung fluid (SLF) imposes the fastest degradation rate of nanoparticles, followed by simulated body fluid (SBF) or PBS. The slowest rate occurred in simulated gastric fluid (SGF).[97] Consequently, the design of MSNs can be used to tune the dissolution rate of silica in biorelevant fluids for specific biomedical purposes.[29,88,89].

3.3.1. Degradability of MSNs by tuning surface area

The synthetic procedures followed to obtain silica nanoparticles can affect biodegradability kinetics. In particular, modifying the contact area between the framework of MSNs and water molecules can be used to control MSN degradability. Indeed, the accessible surface area is the main factor that determines the MSN dissolution rate, showing a linear relationship.[98].

One of the first studies regarding the biodegradation kinetics of MSNs was performed in 2010.[95] In this study the authors reported a three-stage degradation process of bare MSNs (ca. 100 nm) in simulated body fluid (SBF), consisting of a rapid bulk degradation on an hour-scale (stage 1), followed by a decelerated degradation (stage 2), and finally a sustained slow diffusion of the silicate layer over days (stage 3). The authors found that the biodegradation percentage of MSNs with a high-degree of Si-O-Si bond condensation only reached 32% after 15 days. Importantly, this behavior was not observed for nonporous silica nanoparticles. Later on, Hao *et al.,* demonstrated that sphere-shaped bare MSNs (87 nm diameter) have a faster degradation rate than rod-shaped counterparts (short rods of 194 nm and long rods of 416 nm), because of their external surface area. Moreover, the presence of

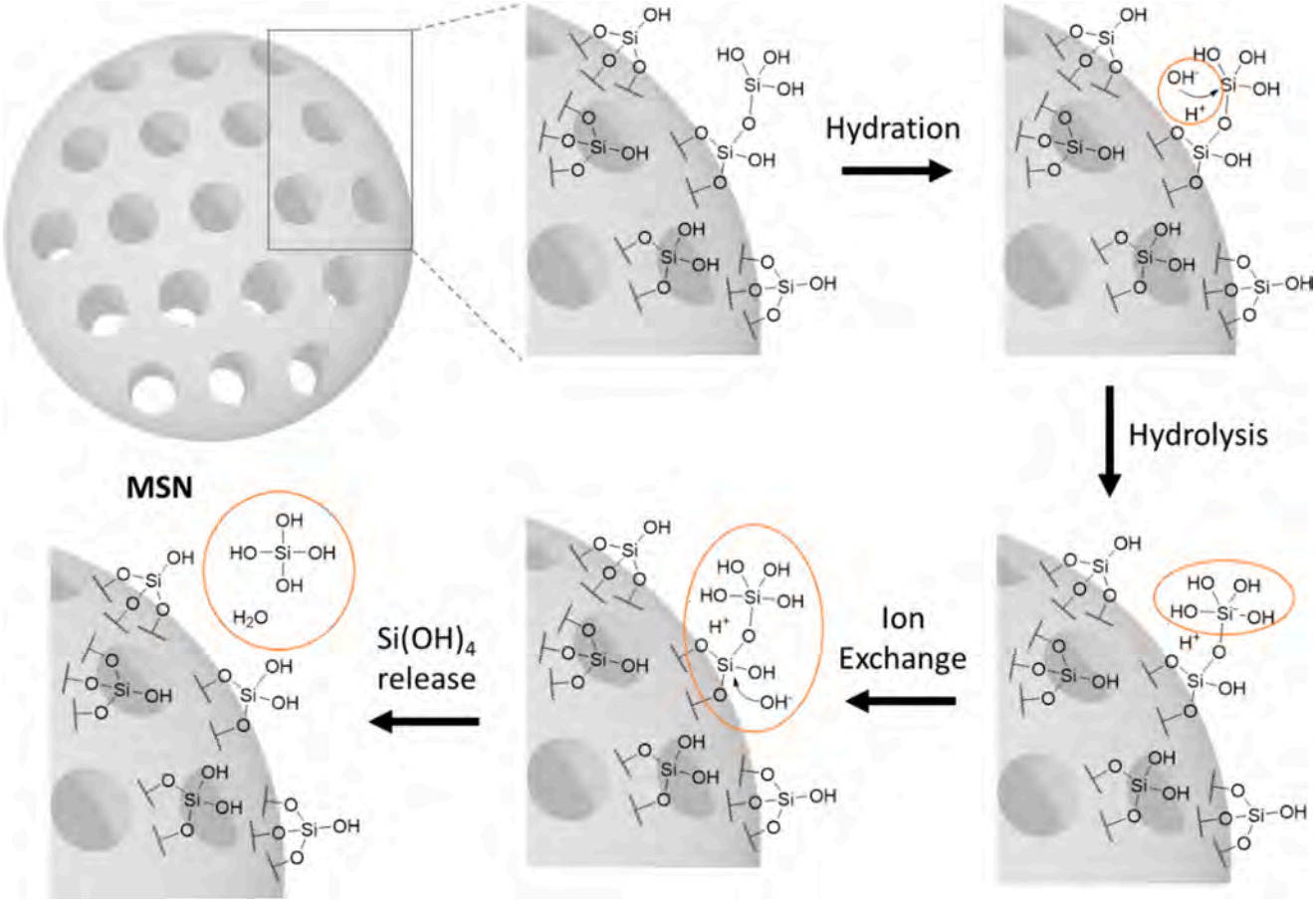

Fig. 4. Schematic representation of the dissolution mechanism of mesoporous silica nanoparticles.

proteins from the FBS accelerates the degradation rates of MSNs. Besides, the authors proposed a mechanism by which naked MSNs are degraded from the external surface, while PEGylated MSNs degraded from the interior of the particles for the steric hindrance of the hydrophilic PEG molecules outside the pore entrance. In contrast, the morphology and structure of solid Stöber silica nanoparticles did not significantly change within 60 days.[99].

Furthermore, it was found that the method for removing the template after the synthesis of MSNs influenced the degradation behavior. Calcined nanoparticles (~100 nm diameter) showed a lower degradation compared to nanoparticles in which the template is removed by refluxing in hydrochloric acid.[95] This study showed that high initial concentrations of the MSNs in SBF and a low surface area prolong the degradation rate. The connection between the degradability with the surface area was explained by the group of Kuroda.[100] For nonporous silica nanoparticles (~5–10 nm diameter), biodegradability was related to particle size. As a result, the smaller the nanoparticles are, the more contact they have with the surrounding medium at the interface, and the more easily they degrade. Unfortunately, the toxicity and hemolytic activity of such small particles increased. Thus, the presence of mesopores in colloidal MSNs showed a much higher degradation rate because of the increased contact area with water molecules, and this effect is independent of their size in a range of 20 to 80 nm diameter.[100,101] Moreover, aggregated MSNs presented a longer degradation rate in contrast to monodispersed MSNs. Zhao et al., showed that uniform monodispersed dendritic mesoporous silica nanospheres (~5–180 nm diameters with ~2.8–13 nm pores) possessed high degradability.[102] The authors concluded that the larger the pore size of MSNs, the faster the degradation rate. A different study also showed that bare MSNs (diameter ranges between 150 and 300 nm) prepared using the Stöber method and immersed in SBF tended to degrade from the inside to the outside, becoming hollow after 36 h and nearly completely degraded after 3 days.[103] Also, biodegradation was demonstrated in human embryo kidney 293 T cells without observing any toxicities. Importantly, Choi et al. evaluated if the presence of cargo in the pores of MSNs has an effect on the degradation of MSNs. The study compared doxorubicin-loaded MSNs (DMSNs), cargo-free MSNs, and nonporous solid silica nanoparticles (nanoparticle sizes < 200 nm) in terms of degradation. Doxorubicin-loaded MSNs degraded more quickly than bare MSNs, while the latter degrade at a similar rate to non-porous solid silica nanoparticles.[104].

Overall, the reported studies indicate that the modification of the different parameters that affect the contact area between MSN's framework and water molecules, such as pore size and porosity, can be used to regulate the degradability of MSNs from days to hours.

3.3.2. *Degradability of MSNs by surface modification*

Besides the surface area, the surface functionalization of MSNs has been demonstrated to affect the biodegradability of MSNs by promoting hydration or hydrolysis progress. Bindini et al reported that blocking the pores with organic or biomolecules (such as albumin present in the blood) reduces the surface of the material exposed to water, and the initial degradation rate is slowed by introducing a lag-time period.[98] Therefore, coatings play a crucial role in modulating the properties and behavior of MSNs having a significant impact on their degradability. While coatings could be categorized as cationic, anionic or neutral, it is important to note that specific coatings within each category can yield different outcomes. Consequently, evaluating each coating individually is necessary to fully understand its impact on MSN behavior. In this regard, Kim et al. showed that coating MSNs with polyethyleneimine

(PEI) to obtain PEI-MSNs (~80 nm diameter), accelerates the hydrolytic degradation of MSNs regardless of the pH value of the PBS medium. [105] The degradation rate of bare MSNs (~80 nm diameter) in acidic PBS was lower than in neutral PBS, which was explained as the nucleophilic attack by OH^- to the Si-O bond in MSNs framework is inhibited in acidic conditions. However, when the coating of PEI is present, the numerous amine residues of PEI could buffer the local pH around MSNs surface allowing the OH^- attack (Fig. 5). Thus, PEI-MSNs degradability is similarly achieved both in acidic PBS (83%) and neutral PBS (81%) at day 7.[105] Cauda et al. also evaluated the influence of the hydrophilic polymer coating PEG and demonstrated that PEGylation significantly retarded the degradation of MSNs in SBF (~60-400 nm diameter), and it depended on the density of the coverage and the molecular weight of the polymer.[106] The same researchers also evaluated different functional groups for coating MSNs (spherical and elliptical with sizes ~50-70 nm diameter) and found that phenyl-functionalized MSNs degraded significantly faster, followed by chloropropyl- and aminopropyl-functionalized MSNs.[107] In another work, it was studied the degradability of modified MSNs with the functional groups $–NH_2$ and –COOH (~10-30 nm diameter). The amino-functionalized nanoparticles ($MSNs\text{-}NH_2$) showed the fastest degradation behavior, followed by carboxylated-functionalized nanoparticles (MSNs-COOH) and non-functionalized nanoparticles when evaluated in PBS.[108].

From these results, it can be concluded that the surface functionalization of MSNs affects their hydrolytic stability and their degradation rate.

3.3.3. *Degradability of MSNs by tuning silica framework*

The biodegradation rate of MSNs is greatly influenced by the condensation degree of the silica framework (Si-O-Si bond), with a higher condensation degree resulting in a lower biodegradation rate. In this line, the synthesis of silica nanoparticles without surfactant leads to looser structures that are easier to hydrolyze in physiological conditions. [109,110] The degradability of MSNs can also be regulated and controlled by changing the chemical composition of the silica framework which has been achieved by doping with metal oxides and organic incorporation.

3.3.3.1. Doping with metal oxides. Degradability of the siliceous framework in physiological fluids of MSNs doped with manganese (Mn, ~60-70 nm diameter)[111], calcium (Ca, ~50-100 nm diameter) [112–114], iron (Fe, ~20-80 nm diameter)[115,116] or copper (Cu, ~160 nm diameter),[117] has been successfully achieved by regulation of the hydrolytic behavior of MSNs (*vide infra*). The presence of ions in the silica network introduces non-bridging oxygens leading to a weaker condensation of Si, and therefore, accelerating the hydrolysis of the silica framework. In contrast, the inclusion of zirconium in the MSN framework had the opposite effect and strongly inhibits degradation. [118].

The first report on metal ion-doped MSNs for biomedical applications was published in 2016.[111] Yu et al., synthesized manganese-doped hollow MSNs (Mn-HMSNs) (~60-70 nm diameter) as a theragnostic platform. The degradation rate was evaluated in SBF solutions at low pH 5.0 and the presence of glutathione (GSH, 5.0 mM and 10.0 mM) to accelerate this process. Also, the intracellular degradation behavior resulted in a significant fusion of degraded products on day 3 with no sign of material after 7 d, demonstrating that biodegraded debris could be easily excreted out of the cells (Fig. 6). Importantly, the rapid biodegradation of Mn-HMSNs in the presence of a mildly acidic and reducing tumor microenvironment resulted in substantially faster anticancer drug release and improved T1-weighted magnetic resonance imaging of the tumor.[111].

Shi and co-workers reported that the addition of calcium salt into the aqueous basic synthesis of MSNs resulted in mesoporous calcium-doped silica spheres (100 nm), containing an amount of CaO up to 8.18 wt%. [112] These particles had similar drug loading and release behavior as pure MSNs, but improved significantly their degradability rate.[112]. Hao and co-workers designed a hybrid mesoporous silica scaffold with hydroxyapatite (MSNs/HAP) which became into debris after 4 h in PBS pH 5.0 and they were found completely broken into small fragments at 12 h [113] (Fig. 7A y 7B). The degradability was improved by Ca^{2+} scape from the skeleton of MSNs in an acid environment. Importantly, the fast breakdown of MSNs/HAP nanospheres improved the penetration ability and release efficiency of the loaded doxorubicin into tumor tissues in mice, which might be more effective in cancer treatment[113] (Fig. 7C).

Iron ions can also be coupled to the silica framework, increasing MSN degradability in a protein-rich environment. Wang et al. produced an iron-doped hollow MSNs nanocatalyst (rFeOx-HMSN) (ca. 80 nm diameter) and found an accelerated biodegradation behavior, attributed to coordination between proteins and Fe ions.[115] The degradation of rFeOx-HMSN was evaluated in presence of SBF at pH = 7.4 and pH = 6.0, where the acidic condition accelerated the fracture of Fe-O bonds showing faster degradation. Also, the presence of deferiprone, which mimics a protein-rich environment and has been proved to coordinate with iron ions, accelerated the process (Fig. 8A). The catalytically active

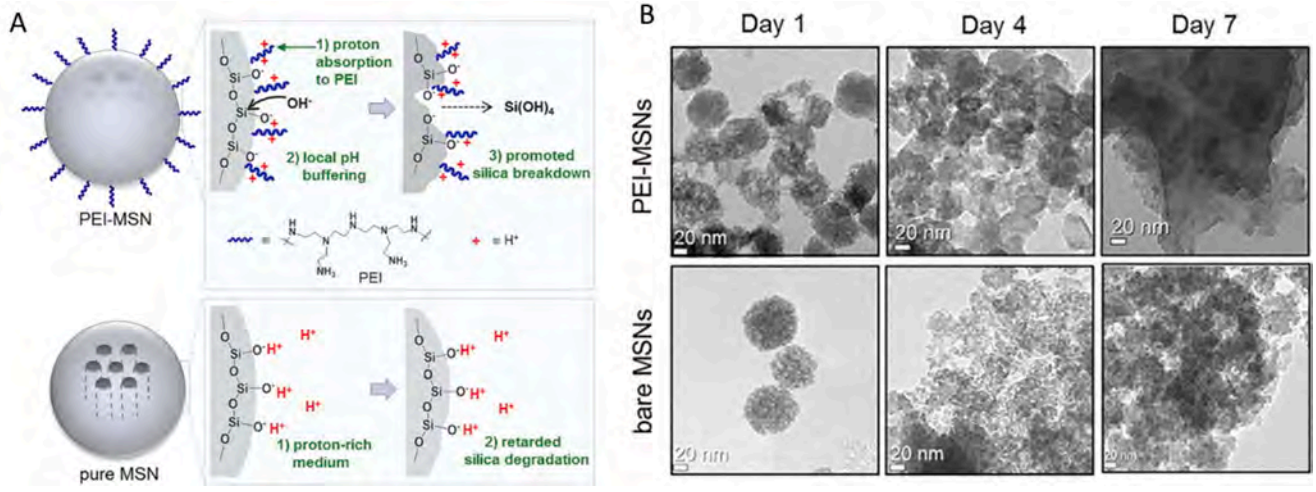

Fig. 5. (A) Schematic depiction of the hydrolytic degradation process of PEI-MSNs (upper) and pure MSNs (bottom) in an acidic medium. (B) TEM images of PEI-MSNs and bare MSNs in PBS at pH 5.0 at different times (1, 4, and day 7). Adapted with permission from J. Colloid Interface Sci. 2019, 533, 463–470. Copyright © 2018 Elsevier Inc. All rights reserved.

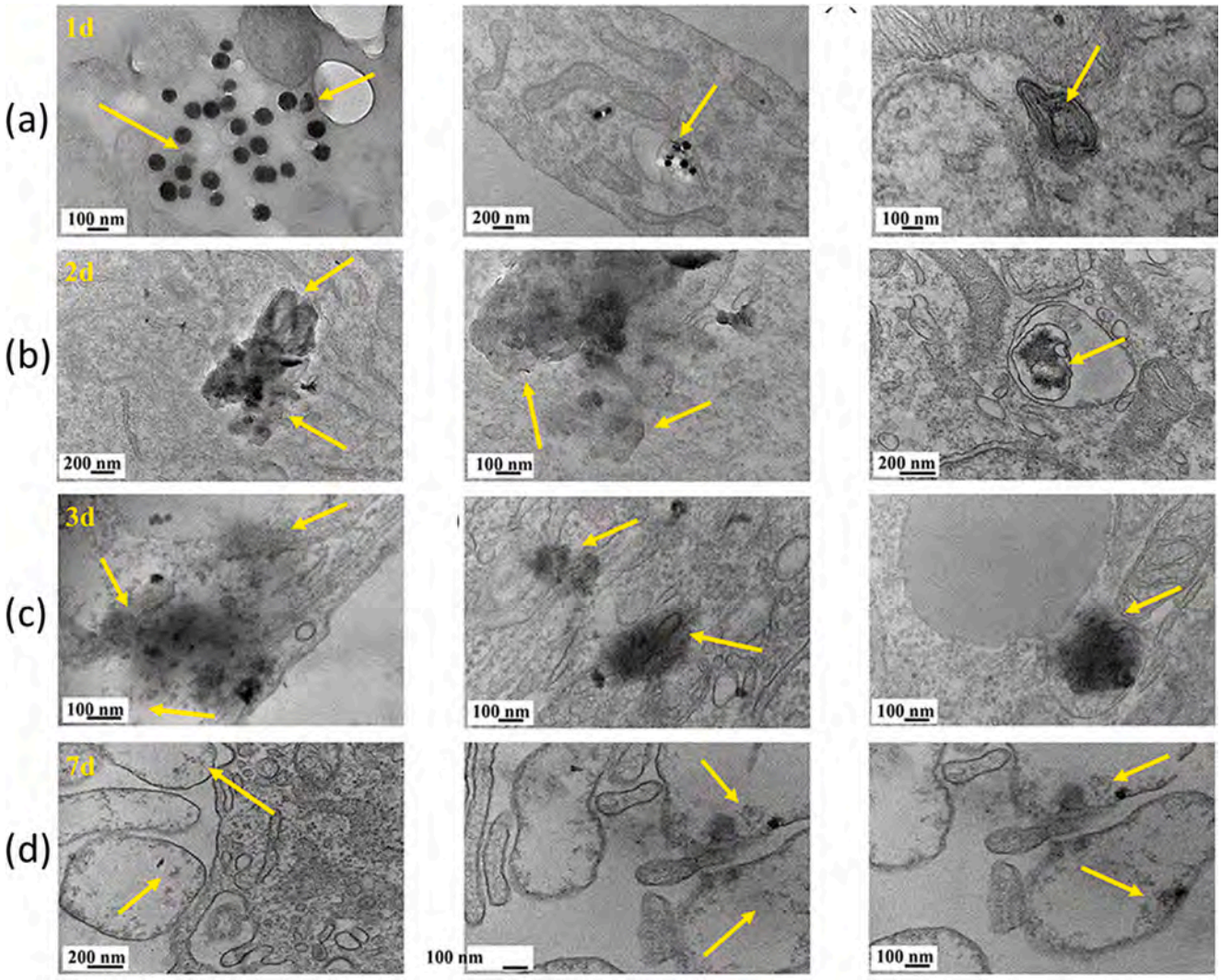

Fig. 6. TEM images of cancer cells after coincubation with Mn-HMSNs to observe the intracellular biodegradation behavior at different time point (a) 1, (b) 2, (c) 3, and (d) 7 d, respectively. At initial stage (a) Mn-HMSNs are endocytosed by cancer cells and accumulate into the cytoplasm. At 48 h (b) after intracellular uptake, is observed the fast biodegradation of Mn-HMSNs, as revealed by the cloudy morphology without a defined spherical structure. At day 3 (c) the biodegradation resulted in a significant fusion of degraded products. No significant material formulations could be found intracellularly after 7 days (d), demonstrating that the biodegraded species could be easily excreted out of the cells. Reprinted with permission from J. Am. Chem. Soc. 2016, 138, 31, 9881–9894. Copyright © 2016, American Chemical Society.

framework of rFeOx-HMSN react with tumor-abundant H_2O_2 to produce toxic hydroxyl radicals (OH^-) via Fenton-like reactions under mildly acidic conditions of the intratumoral microenvironment, resulting in severe oxidative stress conditions as an efficient treatment to damage tumors and enhanced biodegradability. Biocompatibility of rFeOx-HMSN (80 nm diameter) was evaluated *in vivo* on healthy Kunming mice for chronic (30 days) and acute (24 h) modes resulting in biosafety in both periods.[115] A different work reported biodegradable silica-iron oxide hybrid nanovectors of 100 nm with large mesopores (60 nm diameter) for large protein delivery in cancer cells. Half of the content was based on iron oxide nanophases which had an enhanced biodegradability in the presence of proteins from FBS, where the particles were shown mostly degraded as 10 nm pieces after 3 days. In contrast, the same nanoparticles remained intact in water after 3 days [116] (Fig. 8B). Similar degradability results were reported by Liu et al., when doped the silica framework with two transition metals (Fe and Cu; Cu–Fe–MSNs) (ca. 100 nm diameter).[119] The coordination interactions of metals with the silica species facilitated the degradability of the siliceous framework in physiological fluids.

Similar strategies were later described using PEGylated Cu^{2+}-doped hollow MSNs (PEG/Cu-HMSNs) (160 nm diameter), demonstrating that Cu–O bonds accelerate the structural collapse and degradation of the HMSNs carriers after 24 h in SBF (pH 6.5), with only PEG/Cu-HMSNs debris remaining after 72 h.[117] In contrast, the same nanoparticles (160 nm diameter) remained intact in neutral pH. Intracellular biodegradation was gradual in 4 T1 tumor cells, with only a few fragments of the degraded products visible on day 3. As a result, the strategy of doping Cu^{2+} into the MSN framework allowed PEG/Cu-HMSNs to remain intact while circulating in the neutral pH bloodstream but collapse rapidly after entering the weakly acidic tumor tissues, resulting *in situ* release of both encapsulated drugs and Cu^{2+}, reducing off-target release.[117].

In conclusion, the type, content, and structure of the metal doping affect the degradation kinetics of hybrid silica nanoparticles, as well as pH (particularly for Ca and Mn), the presence of certain proteins (for Fe), and glutathione (GSH) (for Mn).

3.3.3.2. Hybrid mesoporous organosilica-based nanomaterials. The incorporation of organic groups within the siloxane framework also leads to degradation under specific controlled conditions. Organosilica

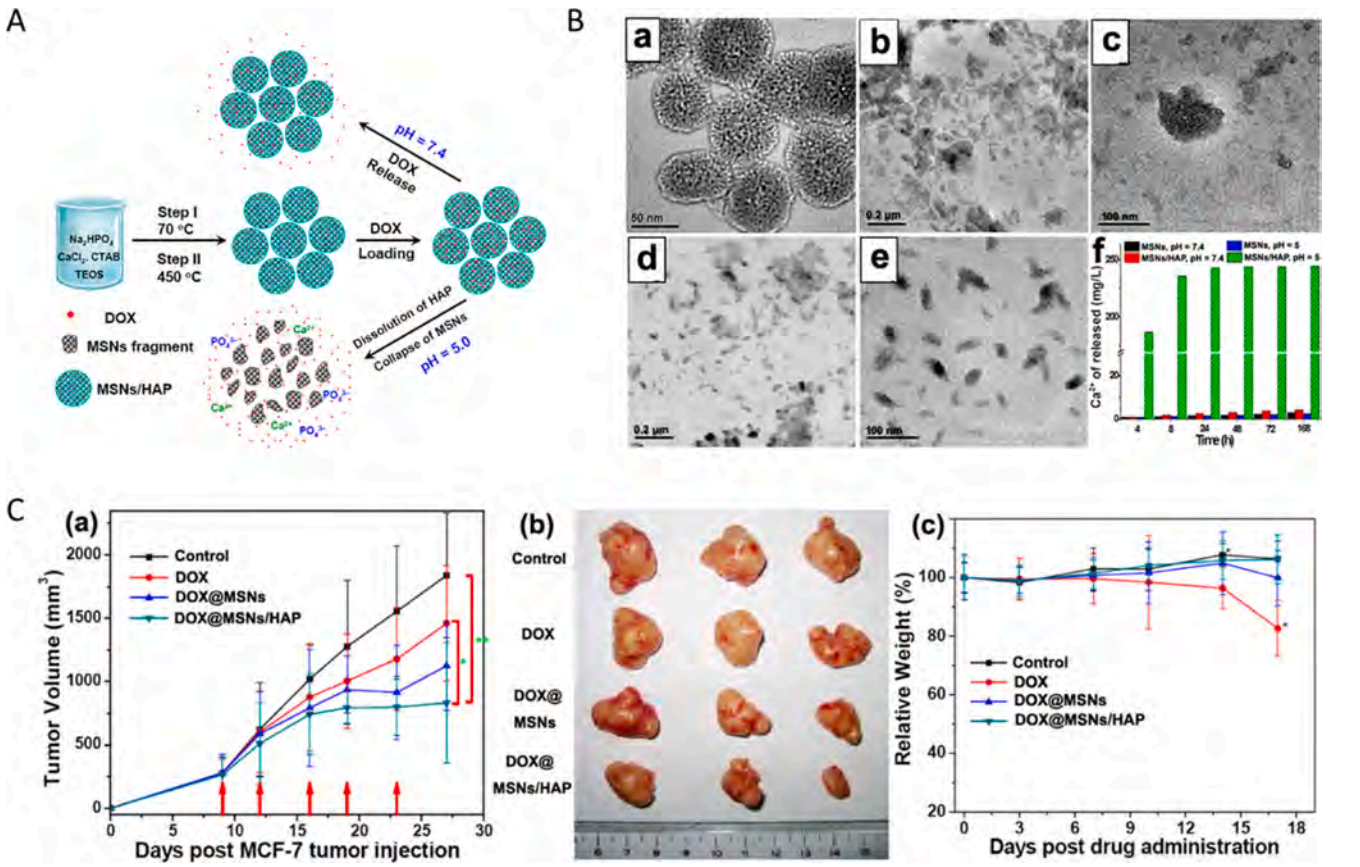

Fig. 7. (A) Schematic illustration of the synthesis, drug loading and controlled release, and degradation process of MSNs/HAP composites. (B) TEM images of the MSNs/HAP sample after degradation in acid buffer solution (pH 5.0) for (a) 0 h, (b, c) 4 h, (d, e) 12 h; (f) the release of Ca^{2+} at pH = 7.4 and 5.0. (C) (a, b) Tumor growth inhibition effect and (c) body weight change upon treatment with DOX, DOX@MSNs, and DOX@MSNs/HAP. Adapted with permission from ACS Nano 2015, 9, 10, 9614–9625. Copyright © 2015, American Chemical Society.

materials are prepared by mixing a silicon alkoxide precursor (i.e., tetraethyl orthosilicate, TEOS) with an organosilane to obtain functional organosilica moieties into the mesoporous silica framework. Depending on the type and ratio of functional organic groups incorporated within the silica framework we can differentiate between mesoporous organosilica nanoparticles (MONs) or periodic mesoporous organosilica (PMOs) when organized mesopores are obtained in MONs.[29] MONs can be prepared by including disulfide [120–123], tetrasulfide [124,125], diselenide[126] or oxamide groups[127,128] into the framework of MSNs, among others. In these organosilicas, the organic functional groups are cleaved under specific physiological conditions, such as enzymatic degradations or acidic conditions, that lead to the disintegration of the MSNs. In contrast to this, mesoporous nanoparticles with ethenylene-bridged silsesquioxane frameworks showed higher hydrolysis resistance under aqueous conditions compared to colloidal MSNs (diameter of ~20 nm). [83] Even if organic incorporation improves the biodegradation behavior of MSNs, organosilica precursors are of high cost and the process and uniformity of the final nanoparticles can be difficult to control.[93] Despite their potential advantages, it is also important to note that organosilicas face certain synthetic limitations compared to MSNs. One significant challenge is the preparation of uniform nanoparticles, while achieving precise control over the size, shape, and uniformity is more complex due to the incorporation of the organic moieties. Additionally, the synthesis of porous organosilica is challenging as the organic components can disrupt the ordered mesoporous structure typically observed in MSNs.

Mesoporous organosilica nanoparticles (MONs, 3.4–3.6 nm and 40 nm diameter) with disulfide bonds on their structure is the most widely studied strategy to enhance biodegradation. It has been demonstrated to improve the biocompatibility and biodegradation behavior of typical MSNs, and also achieve the controlled delivery of a cargo in redox-rich cancer cell environments.[120,121]. According to the valence-bond theoretical model, the bond length of the -Si-C- bond is longer than that of the -Si-O- bond, implying that the bond energy of the -Si-C- bond is lower. Consequently, the -Si-C- bond may be easier to biodegrade than the -Si-O- bond. Additionally, the -S-S- bond is physiologically active and easily biodegradable. As a result, the combined effects lead to the facile biodegradation of organosilica frameworks.[121] For the delivery of serum proteins, degradable dendritic mesoporous organosilica nanovectors (DDMONs) (ca. 200 nm diameter) containing disulfides and covered with a PEI polymer were prepared by Yang et al. with two distinct pore sizes (4.6 and 14 nm).[129] Large pore MONs showed similarly slow degradation compared to small pore MONs in normal cells. In contrast, in the presence of higher levels of GSH in cancer cells, the enhanced diffusion rate of GSH inside the mesoporous structure led to much faster degradation of large-pore MONs than small-pore MONs [129] (Fig. 9A). In a different approach, the biodegradation of ultrasmall disulfide-bridged MONs (<50 nm diameter) was compared to traditional MSNs (ca. 100 nm diameter) into SBF containing different glutathione (GSH) concentrations at different times (Fig. 9B). MONs started to degrade only 6 h after immersion in the reductive solution and were totally disintegrated in 7 d. In contrast, MSNs did not show significant morphological chances in the same periods.[130] Shi and coworkers also confirmed that a hybrid organic–inorganic framework, enhances MSNs biodegradability in tumors and thus high biocompatibility.[121].

A different example includes biodegradable disulfide-doped MSNs (ca. 100 nm diameter), based on hollow MSNs modified with PEG (HMON–PEG) and grafted with Mn–protoporphyrin (MnPorph) applied

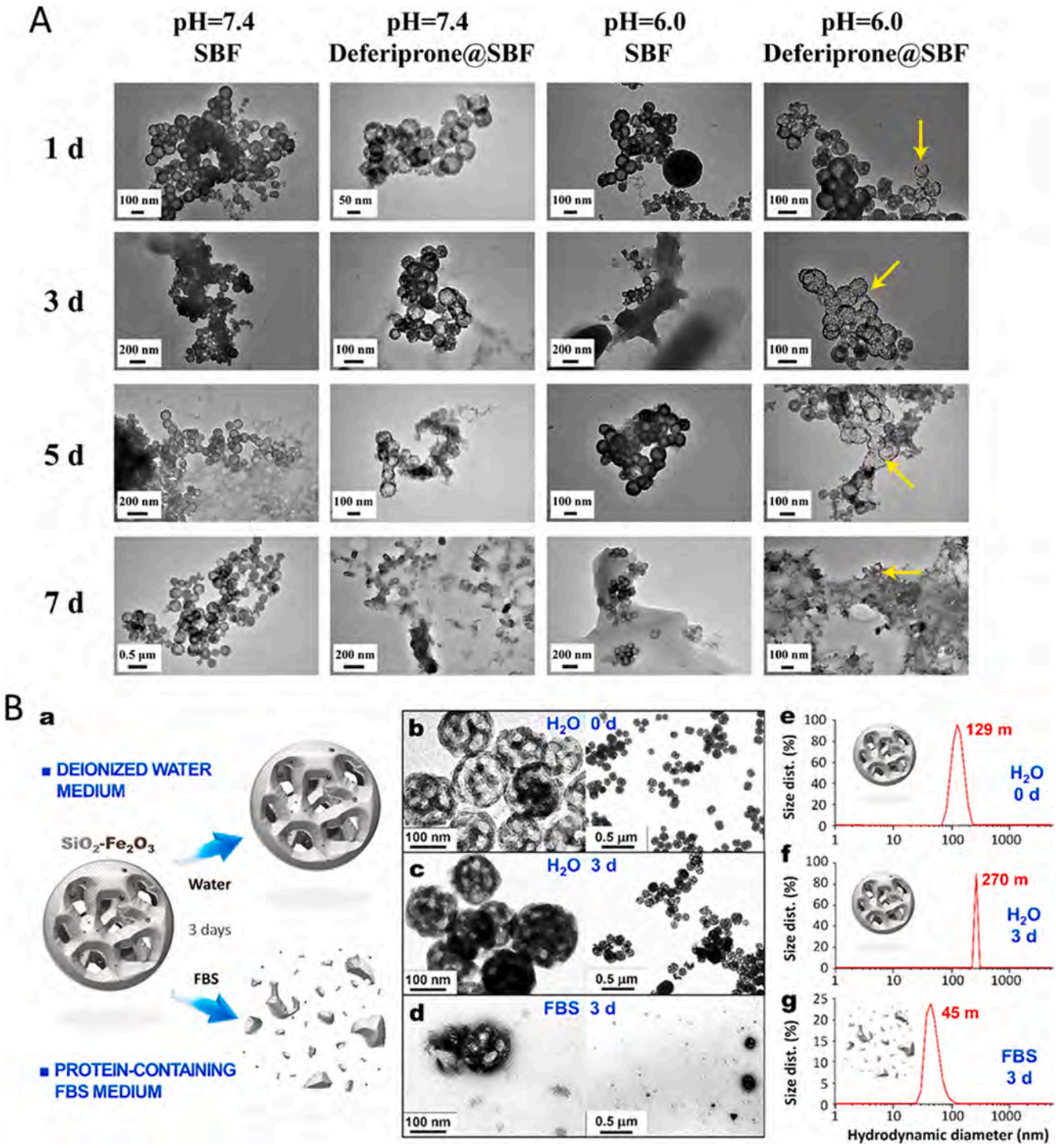

Fig. 8. (A) TEM images showing the biodegradation behavior of rFeOx-HMSN nanocatalyst in SBF with or without deferiprone under neutral (pH = 7.4) and acidic (pH = 6.0) conditions at varied time intervals (1 d, 3 d, 5 d and 7 d). Adapted with permission from Biomaterials 2018, 163, 1–13. Copyright © 2018 Elsevier Ltd. All rights reserved. (B) Representation of the degradability of large-pore silica-iron oxide NPs in water and FBS (a). TEM images of the nanovectors before (b) and after three days of dispersion in water (c) or FBS (d), and the corresponding DLS analyses (e-g). Reprinted with permission from J. Control. Release 2017, 259, 187–194. Copyright © 2016 Published by Elsevier B.V.

for magnetic resonance imaging-guided sonodynamic cancer therapy. [120] The *in vitro* assay in either SBF or intracellular conditions exhibited easy biodegradation behavior. Besides, *in vivo* studies demonstrated the rapid drop in silicon and manganese contents 48 h after injection, as well as the presence of nanoparticles in urine and feces, indicating that the nanoparticles were well excreted, which was likely due to their redox-mediated biodegradability. Additionally, the surface-cloaking with cancer-cell-membrane-derived fragments resulted, apart from an improved homologous tumor-targeting, in lower systemic toxicity.[120].

Shao et al. synthesized biodegradable diselenide-bridge large-pore MSNs (50 nm diameter) for intracellular protein delivery.[126] The organo-bridge MSNs can undergo self-destructive pathways in response to different stimuli, such as reactive oxygen species (ROS) and pH. After 3 days of exposure to redox or oxidative conditions, the MSNs structure was disintegrated into small fragments thus suggesting a facile renal

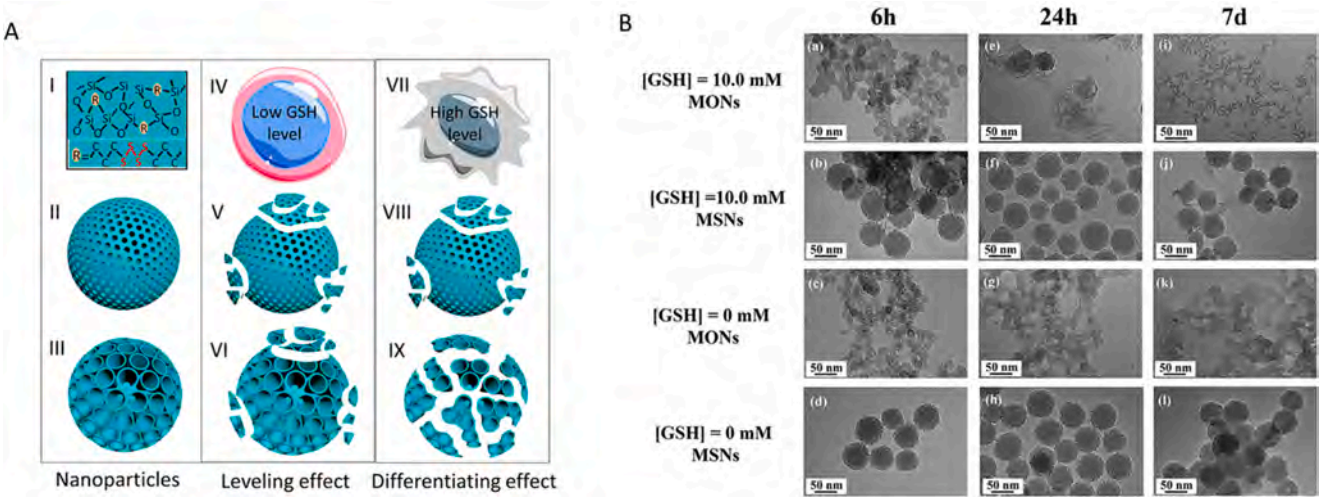

Fig. 9. (A) Schematic illustration for (I) the organic–inorganic hybrid composition of degradable dendritic mesoporous organosilica nanoparticles (DDMONs) (II) small pore MONs, (III) large pore DDMONs, (IV) normal cells, (V) MONs, and (VI) DDMON degradation in normal cells, (VII) cancer cells, (VIII) MONs, and (IX) DDMONs degradation in cancer cells. Reprinted with permission from Chem. Mater. 2016, 28, 24, 9008–9016. Copyright © 2016 American Chemical Society. (B) TEM images of MONs and MSNs after degradation for (a–d) 6 h, (e–h) 24 h and (i–l) 7 d in SBF solutions of GSH concentrations of 10 mM and 0 mM. Reprinted with permission from Biomaterials 2018, 161, 292–305. Copyright © 2018 Elsevier Ltd. All rights reserved.

clearance in further *in vivo* applications.[126] The introduction of oxamide groups into the silica framework was firstly achieved by Kashaḃs group, via a sol–gel method,[127,128] to obtain a homogenous distribution of oxamide groups into the silica framework. The particles degraded into nano fragments after the protein-mediated degradation when treated MSNs with trypsin in PBS for 48 h.

An interesting approach incorporated carbon nanodots (CDs) into mesoporous silica framework (CD@MSNs) following a hydrogen bond/electrostatic-assisted co-assembly strategy.[131] CD@MSNs, nanospheres with sizes of 50—60 nm, resulted biodegradable via CD-induced swelling and hydrolyzable Si-C bonds. The biodegradation was accelerated after the photothermal heating effect by NIR-laser irradiation and the resulting debris enhanced photothermal therapy (PTT) and synergistic immunotherapy *in vitro* and *in vivo*. Furthermore, CD@MSNs could still reach the cell lethal point under NIR-laser irradiation for 5 min even after 12-day degradation. A comparative *in vivo* study with bare MSN showed higher accumulation in the lung, compared to biodegraded CD@MSN which avoided the lung-trapping of nanoparticles, improving biosafety *in vivo*.[131].

3.4. *In vivo degradation of MSNs*

Despite the biodegradation of MSNs being one of the most critical limitations in achieving clinical applications, it is rarely explored in animal models. In this regard, degradation is usually studied using simulated body fluids but there is a need to state if the *in vivo* degradation occurs similarly. In this section, we present representative studies where degradable MSNs have been assessed *in vivo*.

Hao et al.,[113] demonstrated that the incorporation of hydroxyapatite into silica framework (MSNs/HAP, ~80–90 nm diameter) resulted in an increase of accumulated Si element in the kidney in comparison to pure MSNs. This was explained by the presence of Ca in the structure, which facilitated the degradation of the nanoparticle to smaller fragments (<5.5 nm) that are easily excreted through renal clearance. In terms of biocompatibility, MSNs/HAP loaded with doxorubicin (DOX@MSNs/HAP) protected mice from clinical renal lesions as compared to DOX@MSNs, which caused minor edema in the kidneys. [113] Wang et al. found that doped MSNs with Ca, Mg and Zn yielding Ca-MSN (103 nm), Mg-MSN (107 nm), and Zn-MSNs (99 nm) respectively, showed higher degradation rates than pure MSN, with rates of 50.8%, 52.8%, 56.3%, and 24.0%, respectively, one day after subcutaneous injection of 0.1 mL of 50 mg/mL nanospheres into the backs of C57BL/6J mice.[132] Moreover, the presence of Ca, Mg, and Zn in the MSNs framework provide an excellent ability to induce Th1 anticancer immunity, making them potential cancer immunoadjuvants. [132] Choi et al. investigated *in vivo* degradation of microsized mesoporous silica after local subcutaneous injection of 10 mg of SBA-15 (ca. 100 nm diameter) in 200 μL of PBS into the right flank of BALB/c mice inducing a small nodule in the injection site. [133] To assess structural deformation, the material was collected at different time intervals (3, 7, 10, 14, and 28 days). On day 3 post-injection, TEM images revealed that the pore structure was gradually destroyed over time, and distinctive XDR patterns were drastically reduced, indicating a loss of structural integrity. SBA-15 was not retrievable after 28 days, which was attributed to total silica breakdown.[133] Bhavsar et al. correlated the degradation rate of bare MSNs (80–120 nm diameter) from *in vitro* and *in vivo* analyses and showed that MSNs degraded faster *in vivo*.[134] The presence of silicic acid in urine and feces at day 4 indicated the complete degradation of MSNs after intravenous injection (20 mg/kg) in Wistar rats. In contrast, MSNs in PBS (pH 7.4) required 6 days to dissolve completely. They suggest that the explanation might be due to the continuous elimination of soluble silicic acid from the body. This supports the good degradability of MSNs in living organisms.

4. Biodistribution and pharmacokinetics of mesoporous silica nanoparticles

Biodistribution and pharmacokinetics are key parameters as they define the absorption and distribution of the nanoparticles within the organism being highly dependent on the physicochemical features of the nanoparticles (size, shape, and functionalization) as well as the employed route of administration. The principal routes or administration are intravenous (I.V.), intraperitoneal (I.P.), oral gavage (O.G.), and intratracheal administration. Regardless of the route of administration, the organs with the highest accumulation of nanoparticles are the liver, lung, and spleen.[135,136].

A systemic nanoparticle distribution is observed in the bloodstream when nanoparticles are inoculated into the body (as seen in Fig. 10). A protein corona is created as proteins from the plasma and/or intracellular fluid are adsorbed on the nanoparticles' surface.[137] The reticuloendothelial system (RES) immune cells such monocytes, platelets, leukocytes, and dendritic cells quickly opsonize the nanoparticles as a

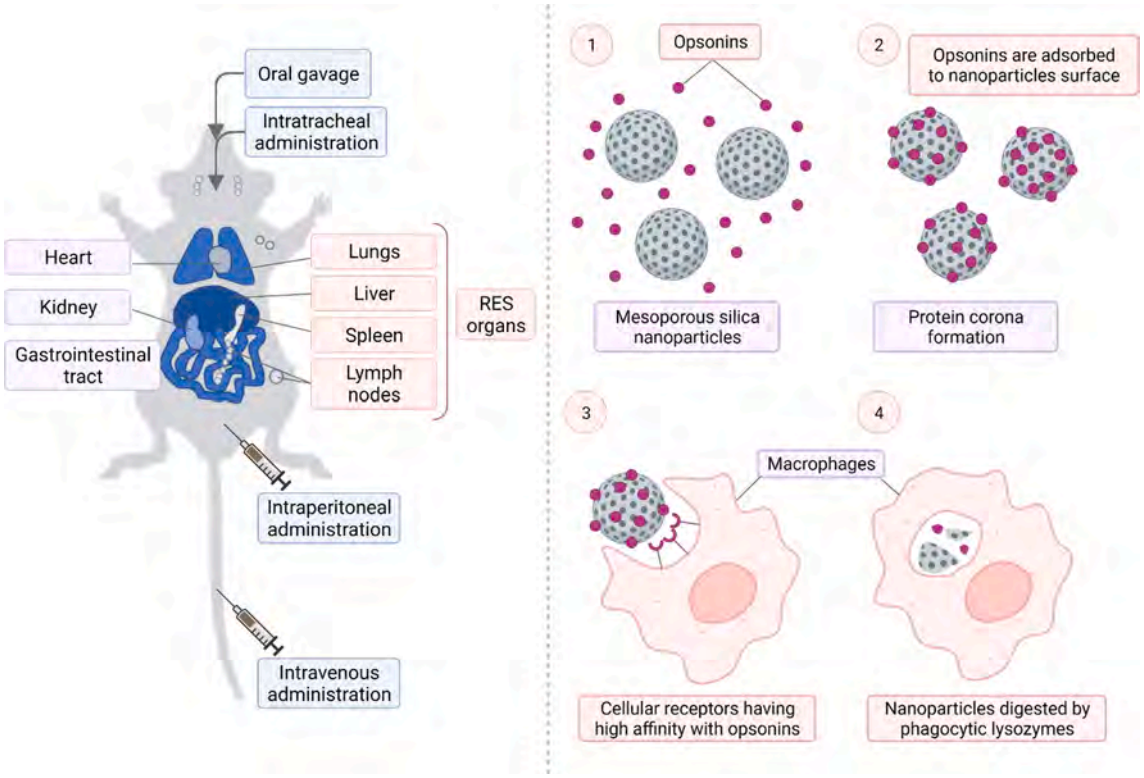

Fig. 10. The four most popular methods of administering nanoparticles in rodent models are intratracheal, intraperitoneal, intravenous, and oral gavage. The scheme also shows reticuloendothelial system (RES) organs like the lungs, spleen, liver, and lymph nodes. When delivered to the body, nanoparticles travel through the bloodstream (1), a protein corona is created when opsonins and other blood plasma proteins adsorb to the surface of the nanoparticles. (2). The circulating RES phagocyte cells, like macrophages, have cellular receptors that have a strong affinity for opsonins (3). This results in the macrophage internalizing and digesting the nanoparticles in the phagocytic lysozymes (4).

result of the protein corona's presence. Due to the presence of resident phagocytes, such as Kupffer cells in the liver, alveolar macrophages in the lung, macrophages and B cells in the spleen, or dendritic cells in lymph nodes, nanoparticles tend to collect in these organs.[138].

4.1. Targeting and cellular uptake of mesoporous silica nanoparticles

In addition to the systemic distribution of nanoparticles in the body nanoparticles can specifically target diseased cells or tissues through passive or active targeting.[139–141] Several factors, including the unique properties of the designed nanoparticles and the target tissue contribute to the nanoparticle accumulation and uptake process.

4.1.1. Passive targeting

There are two described mechanisms by which nanoparticles can passively accumulate in target tissues: the enhanced permeability and retention (EPR) effect in tumors and the ELVIS (Extravasation through Leaky Vasculature and the subsequent Inflammatory cell-mediated Sequestration) mechanism in inflammatory areas. Both mechanisms are based on the alteration of the vasculature that allows the nanoparticles to penetrate easily into the tissue (Fig. 4).

Regarding EPR effect, MSNs exhibits a preferential and large accumulation in the tumours compared to major organs. Matsumura and Maeda initially described the EPR effect in 1986,[142] as result from a dysfunctional lymphatic system and tumor vasculature that increases vascular permeability and limit the elimination of molecules from tumor tissues allowing nanoparticles to accumulate in the tumor (Fig. 4). A clear example of the EPR effect in MSNs was demonstrated by Wei et al. [143], observing that ultrasmall CuSNDs-sealed, doxorubicin-loaded MSNs (abbreviated as [64Cu]MDNs, 110 nm of diameter) initially accumulated in the tumors tissue after 1 h of the intravenous injection (dose of 0.074 MBq per mouse). The accumulation continued increasing at 5 h, reaching the maximum level at 24 h post-administration. At 4 h after the injection, MSNs were also found in the liver, spleen, and bladder. Accumulation in the bladder suggests an excretion method through the renal-urinary system. Another example to highlight is the PEGylated Cu^{2+}-doped hollow MSNs described by Wu et al.[117], these nanoparticles (~160 nm diameter) accumulated in tumor tissue with an efficiency of 4.3% at 48 h after intravenous injection (doses of 10 and 20 mg/Kg).

In a similar way, the leaky vasculature of inflamed tissues facilitates the penetration of nanoparticles due to the "ELVIS mechanism".[144] ELVIS mechanism was firstly described by by Wang D. and Goldring S.R. [144] and has been validated by several inflammatory disease models. [145–147] An example of this effect in MSNs can be found in the preferentially accumulated of MSNs loaded with caspase-1 inhibitor VX-765 capped with poly-l-lysine polymer, after their intravenous administration (~114–122 nm diameter, dose of 75 mg/kg of drug loaded MSNs that corresponds to 4.2 mg/kg of VX-765), in the inflamed tissue of an air pouch mouse model C57BL/6.[148] More recently, the same authors take advantage of this effect for developing targeted-lung nanoparticles for the treatment of pulmonary diseases.[149] MSNs were loaded with dexamethasone and capped with a peptide able to bind TNFR receptor in pro-inflammatory macrophages. After the intravenous administration of the nanoparticles (~194–230 nm diameter, dose of 25 mg/kg of drug loaded MSNs that corresponds to 10 mg/kg of free dexamethasone) in an acute lung injury model in CD-1 mice, IVIS imaging revealed a preferential accumulation of the nanoparticles in the inflamed lungs compared to healthy animals treated with the nanoparticles. Remarkably, the ability of the nanoparticles to reach the inflamed lungs and delivery dexamethasone in a controlled manner enhanced the therapeutic activity of the drug to reduce the inflammatory response and lung injury

while minimizing undesired side effects..

While the passive targeting (EPR effect) has been extensively utilized as a targeting strategy in nanoparticle-based drug delivery systems, it is important to comment that the concept itself is quite generic. The heterogeneity of tumors and the complexity of tumor microenvironments necessitate a deeper understanding of the mechanisms underlying nanoparticle targeting and accumulation in tumors. Merely relying on the EPR effect as a justification for tumor targeting may not be sufficient and future works in the field should provide a more critical discussion and evidence of the specific nature of targeting and accumulation processes in tumors.

4.1.2. *Active targeting*

By adding specific targeting molecules to the surface of nanodevices, active targeting aims to selectively target particular cell types without harming healthy tissues. The most often employed targeted molecules to modify the nanoparticles' surfaces are aptamers, peptides, proteins and antibodies [139] (Fig. 11).

Surface functionalization of MSNs with targeting molecules for specific targeted drug delivery has been extensively studied. Targeted MSNs exhibit a major escape from the uptake by the RES and an increased accumulation in the target organs and cells. [28,150–154] Zhou and coworkers,[155] used hyaluronic acid and collagen I coated MSNs (FMSNs) loaded with doxorubicin to target HeLa tumor-bearing BALB/c nude mice. Hyaluronic acid is one of the most studied agents for tumor targeting, since its receptor, CD44, is overexpressed in many cancers. As expected, FMSNs accumulate mostly in the tumor after 6 and 24 h post-IV injection due to the hyaluronic acid-targeting and EPR effect in the tumor. Another example is described by Goel et al.[156] that designed biodegradable dendritic MSNs (bMSNs, ~150 nm diameter) intrinsically radiolabeled with oxophilic zirconium-^{89} ([^{89}Zr]bMSNs) pegylated and functionalized with anti-CD105 to target tumor vasculature in a 4 T1 breast cancer model. [^{89}Zr]bMSN-PEG5k-TRC105 nanoconjugates demonstrated a long circulation time remaining in the blood even after 24 h post intravenous administration (dose of 50 mg/Kg) in the targeted group. PEGylation resulted critical for longer circulation *in vivo*. Besides, the induction of senescence for cancer treatment has been proposed as a new therapeutic approach. In this way, the development of galactooligosaccharide (galactan) capped nanoparticles has been described to target and selectively eliminate senescent cells in tumors, based on the specific galactan cap hydrolysis by the β-galactosidase overexpressed in senescent cells.[157,158] The *in vivo* imaging studies revealed the preferential accumulation of galactan-capped nanoparticles (80–100 nm diameter, dose 4 mg/mL, 200 μL of dye-loaded MSNs), loaded with different NIR fluorescent dyes (ICG and Nile Blue), in senescent 4 T1 breast tumors in balb/c mice after 24 h.

4.2. *Effect of size and shape modification*

Size and shape change the *in vivo* biodistribution of nanoparticles. Smaller nanoparticles typically have longer blood circulation lifetimes, which may be due to RES cells' delayed uptake of these particles in organs like the liver and spleen. He and coworkers[159] intravenously administered (dose 5 μL/g at concentration of 4 mg/mL) MSNs of different particle sizes (80, 120, 200, and 360 nm) and proved that when the size of the nanoparticles increased, their accumulation in the liver or spleen increased too. Thus, smaller size nanoparticles (80 or 120 nm) escape from being captured by the RES having a slower degradation rate. Dogra et. al[160] also proved that MSNs functionalized with PEG-trimethyl silane (PEG-TMS MSNs) of 25 nm of diameter presented higher

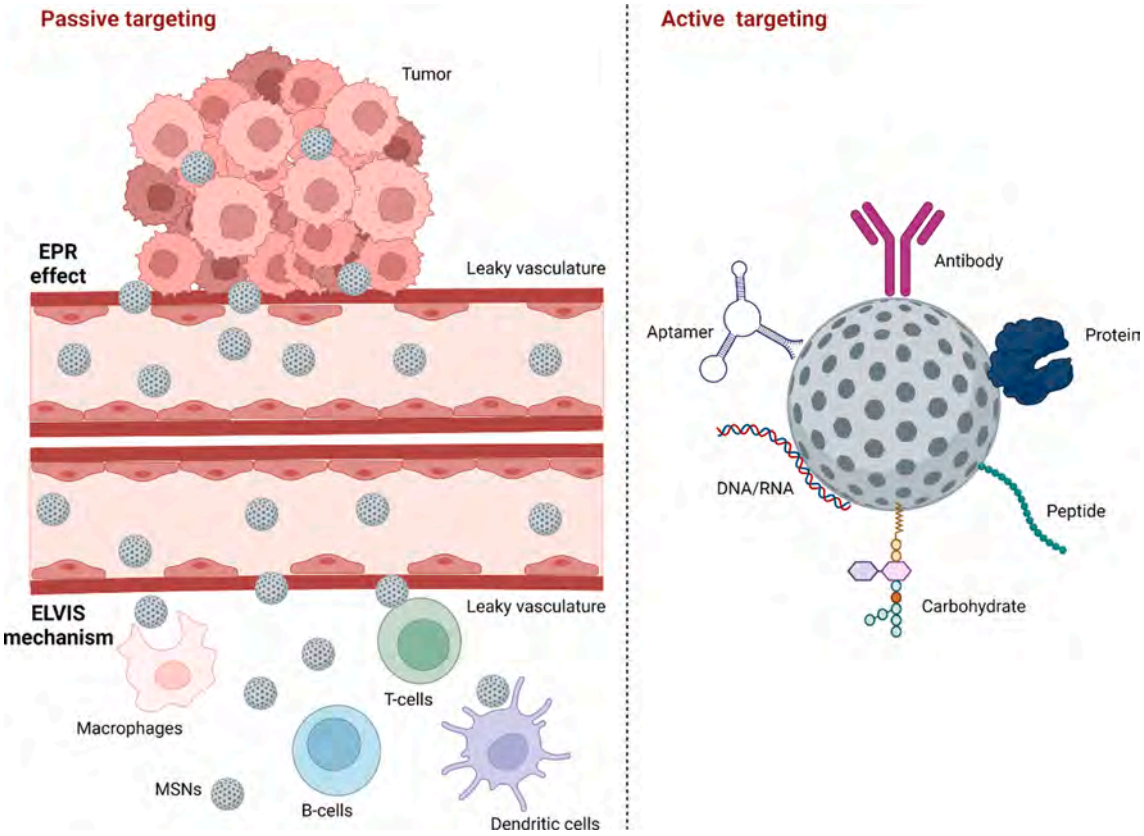

Fig. 11. Schematic illustrating the passive and active cellular targeting. Passive targeting is a consequence of altered vasculature and includes enhanced permeability and retention (EPR) effect in tumors and ELVIS mechanism in inflammatory microenvironment. Active targeting can be achieved by functionalizing nanoparticles with different molecules such as antibodies, proteins, peptides, carbohydrates, aptamers or nucleic acids. ELVIS: Extravasation of nanomedicines through Leaky Vasculature and Subsequent Inflammatory cell-mediated Sequestration.

bioavailability in rats compared to 150 nm PEG-TMS MSNs which were rapidly cleared by the liver and spleen (both MSNs administered at dose of 1 mg of nanoparticles suspended in 200 μL intravenous or intraperitoneal) (Fig. 5).

Particle shape also has a clear effect in *in vivo* behavior including biodistribution and clearance. Intravenously injected short-rod MSNs (185 nm short-rod nanoparticles and 760 nm long-rods nanoparticles, dose 20 mg/Kg) were easily trapped by the liver, while long-rod MSNs had longer blood circulation time and were more accumulated in the spleen.[161].

4.3. Effect of surface modification

The MSNs surface chemical properties of the nanoparticles have a direct impact on the adsorption of proteins, pharmacokinetics, biodistribution, accumulation, and even nanoparticle toxicity.[162] When nanoparticles are exposed to biological systems, a protein corona is created when proteins from the surface of the nanoparticle are adsorbed from the plasma and/or intracellular fluid.[163] The composition of the protein corona is particularly dependent on the nanoparticle composition, surface charge, and hydrophobicity.[164] For example, when nanoparticles are coated with polyethylene glycol (PEG) the stability of nanoparticles increases. PEG-coated nanoparticles have a prolonged blood circulation lifetime due to their ability to evade phagocytosis and avoid being heavily collected by RES cells in the spleen, liver, and lung.[111,159,165] Because of this, there is less breakdown products secreted in the urine.

Another strategy to produce a stealth effect on the RES is to coat the surface of nanoparticles with a lipid bilayer. When core–shell mesoporous silica nanoparticles (Fe_3O_4@MSN) are coated with a 1,2-dimyristoyl-*sn*-glycero-3-phosphocholine (DMPC) lipid bilayer (ca. 150 nm diameter), nanoparticles exhibit a strong accumulation in the liver and a very low accumulation in the lung in comparison with nude (100 nm diameter) or PEG-coated ones (ca. 120–150 nm diameter). At 24 h of the intravenous injection (dose 40 mg/Kg), PEG-coated Fe_3O_4@MSNs are still well present in the blood, suggesting a better circulation time due to the coating.[165] In another work, Shao and coworkers[126] designed diselenide-bridge MSNs (50 nm diameter) with cancer cell membrane coating (HeLa) and RNase A cargo (MSNs@RNaseA@CM) for cancer treatment. The intravenous administration of MSNs@RNaseA@CM (dose 10 mg/Kg) consistently exhibited remarkably improved blood retention compared with MSNs@RNaseA without the cell-membrane coating probably due to the immune-evasive ability of the cancer cell membrane. The elimination half-times were ca. 2.0 times higher (15–20 h) than their comparative without cell-membrane coating (9.7 h).

The copolymer coating of MSNs also alters circulation time in the blood. Dogra et al.[160] proved that strongly positive 50 nm MSNs coated with the copolymer poly(ethylene imine) (PEI) and polyethylene glycol (PEG) (both MSNs administered intravenous or intraperitoneal at a dose of 1 mg, suspended in 200 μL), presented the lowest systemic residence time, being rapidly uptaken by the liver and the spleen. However, PEG-trimethylsilane (neutral) and PEG-quaternary amine (positive) nanoparticles had similar circulating values although PEG-trimethylsilane moved to the liver and spleen and PEG- quaternary amine to the intestinal tract and bladder.

4.4. Effect of the route of administration

Nanoparticles can be administered to the body through different routes including intravenous (I.V.) and intraperitoneal injection (I.P.), oral administration (O.G.), and intratracheal administration. The route of administration can affect the biodistribution of the nanoparticles within the organism and the pharmacokinetics of their cargo. Understanding these factors is crucial for optimizing the therapeutic efficacy and safety profile of nanoparticle-based drug delivery systems. For example, intravenous injection allows the direct systemic circulation and wide distribution throughout the body, while intraperitoneal injection enables localized delivery to the peritoneal cavity. Oral administration offers non-invasive delivery, but it is also subjected to various biological barriers. Intratracheal administration provides targeted delivery to the lungs and respiratory system.

4.4.1. Intravenous administration

Intravenous administration (I.V.) of nanoparticles via the bloodstream allows systemic biodistribution and complete bioavailability facilitating widespread distribution to target tissues and cells and providing several advantages in drug delivery. As described above, when nanoparticles are exposed to plasma and/or intracellular fluid they are subjected to opsonization, protein corona formation, and RES capture.[137,138] This route offers controlled dosing, precise delivery of therapeutic agents, and the potential for targeted delivery. Moreover, intravenous administration is a well-established and widely accepted method in clinical practice.

Laprise-Pelletier and coworkers,[166] demonstrated that MSNs, based on MCM-48 nanospheres (150 nm diameter) functionalized with diethylenetriaminepentaacetic acid (DTPA) and labeled with paramagnetic ions Gd^{3+} (for MRI) as well as radioactive ions $^{64}Cu^{2+}$ (for PET), intravenous administration (dose of 0.31 μmol Gd, kept at a low level at 12.4 μmol/kg) reached the liver and spleen shortly after injection, followed by progressive elimination over time with half-lives of 12.9 h and 14.8 h for the spleen and liver, respectively. Huang et al.[161] found that, 2 h after intravenous administration (dose 20 mg/Kg), 80% of the injected fluorescein-5-isothiocyanate (FITC)-MSNs (ca. 70 nm) were accumulated in the vascular system of the lung and the RES organs such as the liver and spleen. MSNs showed diffused distribution in the lung and liver and aggregated distribution in the borderline of the spleen which correlates to the distribution of mononuclear phagocytes. 6 h after I.V. administration, nanoparticles were mainly located in the liver (35.3%), kidney (9.0%), lung (8.3%), spleen (8.0%) and heart (4.5%).[167,168] Guo and coworkers[169], prepared MSNs nanohybrids (60 nm) functionalized with peptide dendrons and marked with Cy5.5 that were administrated I.V. in healthy nude mice and *in vivo* NIRF imaging was performed at different time points showing the distribution of the MSNs with the time (Fig. 6A). A strong NIRF signal is observed in *ex vivo* imaging in the liver, spleen, and lungs from treated mice at 6 h and 24 h post-administration (I.V.) (Fig. 6B and 6C). Similar results have been obtained by He and coworkers (different particle sizes of 80, 120, 200, and 360 nm; intravenous dose 5 μL/g at concentration 4 mg/mL)[159] and Rojas *et al.* (~60–90 nm diameter, intravenous dose of 0.8 MBq of 18F-MSiNPs)[170] The latter group used the ^{18}F isotope anchored to MSNs (18F-MSiNPs) to determine the biodistribution and found that the radioactivity in the urinary bladder and intestine increased during the 2 h of the scan. At the end of acquisition, only 5 ± 1.2% of the injected dose remained in the circulatory system, suggesting that the removal of the MSNs would occur through feces and urine (see below for more detailed studies on clearance in section 5).

Regarding tumor targeting after I.V. administration, EPR effect with MSNs has been widely validated.[126,129,131,156,171,172] As described above, Wu and coworkers showed that PEGylated Cu^{2+}-doped hollow mesoporous silica nanoparticles (160 nm) accumulated in tumor tissue with an efficiency of 4.3% at 48 h after injection in a 4 T1 breast cancer mice model (intravenous doses of 10 and 20 mg/Kg).[117] In a similar tumor-bearing mice, Wei *et al.*[143] performed photoacoustic imaging of MSNs (100 nm diameter) capped with ^{64}Cu nanodots (6 nm diameter) and demonstrated that nanoparticles accumulated in the tumor tissue at 1 h after I.V. administration (dose of [^{64}Cu]MDNs 0.074 MBq per mouse). With time, the photoacoustic signal increased at 5 h and reached the highest level at 24 h post-injection. PET imaging was also performed to confirm the results, obtaining a gradual increase of radioactivity at the tumor site with the time until 24 h. Besides the tumor, high PET signals were found in the liver, spleen, and bladder

after 4 h of I.V. administration, suggesting that nanoparticles can accumulate in the bladder, and be excreted through the renal-urinary system.

4.4.2. Intraperitoneal administration

Intraperitoneal administration (I.P.) consists of the injection into the peritoneum (abdomen). It is a commonly used method of administration in animal experimentation because it is easy to perform and causes less stress on laboratory rodents being the most suitable technique for long-term administration or chronic therapies. In humans, its application is limited for instance to the treatment of some peritoneal cancer such as gynecological and gastrointestinal cancers.[173–175].

Although I.P. administration requires the absorption of MSNs from the peritoneal cavity into the blood, no significant differences have been found in pharmacokinetics or biodistribution between intravenously and intraperitoneal administration of MSNs. Dogra and coworkers,[160] compared both types of administration (both MSNs administered at a dose of 1 mg of nanoparticles suspended in 200 μL, intravenous or intraperitoneal) (Fig. 12) and observed a generalized nanoparticle distribution after intravenous or intraperitoneal injection of radioactive (^{111}In) MSNs functionalized with the polymer PEG-trimethyl silane. After 30 min of both intravenous and intraperitoneal injections MSNs accumulate in the heart and lungs. Then, the nanoparticles moved from the thoracic region to the spleen and liver (abdominal region) in a particle-type-dependent manner. MSNs accumulation was cleared 24 h after both types of administration.

4.4.3. Oral gavage

Oral delivery is the most common route of drug administration in patients. When MSNs are administered by oral gavage (O.G.), they can remain in the gastrointestinal tract but also can be intestinally absorbed and enter the systemic circulation. Zhao and coworkers,[176] used *ex vivo* optical imaging to qualitatively monitor the distribution of Cy5.5-labeled MSNs (150 nm) in the gastrointestinal tract. At 40 min, the fluorescence signal was mainly in the stomach, duodenum and jejunum while at 2 h, they found that fluorescent nanoparticles moved down gradually from the stomach to the intestine. Also, the fluorescence intensity gradually decreased with time. Regarding general distribution after O.G., L. Li *et al.*,[177] found that at 2 h post-administration (intragastrically dose of 40 mg/Kg), bare MSNs of size 85 nm accumulated in the liver, lung, spleen, and kidney. At 24 h post-administration, the MSNs had approximately a 2 times increased content in the spleen and 2.5 times in the kidney compared to that of 2 h, but it decreased to a low level at 72 h.

Again, the size and shape of MSNs play a role in the distribution of the particles. Zhao and collaborators[176] found that rod nanoparticles (150 nm, orally administration at 80 mg/Kg) had a longer residence time in the gastrointestinal tract compared with spherical nanoparticles (fluorescent Cy5.5-MSNs of 150 nm). It was also found that short rod nanoparticles and spherical nanoparticles both reached a higher content in all the organs than long rod nanoparticles at 2 h and 24 h, while the long rod nanoparticles attained a higher content in all the organs at 7 days. Regarding pharmacokinetics, they found that nifedipine(NI)-loaded long rod nanoparticles have higher bioavailability than NI-loaded short rod nanoparticles and spherical nanoparticles. Also, L. Li *et al.*,[177] proved that after degradation in the intestinal juice, the presence of bare-rod nanoparticles content (85 nm diameter and 146 nm length, intragastrically dose of 40 mg/Kg) was mainly found in the liver and lung, whereas spherical bare nanoparticles (85 nm) was mainly found in the spleen. These results indicated that it was more difficult to remove the long rod MSNs from the RES organs[178] and they were protected from macrophages, resulting in longer blood circulation.

Targeting the gastrointestinal tract can be achieved by oral gavage. Focusing on facilitating drug delivery to the colonic region, MSNs

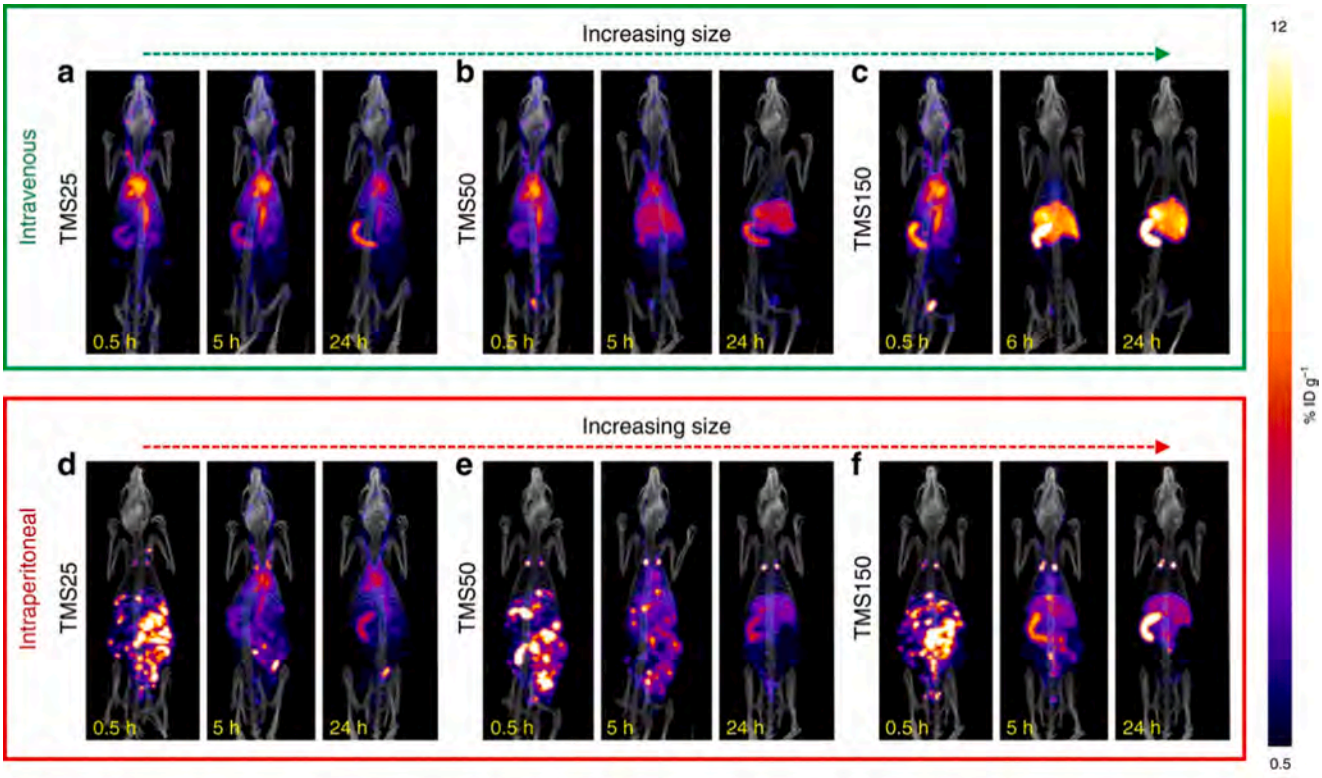

Fig. 12. SPECT/CT images showing the evolution in the biodistribution spatio-temporal of radioactive (^{111}In) MSNs. PEG-trimethyl silane (TMS)-coated radioactive MSNs of nominal sizes 25 nm (a, d), 50 nm (b, e) and 150 nm (c, f) were injected via I.V. (a-c) or I.P. (d–f) route to evaluate the effect of MSN size and route of administration in biodistribution of healthy rats. Injections were followed by SPECT/CT imaging at 30 min, 5 h (6 h in case of TMS150 (I.V.)), and 24 h. All SPECT images were scaled from 0.5 to 12%ID g^{-1}. Reprinted with permission from Nature Commun, 2018, 9, 4551 Copyright © 2018, The Author(s).

containing safranin O (as a model drug) and capped with hydrolyzed starch molecules were administrated in an enteric capsule (~100–200 nm diameter, oral dose of 40 mg) covered by a pH-dependent coating polymer formed by methacrylic acid– methyl methacrylate copolymer (commercially available as Eudragit S), soluble at pH greater than 7. The distribution of safranin O in the colon, plasma, and other organs at 24, 48, and 72 h was compared (e.g., pancreas, heart, kidney, brain, liver, spleen and lung) (Fig. 6E). According to the findings, when safranin O was given freely, it did not build up in the colon or other organs and was practically eliminated after 24 h. In contrast, when safranin O was administered with the enteric capsule formulation, a high dye content in colon tissue was observed after 24 h, while a very low content was found in blood and other tissues. Furthermore, after 72 h, the amount of safranin O in colon tissue decreased significantly. These nanoparticles allow the retention of the MSNs in the colon and the release of the drug in this target organ.[179–181].

Besides, to efficiently treat intestinal diseases nanoparticles can be designed to reach distinct regions of the gastrointestinal tract as demonstrated Desai and co-workers.[182] The authors evaluate the effect of the different combinations of PEI-, PEG-, and FA- coated MSNs (ca. 400–500 nm) on intestinal targeting. The therapeutic potential of MSNs loaded with DAPT (γ-secretase inhibitor) for targeted delivery to the intestinal epithelium was evaluated. PEG-, FA-PEI-MSNs and FA-PEG-PEI-MSNs was fed to mice by oral gavage for 3 consecutive days. Unloaded nanoparticles and free DAPT was used as a control. The combination of FA-PEG-PEI DAPT-loaded MSNs resulted in a higher drug efficacy compared to free drug in the intestine. In addition, the authors evaluate the role of surface modifications to specific regions of the gastrointestinal trac. PEI-MSNs have more affinity for the small intestine and PEG-PEI coating for the colon. PEGylated nanoparticles showed a higher ability for mucosal penetration, being a useful modification for targeting the colon and thus offering better therapeutic options for diseases that occur in the colon such as colorectal cancer and inflammatory bowel disease.

Another interesting approach to target specific regions of GI is the development of programmable nanoparticles taking advantage of the difference in pH values in the stomach (pH 1.2), small intestine (pH 6.5–7.5) and the inflamed colon (pH 3). Fu et al. developed programmed pH-responsive core–shell nanoparticles (CNs) for the precisely drug delivery in ulcerative colitis.[183] Eudragit® EPO and L100, two pH-sensitive materials (pH 6.5 and pH 1.2, respectively), were used to coat nano-sized curcumin to fabricate core–shell nanoparticles (ca. 300 nm). The developed CNs@EPO@L100 exhibited programmed pH-responsive drug release behavior in solutions mimicking pH in the transit through gastrointestinal tract. Due to the presence of EPO layer, which is degraded at pH 1.2 a negligible cargo release was observed from CNs@EPO@L100 at this stage. In the second, the second layer (L100) was slowly degraded at pH 6.8 allowing that nanoparticles reached the final step and efficiently release their content at pH 3.0. This effect was also confirmed in animal experiments. The biodistribution of CNs@EPO@L100 in the gastrointestinal tract from ulcerative colitis mice model was monitored after a single oral administration. A strong fluorescence signal was observed in the colon of those animals treated with the CNs@EPO@L100 compared with control nanoparticles (CNs, and CNs@EPO) present in the stomach and the small intestine. The design of programmed pH-responsive release nanoparticles could be a potential tool for efficiently treat gastrointestinal disorders.

4.4.4. Intratracheal/intranasal administration

In some studies, the MSNs were directly administered into the lungs, by intratracheal instillation or by inhalation. Over years, the use of silica nanoparticles has been concerned with safety issues related to lung accumulation and thus damage, mainly ascribed to inhaled nanoparticles. However, these problems can be overcome through the modulation of the physicochemical properties of the nanoparticles, as well as dose and exposure.[35] Biodistribution of MSNs after intratracheal administration performed by Van Rijt et al. demonstrated the suitability of MSNs as drug delivery carriers in the lung (tested doses of 20 and 100 μg per mouse).[184] The authors prepared MSNs functionalized with amino groups (MSNs-NH_2) of ca. 105 nm, or with avidin protein (MSNs-AVI) of ca. 165 nm of size. The toxicity, biodistribution and clearance rate were evaluated in BALB/c mice. Whereas MSNs-NH_2 showed a significant inflammatory response and some pulmonary toxicity, no evidence of toxic effects or inflammatory response was observed for coated MSNs-AVI. When MSNs were coated with the glycoprotein avidin, the nanoparticles were able to reach the deeper alveolar regions and they were found dispersed over the lungs, remaining in the lung epithelium at least for 7 days.

There are several reports in which MSNs are used for treating pulmonary diseases. In these cases, intratracheal instillation or inhalation was used, without any sign of toxicity achieving a direct lung delivery. For example, the effectiveness of MSNs was proven for lung cancer treatment. Minko and colleagues[185] prepared Cy5.5-labelled MSNs (ca. 150 nm) loaded with doxorubicin and functionalized, via disulfide linkages, with siRNA for drug-resistance and PEG-LHRH (luteinizing hormone-releasing hormone receptor) for lung targeting. The accumulation of the prepared nanoparticles was evaluated in mice bearing an orthotopic A549 lung cancer treated by inhalation or intravenous injection (dose in both cases of 2.5 mg/Kg). After 3 h, IVIS imaging revealed an enhanced accumulation of the inhaled MSNs into the lungs as well as reduced dissemination in other organs, compared to intravenous administration. Besides, Godaly and coworkers[186] developed a MSN loaded with the NZX peptide (NZX-MPSs) of 200 nm size for the treatment of Tuberculosis. The results exhibited a greater reduction of the bacteria burden in BALB/c mice infected with *M. tuberculosis* after the intranasal administration of the MSNs when compared to that obtained with the free treatments. This effect was mainly attributed to the ability of the MSNs to reach the infected lungs.

4.5. Miscellaneous: Blood-brain barrier

The blood–brain barrier is a highly selective semipermeable endothelium whose main function is to regulate the entry of molecules into the central nervous system. It is not yet clear whether MSNs can cross the blood–brain barrier to reach lymph nodes and brain parenchyma. Some reports have indicated the presence of nanoparticles in these brain areas. [187–190] However, other reports [161,170] did not find any presence of nanoparticles in limb lymph nodes or the brain after 2 h or 7 d post-I.V.-injection even changing nanoparticles size or shape (185 nm short-rod nanoparticles and 760 nm long-rods nanoparticles with intravenous dose of 20 mg/kg and ~ 60–90 nm diameter intravenous dose of 0.8 MBq of ^{18}F-conjugated MSNs). The reason for these differences may be related to the intrinsic properties of the nanoparticles.[191] In this regard, MSN formulations can enhance drug delivery by overcoming the BBB through specific transport processes.[192] As an example, Hernan Li and collaborators[193], have synthetized FITC labeled biomimetically MSNs (BMS), with a size of 200 nm, using three heterocyclic amino acid derivatives (C16-L-histidine, C16-L-poline and C16-L-tryptophan) as a template. After 1 h of intragastric administration (dose 200 mg/Kg), BMS were found in the brain exhibiting the highest peaked at 4 h (Fig. 13D). The fluorescence intensity started to decline at 8 h post-administration.

Fortin, Calon, Kleitz, and coworkers performed *in vivo* studies to evaluate the BBB targeting ability of Ri7-MSN50 nanoparticles based on MCM-48 conjugated with DPTA–Gd(III) and the monoclonal antibody (Ri7) with affinity to brain endothelial and neuronal cells (50 nm and 160 nm diameter). The nanoparticles were injected intravenously into mice (dose 0.25 nmol per mice), resulting in their specific interaction with transferrin receptors on brain microvascular endothelial cells (BMECs). The nanoparticles were efficiently internalized by BMECs and accumulated in intracellular vesicles. While the smaller MSNs (50 nm) demonstrated specific targeting, the larger MSNs (160 nm) showed

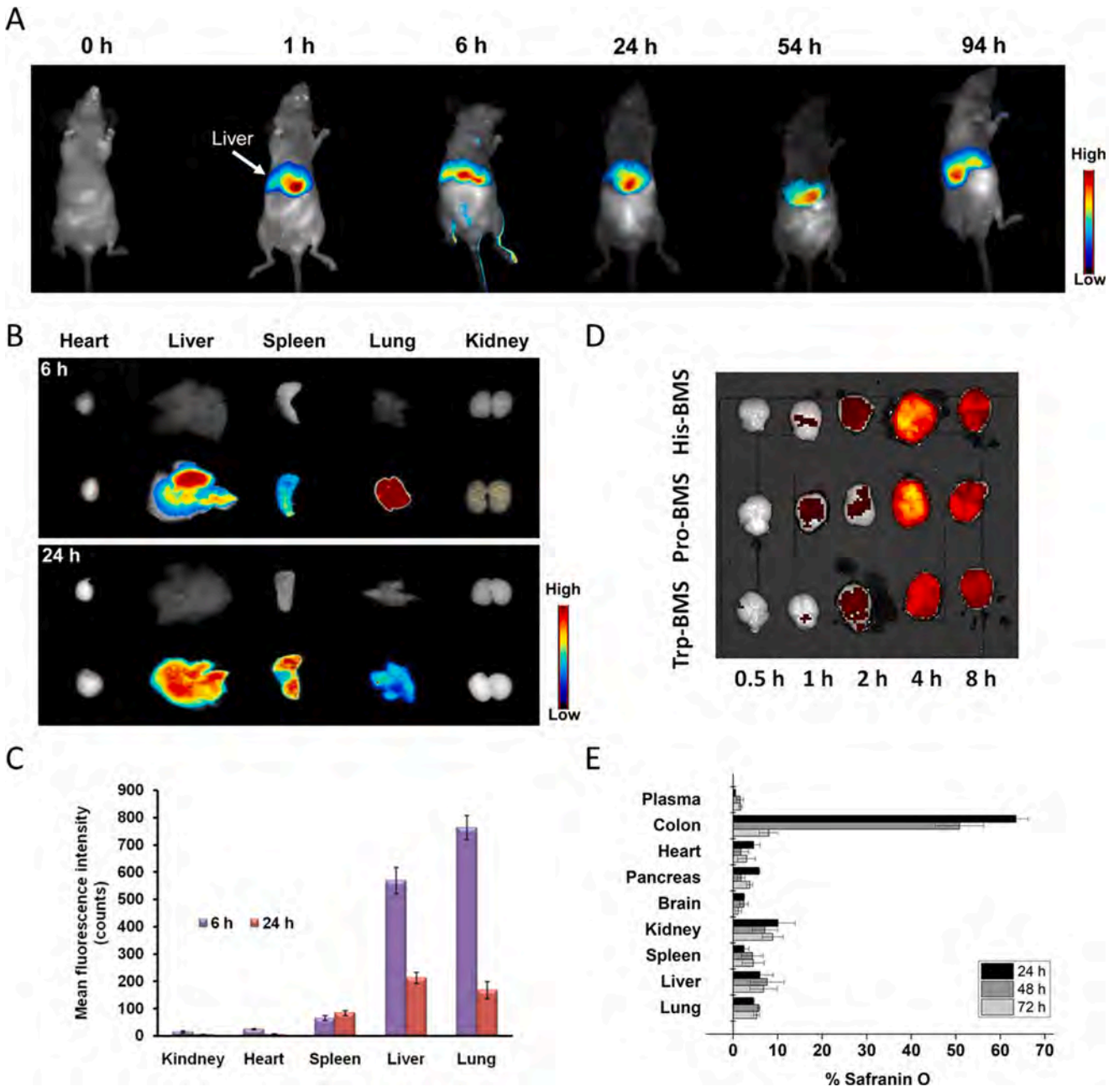

Fig. 13. Biodistribution of MSNs after intravenous and oral administration. (A) An example of intravenous administration of MSNs. MSN-dendron-Cy5.5-based nanohybrids were administrated I.V. in healthy nude mice and NIRF imaging was performed *in vivo* at different time points showing the distribution of the MSNs with the time. (B) A strong NIRF signal is observed in *ex vivo* imaging of the main organs from treated mice at 6 h and 24 h post-administration (I.V.). The first row represents the saline control group. (C) Mean fluorescence intensity of each organ at 6 and 24 h post-administration (n = 5). (D) FITC-MSNs (biomimetically synthesized using the amino acid derivatives C_{16}-l-histidine (His-BMS), C_{16}-l-proline (Pro-BMS) and C_{16}-l-tryptophan (Trp-BMS) as template via the sol–gel procedures) were intragastrically administrated in mice. At different time intervals of 0.5 h, 1 h, 2 h, 4 h and 8 h, animals were sacrificed, and the brains were rapidly collected for *ex vivo* IVIS imaging. (E) MSNs loaded with safranin O and capped with a starch derivative that hydrolyzes in the presence of the enzyme amylase were administered orally in an enteric capsule covered by Eudragit FS 30 D. Percentage of safranin O in plasma and different tissues at 24 (black), 48 (dark gray), and 72 h (light gray). Adapted with permission from Mat. Sci. and Eng.: C. 2019, 94, 453–464. Copyright © 2018 Elsevier B.V. All rights reserved. From Mol. Pharmaceutics 2017, mendeley14, 12, 4442–4453 Copyright © 2017, American Chemical Society. Form ACS Biomater. Sci. Eng. 2016, 2, 5, 860–870 Copyright © 2016, American Chemical Society.

considerable non-specific binding. However, no penetration of the nanoparticles into the brain parenchyma was observed within a one-hour timeframe. These results, show the potential of these nanoparticles for a specific interaction and internalization by BMECs due to the small size of such nano-particles and to the conjugation with Ri7 antibody.[194].

In recent approaches, the combination of liposomes with MSNs was evaluated to improve the biological/cellular interaction through BBB with the aim to improve the delivery of thymoquinone (TQ).[195] The distribution of TQ delivery in the brain areas was compared when using free TQ and TQ-loaded LB-MSNs in Wistar rats receiving an oral daily dose for 14 days (60 mg/Kg). Then the brains of the animals were

analyzed and TQ quantified by HPLC. The results exhibited that LB-MSNs successfully delivered TQ into the different brain areas as well as in the liver, and kidney. A remarkable increase in TQ delivery in the thalamus (81.74%) was observed in comparison with the free TQ group and a considerable reduction in the cortex (−44%). In contrast, LB-MSNs had no significant effect on TQ delivery in the cerebellum, striatum, liver, and kidney. These results evidence the adding effect of combine liposomes and MSNs to cross the BBB, and results in increased drug access.

Another example to improve the cross through BBB was reported by A. Popat et al using ultrasmall large-pore (USLP) silica nanoparticles. [196,197] The authors develop USLP nanoparticles of ~30 nm with a pore size greater than 7 nm with the ability to load high amounts of drugs and be coated with targeting moieties, such as Lactoferrin (Lf). The lactoferrin-coated USLP showed improved penetration into U87 tumor spheroids and enhanced the efficacy of doxorubicin-mediated apoptosis in both 2D and 3D models. Using this strategy, Kavallaris, Thurecht, Popat, and co-workers in a second study used USLP (30 nm diameter) functionalized with lactoferrin and loaded with temozolomide (TMZ) as drug carriers to enhance the permeability of the BBB and increase TMZ delivery in glioblastoma tissues. *In vivo* experiments of nanoparticle distribution were performed in healthy Balb/C mice with in real-time on live mice and on excised organs at 1, 4 and 24 h post treatment. Pegylated USLP nanoparticles and Lactoferrin-Peglyated nanoparticles labelled with a Cy5 dye were administered by intravenous injection. The results confirmed the ability of USLP to reach the brain. In addition, lactoferrin promotes the faster accumulation of the nanoparticles (1 h) compared with the pegylated nanoparticles (4 h). This effect can be attributed to the to the overexpression of lactoferrin receptors on the BBB which favors the trafficking to the tissue. The authors also demonstrated reduced efflux of TMZ, enhanced cytotoxicity against glioblastoma cells, and effective accumulation of USLP in the brain parenchyma in preclinical mouse models (doses of 10 μg/mL and 100 μg/mL).

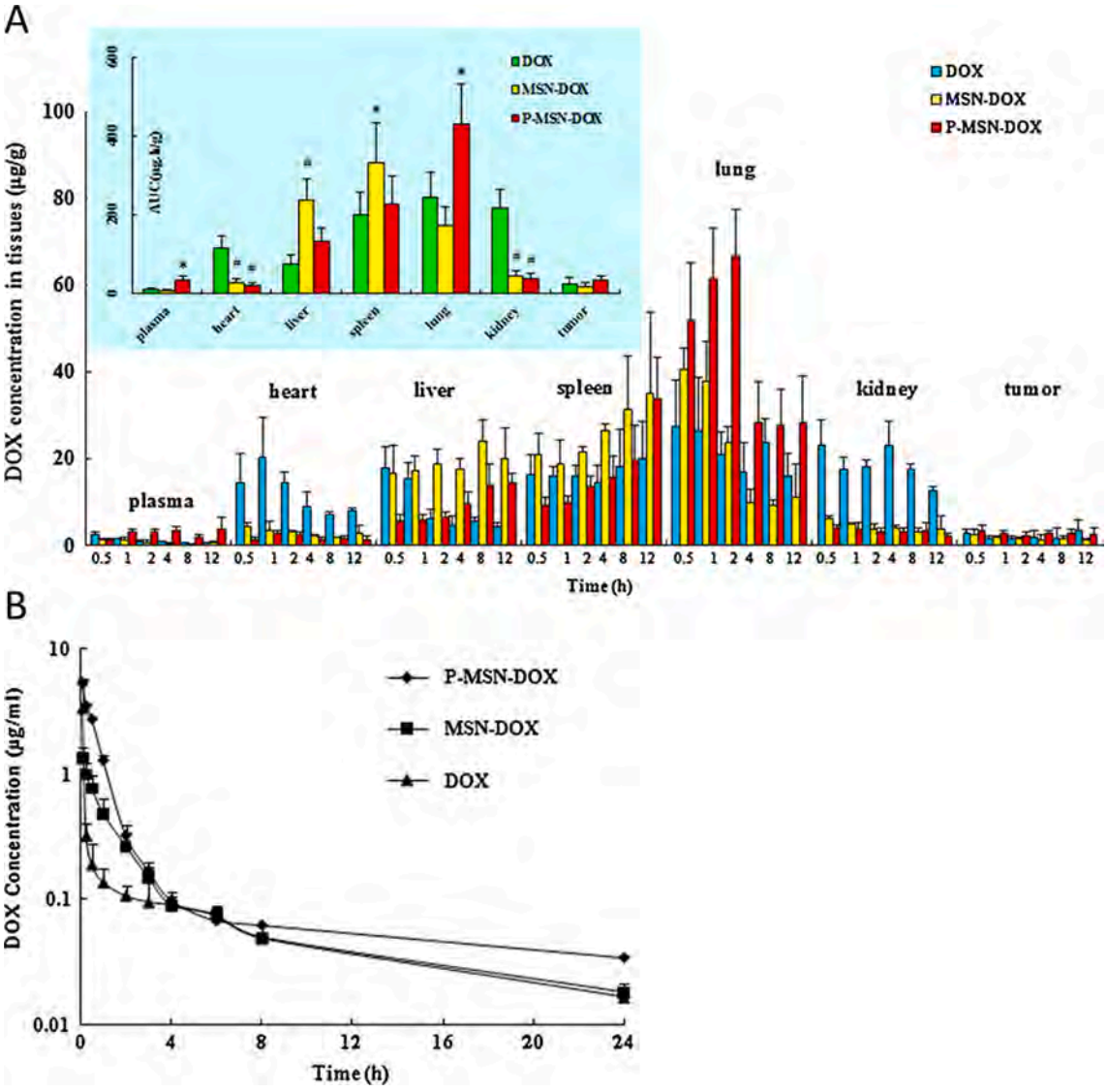

Fig. 14. Compared doxorubicin pharmacokinetic profile of free doxorubicin (DOX) vs encapsulated in MSNs. (A) MSNs loaded with DOX coated with pH-responsive poly (N-isopropylacrylamide-co-methacrylic acid (P-MSN-DOX) were I.V. administrated to SD rats and tissue distribution was analyzed ($AUC_{0\rightarrow 12h}$) ($n = 4$; $^{*}p < 0.05$, $^{\#}p < 0.01$, compared with free DOX). MSNs loaded with DOX without coating (MSN-DOX) were employed as control. (B) Plasma concentration–time curves after I.V. administration of free DOX, MSN-DOX, and P-MSN-DOX to SD rats (DOX = 5 mg/kg; n = 5). Adapted with permission from Eur J Pharm Biopharm. 2013, 85 (3A), 406–412. Copyright © 2013 Elsevier B.V. All rights reserved.

4.6. Doxorubicin pharmacokinetics profile: An example of free drug versus drug-loaded MSNs

MSNs have the unique capability to be loaded with drugs of several nature within their porous structure, being the comparison of the efficacy of the drug loaded on MSNs to that of the free drug a key factor. Drug loading capacity of MSNs (from typical mesoporous to higher pore-volume ratios) usually vary between 25% and 69% weight which highlights their efficiency as drug carriers.[198] To illustrate the concept of drug distribution and to provide a clear understanding of the drug distribution phenomenon and the general principles and implications of drug encapsulation in MSNs, we have chosen doxorubicin (DOX) as an example to show the change in distribution between free and encapsulated drug when utilizing MSNs and highlight the advantages of MSNs encapsulation improving the therapeutic profile of common drugs.

Doxorubicin (DOX) has been widely used as cargo in MSNs due to its activity as a potent antitumoral agent and its intrinsic fluorescence which serves as a valuable tool in imaging. These are the reasons why the pharmacokinetics profile of MSNs loaded with doxorubicin have been extensively studied in comparison with the pharmacokinetic profile of free doxorubicin. Chen et al.,[135] demonstrated that DOX-loaded MSNs coated with pH-responsive poly (N-isopropylacrylamide-co-methacrylic) acid (P-MSN-DOX) (190 nm diameter) circulated longer and had a slower plasma elimination rate than DOX treatment alone (intravenous dose of MSNs equivalent to 4 mg/Kg DOX) (Fig. 14). P-MSN-DOX extended half-time ($t_{1/2}$) of DOX from 0.08 ± 0.08 h (DOX) to 0.71 ± 0.21 h (P-MSN-DOX). Such increased circulation time may be attributed to DOX molecules being stabilized within the MSNs nanochannels, preventing them from leaching and being metabolized. The DOX area under the curve ($AUC_{0\rightarrow 12h}$) of P-MSN-DOX was higher in the liver and spleen and lower in the heart and kidney, compared to DOX. Feng and collaborators[199] demonstrated similar results; free DOX exhibited a biphasic and more rapid blood clearance compared with MSNs loaded with doxorubicin and functionalized with polyelectrolyte multilayers of alginate/chitosan (PEM) (DOX@PEM-MSNs) (200 nm). Free DOX has a $t_{1/2}$ of 64.8 h and an $AUC_{0\rightarrow\infty}$ of 4.9 μg·h/mL, whereas DOX@PEM-MSNs formulation displayed a relatively slow and steady DOX release than free DOX, giving a $t_{1/2}$ of 262.5 h and $AUC_{0\rightarrow\infty}$ of 27.98 μg·h/mL, which were 4.1 times longer and 5.7 times higher than free DOX, respectively.

MSN coating plays an essential role in DOX bioavailability, Feng and collaborators[200] proved that MSNs coated with polyelectrolyte multilayers (PEMs) composed of poly(allylamine hydrochloride) (PAH) and poly(styrene sulfonate) (PSS) and loaded with DOX (ca. 300 nm hydrodynamic size) showed a very slow and steady DOX release in rat plasma up to 24 h post-injection (intravenous dose of MSNs equivalent to 2 mg/Kg) in comparison with non-coated MSNs. Also, Zhou et al., [201] demonstrated that fluorescence MSNs shelled with collagen I and hyaluronic acid and loaded with doxorubicin (FMSN-Dox-C2H) presented a clearance half-time about 6.2 h which was much longer than the free drug (2.2 h).

5. Clearance

Recent preclinical research using MSNs has demonstrated their potential for diagnostic and therapeutic applications, however, the clearance of these nanoparticles from the body has still clinical concerns. [202,203]. All information described above corroborates that MSNs can be degraded and thus excreted, which indicates that MSNs do not

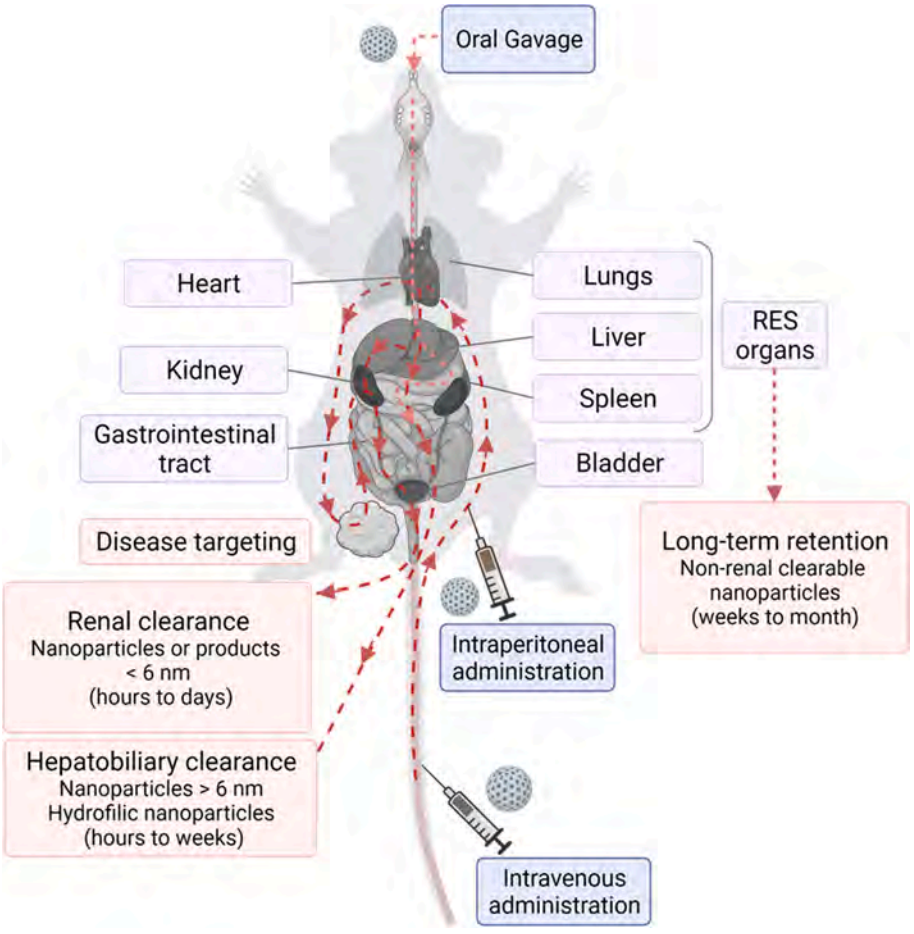

Fig. 15. Scheme of the main pathways from MSNs clearance. After intravenous, or intraperitoneal administration, MSNs circulate in the blood reaching the target tissue (such as tumors) as well as untargeted MSNs are captured by the RES. The MSNs are degraded into small fragments or products and then re-enter blood circulation before being eliminated. Products eliminated by the renal excretion reach the kidneys and are filtered and eliminated through the urine. In the case of hepatobiliary clearance, MSNs reach the liver with the subsequent processing in the biliary conduct and elimination through feces. In the case of oral gavage administration, MSNs reach the gastrointestinal tract, are degraded, and finally adsorbed to the blood and are mainly removed by hepatobiliary clearance.

accumulate in the body (Fig. 15). It has been commonly reported that renal clearance directly removes nanoparticles smaller than 6 nm from the body through the kidneys.[31] In contrast, nanoparticles larger than 6 nm circulate in the blood, reaching the target tissue, and are caught by the RES before being excreted by renal and hepatobiliary excretion. [204,205] Nanoparticles that can be degraded into small fragments or constituents, such as MSNs, are handled by the RES or in the diseased target (such as tumors) before returning to blood circulation and being cleared by the renal excretion or the hepatobiliary system. For MSNs, renal clearance is accepted as the primary excretion route, with hepatobiliary clearance coming in second.[101,205] The physicochemical characteristics of the nanoparticles, such as their charge, porosity, surface functionalization, and particle size, are crucial to this process. In this section, we describe the different studies in which MSNs clearance was evaluated.

5.1. Renal clearance of MSNs

Renal clearance is referred to the mechanism of elimination of any substance from the plasma by the kidneys being finally excreted through urinary excretion. The general process takes place at molecular level, involving the molecules crossing through the globular filtration barrier of the kidneys. In the case of MSNs, different works have described that MSN scaffold is degraded in water-soluble orthosilicic acid, which is well-tolerated by the organism, and finally excreted through the urine in the same manner that silicon sources from ingested food are excreted in the urine as silicic acid.[206,207] Sailor and co-workers demonstrated in 2009 the clear excretion of porous silicon nanostructures, close related to the silica scaffolds (126 nm diameter, intravenous dose of 20 mg/Kg).[208] The authors developed luminescent porous Si nanoparticles (LPSiNPs) (126 nm) for *in vivo* imaging monitoring. Besides, these nanomaterials were coated with a dextran polymer (D-LPSiNPs) or loaded with doxorubicin for therapeutic purposes (Dox-LPSiNPs). The degradability of the silicon scaffold in the different materials was demonstrated *in vitro* in PBS by the appearance of silicic acid. In terms of clearance, the silicon analysis by ICP-OES in different organs (spleen, kidney, brain, lung, etc) over four weeks revealed the complete elimination of the nanoparticles from the animals. These findings contrast with the clearance concerns related to nanoparticles larger than 6–8 nm [209,210] evidencing the degradation of silicon into silicic acid which is rapidly cleared by kidneys. Besides, the authors supported their findings with the histological evaluation of different organs. No significant toxicity was observed in the different organs (liver, spleen, kidneys, etc.) after nanoparticle treatment over time, however, macrophages from the liver appeared swollen after 1 day of the nanoparticle administration and then turned to the normal state. The authors suggested the proper nanoparticle uptake by macrophages with the subsequent degradation into soluble products which finally are released from the cells and eliminated by the body through urinary excretion. Therefore, this study gives evidence of the biodegradability and renal clearance of silicon nanoparticles in live animals.

Along the same lines, different works over the years have also confirmed the renal clearance of MSNs. Vivero-Escoto et al. developed pegylated MSNs with cleavable Gd(III) chelates (PEG-Gd-MSNs) (145 nm diameter, dose of 0.080 mmol/Kg of Gd via tail vein injection) for MRI *in vivo* imaging.[211] *In vivo* studies carried out in female athymic nude mice revealed the presence of Gd(III) in the urinary bladder, liver, and kidneys. The results demonstrated a faster accumulation of the MSN-based MR imaging agent in the bladder after 15 min of nanoparticle intravenous administration, which increased over time, with the subsequent renal excretion. Besides, in the work of Herance and colleagues [170] after the intravenous administration of ^{18}F positron emission isotope conjugated MSNs (^{18}F-MSiNPs) (range size 60–90 nm, intravenous dose of 0.8 MBg) a high concentration of radioactivity was observed in the urinary bladder (27 ± 7.3 %ID/g) and intestine (58.3 ± 13.2 %ID/g) after 2 h. Blood analysis also revealed that at that time, the presence of ^{18}F-MSiNPs was lower thus corroborating the trapping of nanoparticles by the reticuloendothelial system and their active excretion into the bile and urine. Lu et al. described a similar effect for their siRNA-loaded photoluminescent MSNs functionalized with PEI (PMSNs-siRNA-PEI) (ca. 245 nm diameter, intravenous dose of 25 mg/Kg).[212] In this case, an acute myocardial infarction (AMI) mouse model was established and nanoparticles were administered intravenously. Dynamic near-infrared fluorescence imaging over 24 h revealed the rapid accumulation of the nanoparticles in the spleen. Finally, the loss of photoluminescence evidenced the removal of the particles by hepatobiliary and renal clearance because of MSNs degradation.

Tamanoi and co-workers described folate-conjugated MSNs (FMSN) (100–130 nm diameter, intraperitoneal doses ranging from 0.125 mg to 0.5 mg per mouse) loaded with camptothecin (CPT).[213] In this case, the biocompatibility and excretion of MSNs were determined by quantifying the Si content in the urine in BALB/c mice. MSNs and FMSN were intraperitoneally (i.p.) injected and urine and feces were collected and mixed at different time points. A cumulative amount of Si was detected in the samples over time for a week, suggesting the proper MSNs excretion. Surprisingly, the analysis of TEM images from urine samples showed intact MSNs, which correlated with the Si detected in the urine. These results can be explained through MSNs causing some dysfunction of biliary excretion and glomerular filtration process; however, these findings are still controversial.[30,214].

5.1.1. Evaluation of clearance in tumoral models

Overall, the results demonstrated the suitability of MSNs as imaging and drug delivery systems in terms of biocompatibility and clearance. However, most of the systems described above were evaluated in healthy mice, and considering that MSNs are mainly used for therapy, mainly cancer therapy, some studies have also focused on studying MSNs clearance in tumoral models.[34] Moreover, it has been widely described the passive accumulation of nanoparticles in tumors as well as the presence of high ROS levels in tumors,[215,216] is an important issue to consider for nanoparticle degradation and thus clearance.

Recent studies using MSNs systems for therapeutic purposes have already started to evaluate the clearance of MSNs in tumor-bearing mice models. Yang et al. developed a 50 nm sized hyperbranched polyglycerol (PG) doped MSNs (PGSNs) for cancer therapy.[110] After intravenous administration of Cy7-labeled PGSN (dose 200 μL of 2.5 mg/mL) in a breast cancer tumor-bearing mice model, the nanoparticles were clearly observed on the tumor after 32 h. Then, the associated fluorescence signal from the PGSNs disappeared from the body gradually after 56 h post-injection, due to nanoparticles' clearance, attributed to MSNs degradation into smaller sizes which were small enough for renal elimination (<5.5 nm) (Fig. 16).

In the same line, Yu and co-workers described a "metal ion-doping" hollow mesoporous silica nanoparticles functionalized with PEG (PEG/Mn-HMSNs, 60–70 nm diameter.) with tumor-sensitive biodegradation which is finally excreted by the urine.[111] *In vivo* biodistribution and excretion were evaluated after intravenous administration of PEG/Mn-HMSNs (intravenous doses of 5, 10 and 20 mg/Kg), compared to conventional MSNs, in hepatoma tumor-bearing mice. The results of Mn and Si content in the different organs, urine, and feces revealed a rapid excretion of PEG/Mn-HMSNs compared to conventional MSNs. A higher Si content attributed to PEG/Mn-HMSNs was observed in the urine after 48 h, thus confirming the proper renal clearance. The rapid clearance of PEG/Mn-HMSNs was attributed to their easy disintegration in the mild acidic and reducing microenvironment of the tumor which improves drug release as well as renal excretion.

A similar result was observed by Wei and co-workers, which prepared a renal clearable nanoparticle for multi-modal imaging and combined chemo-photothermal cancer therapy.[143] MSNs (100 nm diameter) were loaded with doxorubicin and Cu nanodots (CuSNDs) ([^{64}Cu]MDNs, 6 nm diameter) and were used for photoacoustic and PET imaging to evaluate the dynamic process of nanoparticles after

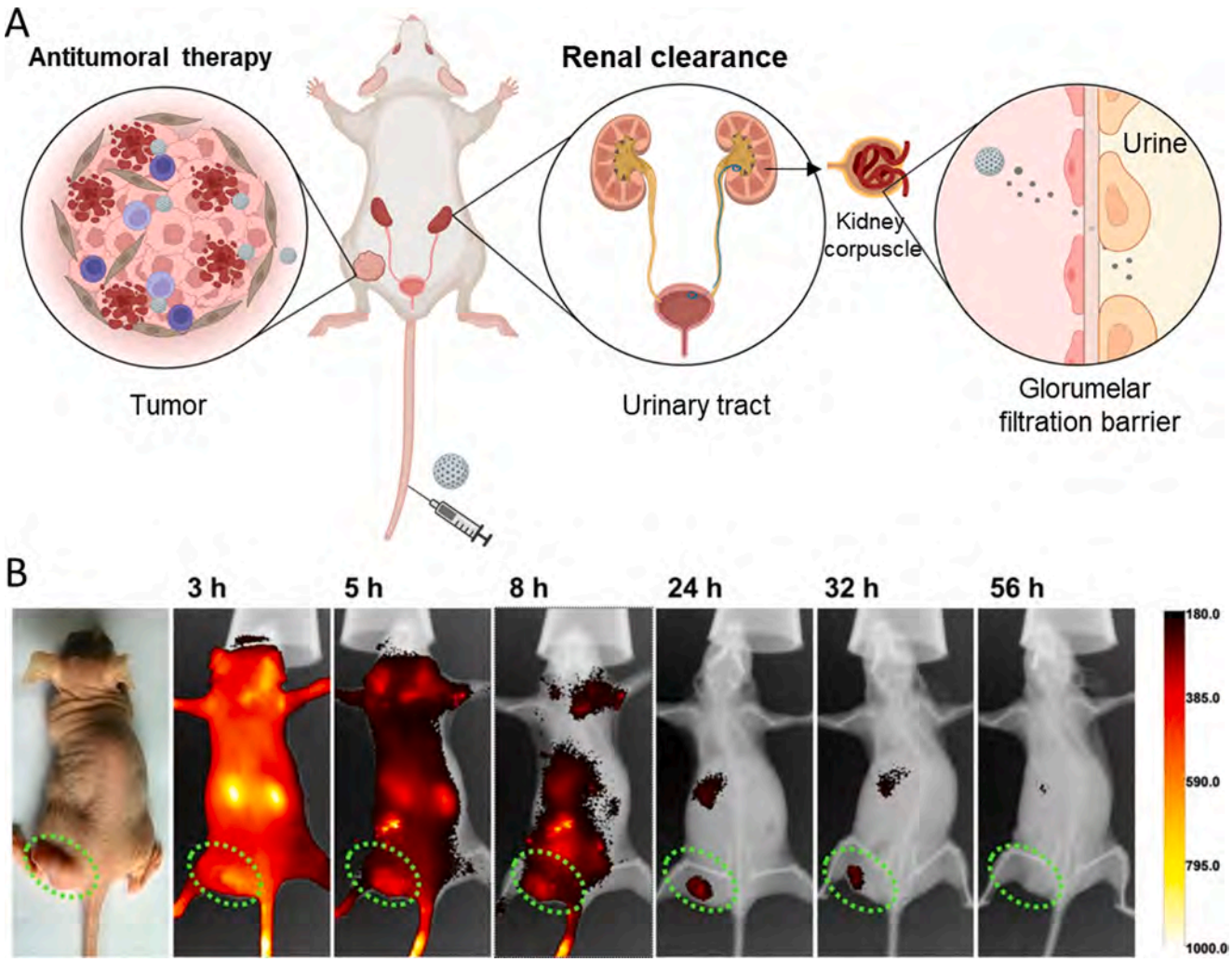

Fig. 16. Clearance of MSNs applied for tumor therapy. A) Representation of biodistribution and clearance of MSNs applied for tumor therapy after intravenous injection. After reaching the tumor MSNs are degraded and removed from the body through renal clearance. The glomerular filtration to the urine takes place in the kidneys at the nanoscale for products < 6 nm. B) *In vivo* real-time images of Cy7-labeled PGSN biodistribution from 3 to 56 h after intravenous injection. Near-infrared fluorescence and X-ray spectra merge images. The PGSNs reach breast cancer tumors as well as the urinary tract after a few hours (3–8 h) of administration. After longer times (ca. 1–3 days), the associated fluorescence-PGSNs signal disappeared from the body, ascribed to renal excretion of the nanomaterial. Reprinted with permission from ChemistryOpen. 2016, 6, 158–164.© 2016 Wiley-VCH Verlag GmbH & Co. KGaA.

intravenous administration in MDA-MB-231 tumor-bearing mice (dose 0.074 MBg per mouse). A significant accumulation of MDNs in the tumor after 1 h of I.V. administration was observed, reaching the highest level after 24 h post-injection. Besides, strong signals were found in the liver and spleen, and after 4 h of injection, a significant signal was registered in the bladder, suggesting that nanoparticles were excreted by the renal-urinary system. Besides, the nanoparticles' fate was deeply studied in Swiss mice. For this purpose, Si and Cu were measured in different organs by inductively coupled plasma mass spectrometry (ICP-MS). High levels of Cu and Si were found in the liver and spleen after 4 h post-injection. Besides, high amounts of Cu were found in the kidney after 4 h compared with lower Si residues in the kidneys. Urine samples analyzed by TEM and UV–vis-NIR spectroscopy confirmed the presence of ultrasmall CuSNDs after 4 h post-injection. These results suggested a rapid clearance by the renal-urinary system of CuSNDs whereas MSNs degraded slower. Si and Cu signals decreased in the RES organs after 14 d and finally disappeared after 30 d thus suggesting the complete metabolization of the nanoparticles.

5.1.2. Effect of the physicochemical properties in renal clearance

Regarding the effect of the physicochemical properties of the nanoparticles in the process of clearance, just a few studies explored the effect of size, shape, and surface properties of MSNs. Shi and co-workers studied the effect of particle size and PEGylation in the biodistribution and urinary excretion in ICR mice or Sprague–Dawley rats over different periods of up to 1 month.[159] For this purpose, FITC-MSNs of different sizes (80, 120, 200, and 360 nm) were prepared and PEGylated or not in each case. The authors observed a preferential accumulation of nanoparticles in the liver and spleen, which increased in a size-dependent manner. After only 30 min of nanoparticle administration (intravenous dose 5 μL/g at concentration 4 mg/mL), a noticeable number of silica degradation products were observed in urine, reaching the highest value of urinary excretion for larger MSNs or PEG-MSNs (360 nm). This different size-dependent kinetics of elimination can be explained by the rapid capture of larger MSNs by RES organs, which led to faster biodegradation and thus excretion. On the other hand, PEGylated MSNs showed a slower degradation and excretion rate, which can be attributed to the enhanced blood-circulation lifetime of these materials.

Besides, Huang et al. prepared long-rod FITC-MSNs (NLR) and short-

rod FITC-MSNs (NSR), functionalized or not with PEG (185 nm short-rod nanoparticles and 760 nm long-rods nanoparticles), and evaluated their effect in ICR mice after intravenous administration (dose 20 mg/Kg). [161] While fluorescence imaging revealed a higher accumulation of nanoparticles in the main organs (liver, spleen, and lung) after 2 h after injection, fluorescence decreased after 7 days of administration suggesting the biodegradation and excretion of silica particles from the body. To study the excretion mechanism of nanoparticles Si content was measured in blood, organs, urine, and feces. The Si content decreased over time, indicating the proper clearance of nanoparticles from the main organs. In fact, after 2 h post-injection, Si was observed in the urine for different materials, reaching a higher rate for NSR compared to NLR. Finally, after 7 days the Si content in urine was decreased to negligible levels for all the nanoparticles. In contrast, at 7 d post-injection, a clear feces excretion mechanism was observed, being again the highest Si content attributed to NSR nanoparticles. These results evidence the implication of both renal and hepatobiliary routes for nanoparticle elimination. In this case, a rapid renal clearance occurred followed by hepatic and biliary excretion, which is relatively slower compared to renal clearance. Despite the presence of intact nanoparticles in urine and fecal samples are still not understood, the authors observed by TEM analysis intact NSR and NLR in urine and feces. Regarding PEGylation, a remarkable decrease in the nanoparticle clearance rate was observed regardless of nanoparticle shape. Overall, these findings exhibited that nanoparticle shape and surface modification influence organ accumulation and retention which finally determine the clearance process.

The structure–activity relationships (SAR) of mesoporous silica nanoparticles *in vivo* for further preclinical development and clinical translation were also studied by Dogra and co-workers.[160] For this purpose, ^{111}In-labeled MSNs of 50 nm were prepared and functionalized

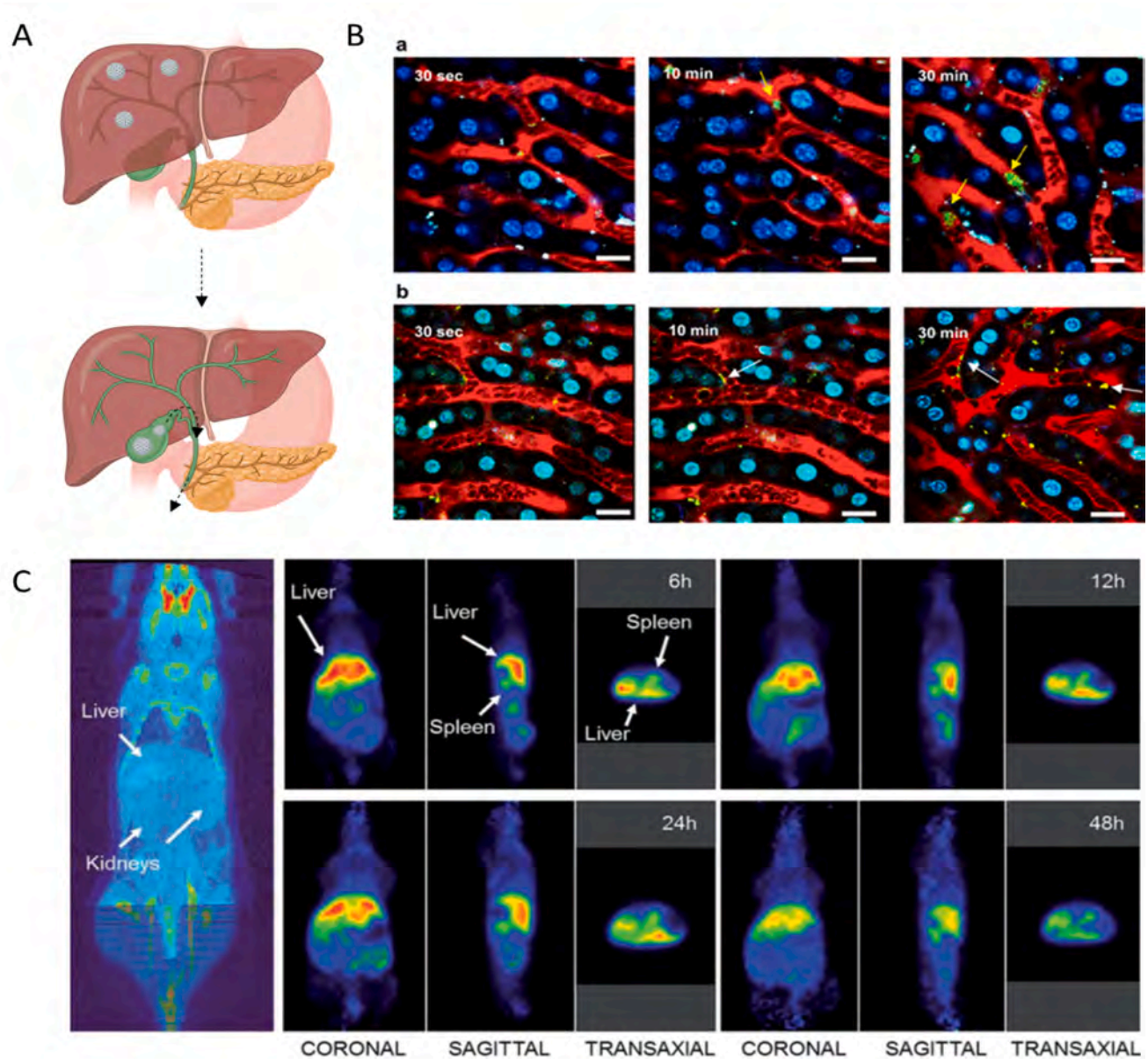

Fig. 17. MSNs can be excreted through the hepatobiliary system. A) Representation of MSNs trafficking undergoing hepatobiliary clearance. MSNs reach the liver and after some hours migrated into the biliary duct. B) Real-time hepatic visualization of negatively and positively charged FITC-labeled MSNs at different periods of postinjection time. Red: rhodamine/dextran R6G (MW 70 000) staining of sinusoids. Green: fluorescence of FITC-MSNs. Blue: hepatocyte nuclei labeled with Hoechst 33342. Reprinted with permission from ACS Nano 2012, 6, 4122–4131 © 2016 American Chemical Society. C) PET images of mice injected with at time points identifying the accumulation of nanoparticles in the liver and spleen, while no evidence of signal was found in the kidneys. Reprinted with permission from J. Mater. Chem. B, 2015,3, 748–758 © 2015 Royal Society of Chemistry Society.

with PEG-polyethyleneimine (PEG-PEI), PEG-quaternary amine (PEG-QA) and PEG-trimethyl silane (PEG-TMS), respectively. Besides, PEG-TMS were also synthesized at different sizes of 25, 90, and 150 nm. PEG-TMS MSNs presented neutrally charge (-4 to −7 mV) and PEG-PEI and PEG-QA modified MSNs showed strong positive charges (+37 and + 38 mV, respectively). The effect of MSN size and route of administration was evaluated using PEG-TMS MSNs of different sizes (25, 50, 90, and 150 nm) by intravenous or intraperitoneal injection in healthy rats (MSNs administered at a dose of 1 mg of nanoparticles suspended in 200 μL to each rat intravenous or intraperitoneal). Finally, the influence of surface chemistry was evaluated using PEG-QA MSNs and PEG-PEI MSNs of 50 nm. In all cases, MSNs conjugated with the radioactive ^{111}In were monitored by SPECT/CT imaging in rats over 24 h. In all cases, a primary mechanism of renal excretion was observed. The results showed that the size or route of administration did not affect the excretion; a signal profile for all the MSNs after i.v. or i.p injection was observed in the kidneys only after 30 min followed by a significant radioactivity pattern in the urinary bladder. In contrast, the surface chemistry of MSNs played an important role in the kinetics excretion, being faster the renal clearance of PEG-QA nanoparticles that are strongly positive with the presence of quaternary ammonium salts, which is mainly attributed to the lower sequestration by the liver compared to PEG-TMS and PEG-PEI MSNs. The authors conclude that small TMS-alkylated MSNs (32 nm diameter) and QA-aminated MSNs (56 nm diameter) were suitable for therapeutic applications in which higher bioavailability is needed, being neutral MSNs a better choice for developing antitumoral drug delivery systems compared to positively charged nanoparticles which are more rapidly removed from the circulation.

5.2. Hepatobiliary clearance of MSNs

The hepatobiliary system is established as the second route for nanoparticle excretion.[31,204] Foreign substances and particles are processed in the liver by specialized phagocytic cells and finally processed in the intestines, being this route more complex and slower than renal clearance (Fig. 17A). Hepatocytes catabolize the substances eliminated by the bile and Kupffer cells, included in the RES, and degrade particles and substances intracellularly by enzymatic processes.[217].

Taking into account these premises, Chen et al. used intravital multiphoton imaging to monitor in real-time the hepatic metabolism, at subcellular resolution, of MSNs.[218] For this purpose, MSNs were prepared and labeled with FITC. Then, MSNs' (ca. 100 nm diameter) surface was modified with different amounts of 3-aminopropyltrimethoxysilane (APTMS) (referred as 1X and 3X) giving unmodified FITC-MSNs, FITC-MSN-1X and FITC-MSNs-3X. The surface charge of different FITC-MSNs was characterized by zeta potential corresponding to negative, moderately positive, and highly positive for FITC-MSNs, FITC-MSN-1X, and FITC-MSN-3X, respectively. In the first step, the cellular uptake efficiency was assessed for each material in HepG2 cells by flow cytometry assays. The results showed low uptake when negatively charged FITC-MSNs were used while higher uptake was achieved using FITC-MSN-1X and FITC-MSN-3X. Then, a hepatic imaging window was installed on the upper abdomen of C57BL/6 mice for liver surface area image acquisition through multiphoton microscopy. The different FITC-MSNs were administered through the right jugular vein (dose 16 mg/Kg) and rhodamine B isothiocyanate/dextran 70,000 and Hoechst 33,342 were also administered to label blood vessels and cell nuclei. The results showed a significant uptake of positively charged MSNs by hepatocytes, confirming the possible clearance via hepatobiliary excretion. In contrast, negatively charged MSNs were mainly accumulated in Kupffer cells in liver sinusoids which could result in significant hepatoxicity (Fig. 17B). TEM analysis of excised tissues confirmed the presence of FITC-MSN-1X and FITC-MSN-3X in hepatocytes as well as the presence of negatively charged FITC-MSNs in Kupffer cells. The authors demonstrated that the intravital multiphoton imagen technique can be useful to elucidate hepatotoxicity and clearance of MSNs in further *in vivo* applications.

Hepatobiliary clearance was also observed in other works. Guo et al. prepared MSNs of 60 nm diameter, labeled with Cy5.5 fluorophore and functionalized with peptide dendrons for achieving enhanced biocompatibility.[169] After *in vivo* biodistribution analysis of nanoparticles in BALB/c mice (dose 20 mg/Kg via tail vein injection) and *ex vivo* analysis of different organs, the authors observed a clear fluorescence signal of the nanoparticles in the liver, which remained strongly up to 4 days post-injection, thus indicating a hepatobiliary excretion process for nanoparticle elimination. Goel and co-workers also developed biodegradable dendritic MSNs (bMSNs) (160 nm diameter), radiolabeled with oxophilic zirconium-89, for targeting CD105 tumor vasculature in breast cancer models.[156] Despite the preferential accumulation of the nanoparticles into the target site after intravenous administration (dose 50 mg/Kg) in 4 T1 breast cancer tumor-bearing mice, some nanoparticles accumulated in non-target organs such as the liver and spleen. The presence of radioactivity up to day 3 post-injection in the liver suggested the elimination of bMSNs by the hepatobiliary route. Li et al. also suggested a hepatobiliary excretion mechanism for the elimination of folic acid (FA) conjugated biodegradable MSNs (100–130 nm diameter, tail vein injection of 200 μL, no concentration of MSNs was reported), based on the presence of fluorescence signals in the liver in a pancreatic tumor mice model.[219].

Laprise-Pelletier and co-workers observed a significant quantity of MSNs in the gastrointestinal system after intravenous administration in BALB/c mice (dose of 0.31 μmol Gd, kept at a low level at 12.4 μmol/kg), suggesting elimination by the hepatobiliary system.[166] The authors prepared metal chelate MSNs, based on MCM-48 nanospheres (150 nm) functionalized with diethylenetriaminepentaacetic acid (DTPA) and labeled with paramagnetic ions Gd^{3+} (for MRI) as well as radioactive ions $^{64}Cu^{2+}$ (for PET) (Gd^{3+}/$^{64}Cu^{2+}$-DTPA-M48SNs) for biomedical imaging. PET and MRI scans as well as *ex vivo* biodistribution studies showed a clear accumulation of nanoparticles in the liver and spleen. In addition, some MSNs, were found in the gastrointestinal tract. After 48 h higher levels of Gd^{3+}/$^{64}Cu^{2+}$-DTPA-M48SNs were found in the liver (30,1% ID) and intestine (18.1%) whereas a lower presence of nanoparticles was observed in the blood, spleen, lungs, heart, etc (Fig. 17C). Similar results were observed by Souries et al. who examined the hepatobiliary clearance of positive and negative MSNs (50–100 nm diameter, dose by tail-vein bolus injections of 12, 24, or 30 mg/kg).[220] The authors prepared two indocyanine green (ICG)-loaded MSNs, one amino-modified (MSN-NH_2-ICG) with a positive zeta potential and the other trimethylammonium-modified (MSN-TA-ICG) with a negatively zeta potential. Fluorescence imaging *in vivo* and *ex vivo* revealed a quick elimination of positively charged nanoparticles through feces, while negatively charged nanoparticles showed an increased residence time in the body. Then, the biodistribution and clearance of MSN-NH_2-ICG were studied in more detail. After ten minutes of I.V. injection, positively charged nanoparticles reach the liver and migrated to the duodenum in 60 min through the biliary duct. After 4 h, a negligible fluorescence signal was observed in the liver whereas the majority of MSNs accumulate in the gastrointestinal tract. Besides, Si content and TEM images confirmed the liver and gastrointestinal biodistribution of MSN-NH_2-ICG nanoparticles, which are finally removed through feces after 3 days.

In a very complete work, Wang and co-workers described the hepatobiliary elimination for different shaped fluorescent mesoporous silica nanomaterials administered by oral gavage in Kunming mice and Sprague-Dawley (SD) rats.[176] The authors prepared Cy5.5 labeled long rod nanoparticles (NLR) (aspect ratio 4), short rod nanoparticles (NSR) (aspect ratio 2), and spherical nanoparticles (NS) (aspect ratio 1) with the same size distribution (150 nm diameter) All the nanoparticles were administered orally at a dose of 80 mg/kg. The results showed a longer residence time in the gastrointestinal tract for rod nanoparticles compared to spherical MSNs in mice, being spherical MSNs rapidly

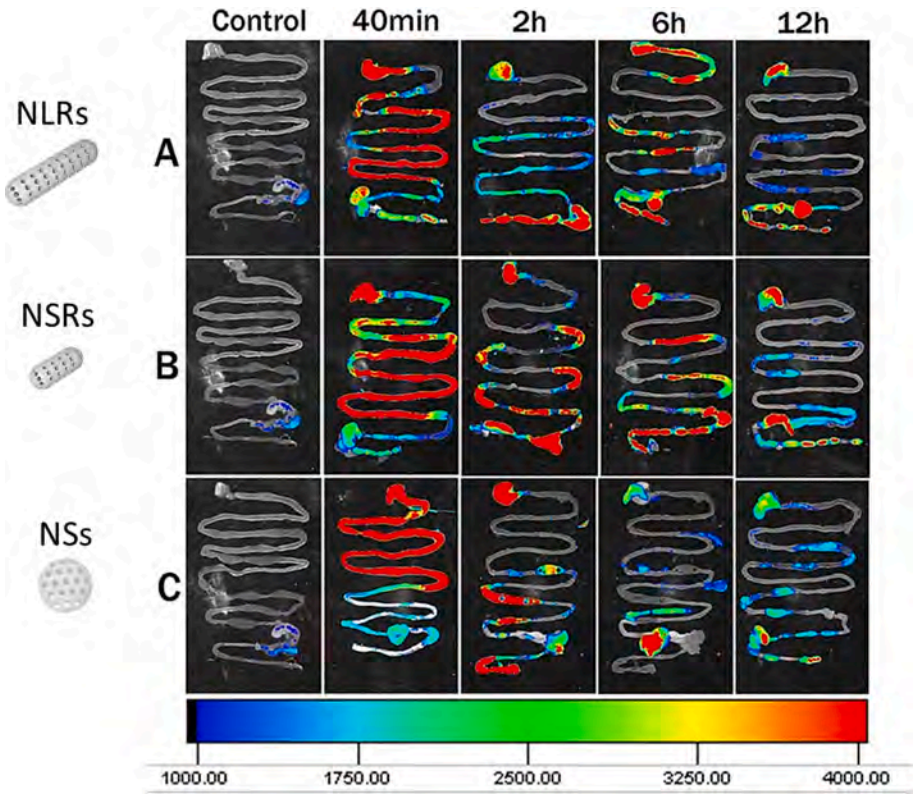

Fig. 18. MSNs removal from the body after oral administration. Gastrointestinal tract of Kunming mice at different points after oral administration of three different mesoporous silica-based nanomaterials: A) Long nanorods (NLR); Short nanorods (NSR) and C) Nanospheres (NS). The *ex vivo* images confirmed the processing of the nanoparticles in the intestines being the nanospheres more rapidly eliminated, compared to long rods, through feces. Reprinted with permission from Adv. Funct. Mater. 2017, 28, 1,704,634.© 2017 Wiley-VCH Verlag GmbH & Co. KGaA Weinheim.

excreted through feces (Fig. 18). Si content analysis of the different organs revealed a preferential accumulation of Si residues, from degraded nanoparticles in the gastrointestinal tract, in the liver and kidney after oral administration. Again, long rod nanoparticles showed the slowest clearance rate, with remaining higher content of Si in all the organs over 7 days. After 7 days, the Si content was reduced in all the organs thus confirming the proper elimination of the nanomaterials from the body. The excretion was studied in more detail by analyzing Si content in feces and urine. In general, the larger Si content was found in the feces, although some Si content from spherical MSNs was also found in the urine. The results evidenced a preferential hepatobiliary mechanism of elimination with a slow rate of clearance taking into account that after 7 days of oral administration a significant Si content was still found in the feces for all the MSNs. This slower elimination could be explained by the reabsorption processes of nanoparticles. After being processed in the gastrointestinal tract, Si nanoparticle residues can be captured by the liver and finally processed thus resulting in higher retention times and thus elimination.

6. Silica nanoparticles in clinical trials

This section includes the description of clinical trials of MSNs but also of silica nanoparticles (which are not porous). There are more clinical trials using silica nanoparticles (not porous) than MSNs. Solid silica nanoparticles are included in this section with the aim to inspire future clinical trial applications in which the particular properties of MSNs could additionally be taken into account. Due to their compatibility and low toxicity, silicon dioxides have been classified as "Generally Recognized as Safe" (GRAS, ID Code: 14808–60-7) for use in cosmetics and food additives by the US Food and Drug Administration (FDA). As a result, silica nanoparticles have been studied in clinical trials for biomedical applications (drug delivery, diagnosis, and therapy). [221] In fact, in the last several years, the number of approved inorganic nanoparticles for therapeutic application has increased. [222] MSNs, in particular, are likely to be important drug transporters in theragnostic applications due to their versatility. Nevertheless, to date, only one study has been conducted using MSN as a proof of concept in humans. [223] In this investigation, 12 healthy men volunteers were given fenofibrate acid orally to compare the bioavailability of the drug loaded onto MSNs to that of the commercially available formulation Lipanthyl. Results demonstrated well tolerance and enhanced bioavailability of fenofibrate when compared to the marketed product. Moreover, in two different human studies, the oral administration of ibuprofen or simvastatin (**ACTRN12618001929291**), in a silica-lipid hybrid (Lipoceramic) formulation, improved the pharmacokinetic when compared to the commercial formulation. [224,225] These findings show that silica nanoparticles improve the pharmacokinetic profile of hydrophobic drugs while also being well-tolerated and having no side effects after oral administration in healthy men. The clinical trials cited in this section are summarized in Table 1.

The initial application of silica-based nanoparticles in the context of clinical therapy was for the treatment of cardiovascular disorders. [226,227] The first clinical research began in 2007 to treat atherosclerotic lesions using plasmonic photothermal therapy. (**NANO-FIM; NCT01270139**). In this study, patients were assigned to receive either nano-intervention with silica–gold nanoparticles in a bioengineered on-artery patch, or nano-intervention with the delivery of silica–gold iron-bearing nanoparticles with targeted micro-bubbles and stem cells using a magnetic navigation system versus stent implantation. Nano-intervention resulted in a considerable regression in coronary atherosclerosis by eliminating atherosclerosis plaque and modifying the arteries. [226] The NANO-FIM trial's long-term results were reported in 2017, and the patients who underwent treatment with silica-gold nanoparticles showed no signs of cytotoxicity or clinical problems. Furthermore, the NANO-FIM trial showed superior safety, with lower rates of mortality, and target lesion revascularization over time, when compared to the stent. [227] Also, in 2010 these researchers generated CD68-targeted microbubbles using silica-gold iron nanoparticles, to target macrophages in atherosclerotic plaques (NANOM PCI; NCT01436123). In this instance, a micro-bubble responsive patch was

Table 1
Silica nanoparticles on clinical trials (Database).

Responsably party	Nanoparticle type	Payload	ClinicalTrials.gov identifiers	Clinical indication	Primary purpose	Title	Start date	Enrollment	Stage
Alexander Kharlamov (Ural State Medical University)	Silica-gold NP/ Silica–gold iron-bearing NP	Plasmonic Nanophotothermal Therapy/and Stem Cell Therapy	NCT01270139	Atherosclerosis, Multivessel Coronary Artery Disease, Stable Angina, Heart Failure	Treatment	Plasmonic Nanophotothermal Therapy of Atherosclerosis (NANOM-FIM)	2007	180 participants	Completed (2016)
			NCT01436123	Atherosclerosis, Coronary Artery Disease	Treatment	Plasmonic Photothermal and Stem Cell Therapy of Atherosclerosis Versus Stenting (NANOM PCI)	2010	62 participants	Terminated (2012)
AuroLase (Nanospectra Biosciences)	PEGylated silica-gold nanoshells	Thermal ablation from near infrared light stimulation	NCT00848042	Head and Neck Cancer	Treatment	Pilot Study of AuroLase(tm) Therapy in Refractory and/or Recurrent Tumors of the Head and Neck	2008	11 participants	Completed (2014)
			NCT02680535	Neoplasms of the Prostate	Treatment	MRI/US Fusion Imaging and Biopsy in Combination With Nanoparticle Directed Focal Therapy for Ablation of Prostate Tissue	2016	45 participants	Completed (2020)
			NCT04240639	Neoplasms of the Prostate	Treatment	An Extension Study MRI/US Fusion Imaging and Biopsy in Combination With Nanoparticle Directed Focal Therapy for Ablation of Prostate Tissue	2020	60 participants	Recruiting (expected, 2023)
			NCT04656678	Prostate Cancer, Prostate Disease	Treatment	An Extension Study MRI/US Fusion Imaging and Biopsy in Combination With Nanoparticle Directed Focal Therapy for Ablation of Prostate Tissue	2020	45 participants	Recruiting (expected, 2023)
Cornell Dots (Memorial Sloan Kettering Cancer Center)	Silica nanoparticles with a NIR fluorophore, PEG coating, and a cRGDY targeting peptide (cRGDY-PEG-C-dots)	NIR fluorophore	NCT01266096	Melanoma and malignant brain tumors: PET scan with 124I-cRGDY-PEG-dots	Diagnostic	PET Imaging of Patients With Melanoma and Malignant Brain Tumors Using an 124I-labeled cRGDY Silica Nanomolecular Particle Tracer: A Microdosing Study	2010	10 participants	Active, not recruiting (expected, 2023)
			NCT02106598	Head and Neck Melanoma	Diagnostic	Targeted Silica Nanoparticles for Real-Time Image-Guided Intraoperative Mapping of Nodal Metastases	2014	86 participants	Recruiting (expected, 2023)
			NCT03465618	Brain Cancer, Pituitary Adenoma: PET scan with 89Zr-DFO-cRGDY-PEG-Cy5-C' dots	Diagnostic	A First in Human Study Using 89Zr-cRGDY Ultrasmall Silica Particle Tracers for Malignant Brain Tumors	2018	10 participants	Recruiting (expected, 2023)
			NCT04167969	Prostate Cancer: PET/MR with 64Cu-NOTA-PSMAi-PEG-Cy5.5-C' dots	Diagnostic	The Use of Nanoparticles to Guide the Surgical Treatment of Prostate Cancer	2019	10 participants	Recruiting (expected, 2023)

Source: ClinicalTrial.gov

destroyed by ultrasounds in order to release the nanoparticles, which were then guided to the target by a magnetic field. The trial was abandoned, though, after toxicity was found in the patients who received the nanoparticle treatment.

A different approach including "Cornell dots" (C-dots) was approved by the FDA in 2012 for their use in the first phase of clinical trials. C-dots are ultrasmall inorganic silica nanoparticles (6–10 nm of diameter) conceived as a fluorescence imaging method for sentinel lymph node detection prior to cancer surgery. [228] To date, the C-dots have been applied in patients with metastatic melanoma, malignant brain tumors, and head and neck melanoma (NCT01266096, NCT02106598, and NCT03465618). The internal silica core of these nanoparticles (cRGDY-PEG-Cy5.5-C dots) is labeled with the Cy5.5 fluorescence dye and coated with a PEG polymer and a tumor cell targeting peptide (cyclic arginine–glycine–aspartic acid peptide; cRGDY).[229] The nanoparticles labeled with ^{124}I were applied for positron emission tomography imaging and fluorescent-based detection for the diagnosis of melanoma and malignant brain tumors (NCT01266096). A different phase II study, (NCT02106598), is being carried out in a total of 86 patients with head and neck melanoma[229] and another one (NCT03465618) includes ^{89}Zr radiolabeled C-dots for PET imaging of malignant brain tumors. The results for these three clinical trials are expected to be published by 2023. However, no hazardous or adverse effects attributed to the particles have been documented yet, suggesting that these nanoparticles are safe for use in human cancer diagnostics. Worth noting that, due to their small size, Cornell dots can be rapidly cleared by the kidneys, which alleviates concerns about silica nanoparticle bioaccumulation.[230] The most recent clinical trials based on this strategy consist in using ^{64}Cu-NOTA-PSMA-PEG-Cy5.5-C dots to identify tumor cells before and during prostate cancer surgery (NCT04167969). The nanoparticles are based on ultrasmall silica scaffold, used to encapsulate the Cy5.5-C dots as a tracer, covered with a protective PEG, the PSMA peptide as active targeting to prostate cancer and a radionuclide chelator, NOTA, for ^{64}Cu-radiolabeling. The overall goal is to investigate if PET/MRI scans performed after injecting the nanoparticles are more accurate than standard imaging scans for locating prostate tumor cell deposits.

Besides, different studies using PEGylated gold–silica nanoshells are in clinical trials conducted by the company AuroLase (Nanospectra Biosciences) for the treatment of prostate cancer, and head and neck cancer (NCT00848042, NCT02680535, NCT04240639, and NCT04656678).[231] After intravenous injection, the AuroShell particles preferentially accumulate in the tumor via the EPR effect, and the thermal ablation of the malignant tumor is carried out using near-infrared stimulation. The estimated completion date for this clinical trial was recently updated to November 2023 but preliminary findings in 16 patients demonstrate that laser excitation of gold–silica nanoshells is a technically feasible and safe procedure for the targeted removal of prostate tumors without significant complications or abnormalities in genitourinary function.[231].

Although the number of probes translated into human clinical trials is still very few, the clinical trials carried out so far in solid silica nanoparticles have indicated that silica is safe for humans and improves therapeutic efficacy. Regarding the scope of this review, these findings could imply that MSNs have a large potential in the clinic due to their additional unique characteristics (good biocompatibility, tunable particle and pore size, high loading capacity, tunable surface using standard chemical reactions, etc.) when compared with non-porous silica nanoparticles. With these promising results, clinical translation of silica nanoparticles is expected to increase in the next years and MSN may open new avenues for nanomedicine. Nevertheless, future studies should focus on critical aspects such as chronic exposure safety and long-term toxicological profiles from different routes of administration. In addition, a greater understanding of the manufacturing process is required, including scaling issues, reproducibility, and cost-effectiveness.

7. Outlook and future perspectives

Today the applications of silica nanoparticles have revolutionized the diagnosis and disease therapy field. Remarkably, mesoporous silica nanoparticles (MSNs) have effectively improved drug stability and solved low drug solubility problems. Furthermore, MSNs enable the controlled release of the cargo which reduces undesirable side effects of free drugs. Compared to other inorganic drug delivery systems, MSNs may have a greater potential for future clinical translation due to their well-established and simple surface modification chemistry, demonstrated tumor-targeted, drug delivery capabilities, and potential to reduce long-term RES accumulation issues. However, immunogenicity and toxicity concern due to bioaccumulation of inorganic materials remain one of the most challenging aspects of clinical translation. Therefore, a great deal of preclinical work is still necessary. A drawback limiting the translation of nanoparticles into clinics is the lack of systematic research in bioaccumulation, biodegradation, clearance, and safety conditions which impairs the comparison between studies. This review recapitulates the most relevant research to encourage MSNs clinical translation.

Future research must include designing MSNs to be non-toxic, excretable, and overall safe for human patients to achieve clinical application. To date, several data show that MSNs are biocompatible in animal models, however, the main focus of the studies has been placed on their application than the evaluation of their toxicity. Therefore, one of the major obstacles to employing MSNs as a delivery strategy for biomedical applications is the insufficient understanding about the long-term safety of nanomaterials and this concern needs to be addressed. Among these challenges, the lack of consistency in literature attending to characterizing protocols or toxicity screening assays hinders the development of these systems for commercialization and clinical applications.

Since biological interaction could significantly alter the behavior and effect of nanoparticles, extensive research is required to understand the physicochemical changes that nanomaterials undergo in biological systems and how they may affect their biological fate. Therefore, engineering MSNs with tunable and controllable bioaccumulation and biodegradation rates would be beneficial for achieving a safer therapeutic translation. Sophisticated control of physicochemical variables such as particle size or surface coating is critical since these characteristics determine the pharmacokinetics and biodegradation properties of the nanoparticles. In recent years, significant progress has been made in developing novel biodegradable and more clearable MSNs with reduced toxicity while retaining useful imaging or therapeutic functions.

However, more extensive pharmacodynamics and pharmacokinetics research is still needed to ensure MSNs fate in the body. Regarding drug delivery, MSNs nanoformulation has been demonstrated to increase drug bioavailability, improving the pharmacokinetics and thus the therapeutic activity of the encapsulated drug by a 10–25% compared with the free drug.[135,200] However, we are still far from achieving all the administered nanoparticles reach the target organ. To ensure this, we must ensure that they have the longest possible circulation time, and that the RES system does not quickly capture them. From the articles included in this review, it can be concluded that long-rod or spherical nanoparticles of 80–150 nm functionalized with a PEG derivative or with a lipid coating such as cell membranes would be ideal for achieving longer retention times.

Related to the routes of administration, the best route depends on the desired application. For cancer therapy, as occurs with chemotherapy, MSNs for antitumor drug delivery should ideally be administered I.V. However, intratumoral administration is also gaining attention recently as a new local way of administrating nanoparticles to target tumors specifically.[232] In oral administration, MSNs could be exploited as carriers to increase bioavailability and the subsequent adsorption of the drug from the intestine, as demonstrated in the only clinical trial conducted on humans with MSNs,[223] which demonstrated its use is beneficial for the treatment for the gastrointestinal tract diseases, as inflammatory bowel disease. For the treatment of lung diseases, a potential effective application is a local administration by inhalation. Much research has been done about inhaled polymer administration; [233,234] however, more research is needed about the administration of MSNs by this route. Moreover, inhaled administration could be functional to achieve that MSNs pass across the blood–brain barrier to target the brain.[235–237].

Concerning the degradation and clearance of MSNs in the organism, more research must be done to get MSNs to the clinic. Little has been evaluated *in vivo* about the degradation of MSNs. Instead, the degradation behavior of MSNs is usually studied in physiologically mimetic solutions which do not perfectly correlate to the biological environment. The experiments are normally carried out in a close environment characterized by a limited amount of aqueous solution which may delay the hydrolysis process resulting in a different fate for organisms. In recent years, the improvement in biodegradable and self-destructing MSNs which degrade into non-toxic byproducts over time has become a promising platform for nanoparticle-based *in vivo* imaging and drug delivery. As summarized, changing the structure of MSNs by modifying surface area, surface functionalization or the inclusion of metal ions or organic moieties in the MSN framework has been demonstrated to accelerate the biodegradation and excretion in a few days after injection. The doping of silica framework and the introduction of degradable organic functional groups on their structure, such as disulfide bonds, enhance the degradability rate and therefore potential applicability. Although there is limited evidence in the literature, it is strongly believed that the controllable biodegradability and easy excretion of MSNs will benefit the low toxicity of MSNs *in vivo*.

Besides, there are different contributions describing the clearance mechanism of MSNs. Several authors confirmed that MSNs are efficiently removed from the body regardless of the route of administration, dose, shape, size, and surface properties generally after a few weeks. MSNs possess unique physicochemical properties (sizes, porosity and composition, surface modification and charge, shape, etc.), and these characteristics determine the nanoparticle pharmacokinetics and biodistribution through the different organs that finally rule the clearance process.[238,239] The way the nanoparticles are degraded and thus eliminated depends on their location in the body if they can reach easily or not the target site in which they are processed, if they remain for longer time in blood circulation or if the liver, spleen, etc.

Four significant factors determined the clearance route and rate: particle size, shape, surface charge, and functionalization. Smaller nanoparticles (<6nm) are directly excreted by the kidney, while larger nanoparticles like MSNs (50–200 nm) are processed in the diseased tissue or by the RES system, degraded, and mainly excreted through urine.[159] Regarding shape, spherical nanoparticles are more easily processed than rod or filament-shaped nanoparticles taking into account the longer circulation and retention time observed for rod or filament MSNs.[161,176] The surface charge and functionalization overall influence the nanoparticle fate. Positive and negatively charged nanoparticles interact with serum proteins in the bloodstream, increasing their hydrodynamic size and thus facilitating their sequestration by the RES system. In fact, most positively charged nanoparticles are mainly cleared by the hepatobiliary route due to the increased size and the preferential uptake of positively charged nanoparticles by hepatocytes. [217,218] In contrast, neutral or PEGylated nanoparticles have longer blood circulation time and are processed more gradually cleared through urinary excretion. It is important to point out that enough circulating time is needed to reach the target site of action before nanoparticle degradation and clearance. Besides, the incorporation of targeting moieties into MSNs surface can help to handle nanoparticle biodistribution to diseased tissue thus favoring enhanced therapeutic effect as well as proper nanoparticle degradation and elimination. [240,241] Even so, establishing general conclusions is still difficult given the diversity of nanoparticles and applications that has been

described. Moreover, specific clearance studies will be required as well as more accurate methods to monitor *in vivo* degradation and excretion mechanisms and routes.

The biosafety profile of MSNs has been confirmed in this review, through the evaluation of key parameters: i.e. biodistribution, biodegradability and clearance. Despite more efforts are required to solidly establish the fate of MSNs in the organism, in a few years there has been an increase in studies giving evidence of the MSNs behavior. Although only one clinical trial includes MSNs, silica nanoparticles are already being evaluated for human treatment in several applications. Nevertheless, this transition must be handled very carefully as many nanomedicines fail in clinical translation. The failure in efficacy may lie in the large physiological differences between humans and small animals. Hopefully, preliminary results indicate the safety, efficacy, and viability of silica nanoparticles under these clinical scenarios.

On the other hand, while the impact of nanomedicines will most certainly benefit a number of diseases, there is a need to overcome industrial production. In this regard, there is a limiting difficulty in scalability and reproducibility in the synthetic manufacture of MSNs, as the batch-to-batch variations hinder the scale-up at industrial production. Consequently, the cost of production rises, and the prospect of its commercialization remains distant. These complications have also hindered the widespread adoption of MSNs in the clinical setting. Besides, the lack of a consensus on the standards and regulatory laws specifically for nanomedicines needed for reaching the market has delayed their potential clinical translation. The major challenges addressed by the regulatory agencies include their concern to classify many systems as medicines or medical devices, the needing for robust quality assurance for nanoparticle preparation and characterization, considering the complex physicochemical characteristics form each nanoparticle which determines their biological activity, as well as the lack of homogeneous, pure, and reproducible nanomedicine batches.[242,243].

Enclosed by a growing nanomedical field, MSNs have attracted attention as potential diagnostic and drug-delivery systems. The publications in nanomedicine are increasing every year, attracting the attention of the market.[244,245] According to a report by Grand View Research Inc., it is expected that by the year 2025, the pharmaceutical market will reach USD 350.8 billion.[246].

Even given that some challenges have still been overcome, all the findings pointed out here suggested the suitability of MSNs for clinical translation. A consensus by the researchers of establishing a standard MSNs scaffold, following the “keep it simple” premise and including tunable biodegradable properties, could be a key factor to reach realistic clinical goals and boost the market with reduced cost and easy industrial production. Considering the increasing knowledge about MSNs in the body and clinical studies, joint to the incipient improvements in silica mesoporous nanoformulations, it is expected that MSNs will finally reach the clinic in the near future.

Declaration of Competing Interest

The authors declare that they have no known competing financial interests or personal relationships that could have appeared to influence the work reported in this paper.

Data availability

Data will be made available on request.

Acknowledgments

This work was supported by project PID2021-126304OB-C41 funded by MCIN/ AEI /10.13039/501100011033/ and by European Regional Development Fund - A way of doing Europe and the Generalitat Valenciana (PROMETEO CIPROM/2021/007). A.E-F. is grateful to the Spanish Government for her Ph.D. grant (FPU17/05454), A.L-V. is grateful to the Instituto de Salud Carlos III for her Ph.D. i-PFIS grant (IFI17/00039). V.M.-C acknowledges the financial support from Project CIDEGENT/2020/031 funded by Generalitat Valenciana and Project PID2020-113256RA-I00 funded by MCIN/AEI/10.13039/50110001 1033. The authors thank the use of BioRender.com for the design of the figures in the manuscript.

References

[1] M.J. Mitchell, M.M. Billingsley, R.M. Haley, M.E. Wechsler, N.A. Peppas, R. Langer, Engineering precision nanoparticles for drug delivery, Nat. Rev. Drug Discov. 202 (20) (2020) 101–124, https://doi.org/10.1038/s41573-020-0090-8.
[2] T. Yanagisawa, T. Shimizu, K. Kuroda, C. Kato, The preparation of alkyltrimethylammonium-kanemite complexes and their conversion to microporous materials, Bull. Chem. Soc. Jpn. 63 (1990) 988–992, https://doi.org/10.1246/bcsj.63.988.
[3] M. Vallet-Regi, A. Rámila, R.P. Del Real, J. Pérez-Pariente, A new property of MCM-41: Drug delivery system, Chem. Mater. 13 (2001) 308–311, https://doi.org/10.1021/cm0011559.
[4] H.A. Santos, J. Salonen, L.M. Bimbo, V.-P. Lehto, L. Peltonen, J. Hirvonen, Mesoporous materials as controlled drug delivery formulations, J. Drug Deliv. Sci. Technol. 21 (2011) 139–155, https://doi.org/10.1016/S1773-2247(11)50016-4.
[5] J. Zhang, J.M. Rosenholm, The viability of mesoporous silica nanoparticles for drug delivery, Ther. Deliv. 6 (2015) 891–893, https://doi.org/10.4155/TDE.15.46.
[6] V. Mamaeva, C. Sahlgren, M. Lindén, Mesoporous silica nanoparticles in medicine—Recent advances, Adv. Drug Deliv. Rev. 65 (2013) 689–702, https://doi.org/10.1016/j.addr.2012.07.018.
[7] E. Aznar, M. Oroval, L. Pascual, J.R. Murguía, R. Martínez-Máñez, F. Sancenón, Gated Materials for On-Command Release of Guest Molecules, Chem. Rev. 116 (2016) 561–718, https://doi.org/10.1021/acs.chemrev.5b00456.
[8] P. Yang, S. Gai, J. Lin, Functionalized mesoporous silica materials for controlled drug delivery, Chem. Soc. Rev. 41 (2012) 3679–3698, https://doi.org/10.1039/C2CS15308D.
[9] S.-H. Wu, C.-Y. Mou, H.-P. Lin, Synthesis of mesoporous silica nanoparticles, Chem. Soc. Rev. 42 (2013) 3862–3875, https://doi.org/10.1039/C3CS35405A.
[10] N.K. Mal, M. Fujiwara, Y. Tanaka, Photocontrolled reversible release of guest molecules from coumarin-modified mesoporous silica, Nature. 421 (2003) 350–353, https://doi.org/10.1038/nature01362.
[11] R. Casasús, M.D. Marcos, R. Martínez-Máñez, J.V. Ros-Lis, J. Soto, L. A. Villaescusa, P. Amorós, D. Beltrán, C. Guillem, J. Latorre, Toward the development of ionically controlled nanoscopic molecular gates, J. Am. Chem. Soc. 126 (2004) 8612–8613, https://doi.org/10.1021/ja048095i.
[12] A. Llopis-Lorente, B. Lozano-Torres, A. Bernardos, R. Martínez-Máñez, F. Sancenón, Mesoporous silica materials for controlled delivery based on enzymes, J. Mater. Chem. B. 5 (2017) 3069–3083, https://doi.org/10.1039/C7TB00348J.
[13] A.B. Descalzo, R. Martínez-Máñez, F. Sancenón, K. Hoffmann, K. Rurack, The Supramolecular Chemistry of Organic-Inorganic Hybrid Materials, Angew. Chemie Int. Ed. 45 (2006) 5924–5948, https://doi.org/10.1002/anie.200600734.
[14] I.I. Slowing, J.L. Vivero-Escoto, C.-W. Wu, V.-S.-Y. Lin, Mesoporous silica nanoparticles as controlled release drug delivery and gene transfection carriers, Adv. Drug Deliv. Rev. 60 (2008) 1278–1288, https://doi.org/10.1016/j.addr.2008.03.012.
[15] B.G. Trewyn, S. Giri, I.I. Slowing, V.-S.-Y. Lin, Mesoporous silica nanoparticle based controlled release{,} drug delivery{,} and biosensor systems, Chem. Commun. (2007) 3236–3245, https://doi.org/10.1039/B701744H.
[16] J.M. Rosenholm, C. Sahlgren, M. Lindén, Towards multifunctional{,} targeted drug delivery systems using mesoporous silica nanoparticles – opportunities & challenges, Nanoscale. 2 (2010) 1870–1883, https://doi.org/10.1039/C0NR00156B.
[17] J.M. Rosenholm, C. Sahlgren, M. Linden, Multifunctional Mesoporous Silica Nanoparticles for Combined Therapeutic, Diagnostic and Targeted Action in Cancer Treatment, Curr. Drug Targets. 12 (2011) 1166–1186, https://doi.org/10.2174/138945011795906624.
[18] S. Jafari, H. Derakhshankhah, L. Alaei, A. Fattahi, B.S. Varnamkhasti, A. A. Saboury, Mesoporous silica nanoparticles for therapeutic/diagnostic applications, Biomed. Pharmacother. 109 (2019) 1100–1111, https://doi.org/10.1016/J.BIOPHA.2018.10.167.
[19] F. Sancenón, L. Pascual, M. Oroval, E. Aznar, R. Martínez-Máñez, Gated Silica Mesoporous Materials in Sensing Applications, ChemistryOpen. 4 (2015) 418–437, https://doi.org/10.1002/open.201500053.
[20] B. de Luis, A. Llopis-Lorente, F. Sancenón, R. Martínez-Máñez, Engineering chemical communication between micro/nanosystems, Chem. Soc. Rev. 50 (2021) 8829–8856, https://doi.org/10.1039/d0cs01048k.
[21] B. de Luis, A. Llopis-Lorente, P. Rincón, J. Gadea, F. Sancenón, E. Aznar, R. Villalonga, J.R. Murguía, R. Martínez-Máñez, An Interactive Model of Communication between Abiotic Nanodevices and Microorganisms, Angew. Chemie Int. Ed. 58 (2019) 14986–14990, https://doi.org/10.1002/anie.201908867.

[22] B. de Luis, Á. Morellá-Aucejo, A. Llopis-Lorente, J. Martínez-Latorre, F. Sancenón, C. López, J.R. Murguía, R. Martínez-Máñez, Nanoprogrammed Cross-Kingdom Communication Between Living Microorganisms, Nano Lett. 22 (2022) 1836–1844, https://doi.org/10.1021/acs.nanolett.1c02435.

[23] X. Pu, J. Li, P. Qiao, M. Li, H. Wang, L. Zong*, Q.Y. and S. Duan*, Mesoporous Silica Nanoparticles as a Prospective and Promising Approach for Drug Delivery and Biomedical Applications, Curr. Cancer Drug Targets. 19 (2019) 285–295. https://doi.org/https://doi.org/10.2174/1568009619666181206114904.

[24] R.R. Castillo, M. Vallet-Regí, Functional Mesoporous Silica Nanocomposites: Biomedical Applications and Biosafety, Int. J. Mol. Sci. 20 (2019), https://doi.org/10.3390/ijms20040929.

[25] P.T. Yin, T. Pongkulapa, H.-Y. Cho, J. Han, N.J. Pasquale, H. Rabie, J.-H. Kim, J.-W. Choi, K.-B. Lee, overcoming chemoresistance in cancer via combined microrna therapeutics with anticancer drugs using multifunctional magnetic core-shell nanoparticles, ACS Appl. Mater. Interfaces. 10 (2018) 26954–26963, https://doi.org/10.1021/acsami.8b09086.

[26] L. Zhang, Y. Chen, Z. Li, L. Li, P. Saint-Cricq, C. Li, J. Lin, C. Wang, Z. Su, J.I. Zink, Tailored Synthesis of Octopus-type Janus Nanoparticles for Synergistic Actively-Targeted and Chemo-Photothermal Therapy, Angew. Chemie Int. Ed. 55 (2016) 2118–2121, https://doi.org/10.1002/anie.201510409.

[27] J.-J. Hu, Q. Lei, M.-Y. Peng, D.-W. Zheng, Y.-X. Chen, X.-Z. Zhang, A positive feedback strategy for enhanced chemotherapy based on ROS-triggered self-accelerating drug release nanosystem, Biomaterials. 128 (2017) 136–146, https://doi.org/10.1016/j.biomaterials.2017.03.010.

[28] D. Muñoz-Espín, M. Rovira, I. Galiana, C. Giménez, B. Lozano-Torres, M. Paez-Ribes, S. Llanos, S. Chaib, M. Muñoz-Martín, A.C. Ucero, G. Garaulet, F. Mulero, S.G. Dann, T. VanArsdale, D.J. Shields, A. Bernardos, J.R. Murguía, R. Martínez-Máñez, M. Serrano, A versatile drug delivery system targeting senescent cells, EMBO Mol. Med. 10 (2018) e9355.

[29] J.G. Croissant, Y. Fatieiev, A. Almalik, N.M. Khashab, Mesoporous Silica and Organosilica Nanoparticles: Physical Chemistry, Biosafety, Delivery Strategies, and Biomedical Applications, Adv. Healthc. Mater. 7 (2018), https://doi.org/10.1002/adhm.201700831.

[30] Y. Chen, H. Chen, J. Shi, In vivo bio-safety evaluations and diagnostic/therapeutic applications of chemically designed mesoporous silica nanoparticles, Adv. Mater. 25 (2013) 3144–3176, https://doi.org/10.1002/adma.201205292.

[31] M. Longmire, P.L. Choyke, H. Kobayashi, Clearance properties of nano-sized particles and molecules as imaging agents: considerations and caveats, Nanomedicine (Lond). 3 (2008) 703–717, https://doi.org/10.2217/17435889.3.5.703.

[32] Y. Yang, M. Zhang, H. Song, C. Yu, Silica-Based Nanoparticles for Biomedical Applications: From Nanocarriers to Biomodulators, Acc. Chem. Res. 53 (2020) 1545–1556, https://doi.org/10.1021/ACS.ACCOUNTS.0C00280.

[33] Q. Lei, J. Guo, A. Noureddine, A. Wang, S. Wuttke, C.J. Brinker, W. Zhu, Sol–Gel-Based Advanced Porous Silica Materials for Biomedical Applications, Adv. Funct. Mater. 1909539 (2020) 1–28, https://doi.org/10.1002/adfm.201909539.

[34] A. García-Fernández, E. Aznar, R. Martínez-Máñez, F. Sancenón, A. García-Fernández, E. Aznar, R. Martínez-Máñez, F. Sancenón, New Advances in In Vivo Applications of Gated Mesoporous Silica as Drug Delivery Nanocarriers, Small. 16 (2020) 1–62, https://doi.org/10.1002/smll.201902242.

[35] A. García-Fernández, F. Sancenón, R. Martínez-Máñez, Mesoporous silica nanoparticles for pulmonary drug delivery, Adv. Drug Deliv. Rev. 177 (2021), 113953, https://doi.org/10.1016/j.addr.2021.113953.

[36] J. Wen, K. Yang, F. Liu, H. Li, Y. Xu, S. Sun, Diverse gatekeepers for mesoporous silica nanoparticle based drug delivery systems, Chem. Soc. Rev. 46 (2017) 6024–6045, https://doi.org/10.1039/C7CS00219J.

[37] M. Manzano, M. Vallet-Regí, Mesoporous Silica Nanoparticles for Drug Delivery, Adv. Funct. Mater. 30 (2020) 1902634, https://doi.org/10.1002/ADFM.201902634.

[38] A.N. Frickenstein, J.M. Hagood, C.N. Britten, B.S. Abbott, M.W. McNally, C. A. Vopat, E.G. Patterson, W.M. Maccuaig, A. Jain, K.B. Walters, L.R. McNally, Mesoporous silica nanoparticles: Properties and strategies for enhancing clinical effect, Pharmaceutics. 13 (2021) 1–27, https://doi.org/10.3390/pharmaceutics13040570.

[39] K.S.W. Sing, Reporting physisorption data for gas/solid systems with special reference to the determination of surface area and porosity (Recommendations 1984), Pure Appl. Chem. 57 (1985) 603–619. https://doi.org/doi:10.1351/pac198557040603.

[40] C.T. Kresge, W.J. Roth, The discovery of mesoporous molecular sieves from the twenty year perspective, Chem. Soc. Rev. 42 (2013) 3663–3670, https://doi.org/10.1039/C3CS60016E.

[41] L.T. Gibson, Mesosilica materials and organic pollutant adsorption: part A removal from air, Chem. Soc. Rev. 43 (2014) 5163–5172, https://doi.org/10.1039/C3CS60096C.

[42] J.S. Beck, J.C. Vartuli, W.J. Roth, M.E. Leonowicz, C.T. Kresge, K.D. Schmitt, C.T. W. Chu, D.H. Olson, E.W. Sheppard, S.B. McCullen, J.B. Higgins, J.L. Schlenker, A new family of mesoporous molecular sieves prepared with liquid crystal templates, J. Am. Chem. Soc. 114 (1992) 10834–10843, https://doi.org/10.1021/JA00053A020.

[43] Z. Dongyuan, F. Jianglin, H. Qisheng, M. Nicholas, F.G. H., C.B. F., S.G. D., Triblock Copolymer Syntheses of Mesoporous Silica with Periodic 50 to 300 Angstrom Pores, Science (80-.). 279 (1998) 548–552. https://doi.org/10.1126/science.279.5350.548.

[44] W. Stober, A. Fink, D. Ernst Bohn, Controlled Growth of Monodisperse Silica Spheres in the Micron Size Range 1, J. Colloid Interface Sci. 26 (1968) 62–69.

[45] T.T. Hoang Thi, V. Du Cao, T.N.Q. Nguyen, D.T. Hoang, V.C. Ngo, D.H. Nguyen, Functionalized mesoporous silica nanoparticles and biomedical applications, Mater. Sci. Eng. C. Mater. Biol. Appl. 99 (2019) 631–656, https://doi.org/10.1016/j.msec.2019.01.129.

[46] Q. Cai, W.-Y. Lin, F.-S. Xiao, W.-Q. Pang, X.-H. Chen, B.-S. Zou, The preparation of highly ordered MCM-41 with extremely low surfactant concentration, Microporous Mesoporous Mater. 32 (1999) 1–15, https://doi.org/10.1016/S1387-1811(99)00082-7.

[47] A.B.D. Nandiyanto, S.-G. Kim, F. Iskandar, K. Okuyama, Synthesis of spherical mesoporous silica nanoparticles with nanometer-size controllable pores and outer diameters, Microporous Mesoporous Mater. 120 (2009) 447–453, https://doi.org/10.1016/j.micromeso.2008.12.019.

[48] H. Zhang, Y. Zhou, Y. Li, T.J. Bandosz, D.L. Akins, Synthesis of hollow ellipsoidal silica nanostructures using a wet-chemical etching approach, J. Colloid Interface Sci. 375 (2012) 106–111, https://doi.org/10.1016/j.jcis.2012.02.046.

[49] T. Sánchez, P. Salagre, Y. Cesteros, Ultrasounds and microwave-assisted synthesis of mesoporous hectorites, Microporous Mesoporous Mater. 171 (2013) 24–34, https://doi.org/10.1016/j.micromeso.2013.01.001.

[50] N.I. Vazquez, Z. Gonzalez, B. Ferrari, Y. Castro, Synthesis of mesoporous silica nanoparticles by sol–gel as nanocontainer for future drug delivery applications, Boletín La Soc, Española Cerámica y Vidr. 56 (2017) 139–145, https://doi.org/10.1016/j.bsecv.2017.03.002.

[51] D. Bokov, A. Turki Jalil, S. Chupradit, W. Suksatan, M. Javed Ansari, I. H. Shewael, G.H. Valiev, E. Kianfar, Nanomaterial by Sol-Gel Method: Synthesis and Application, Adv. Mater. Sci. Eng. 2021 (2021) 5102014, https://doi.org/10.1155/2021/5102014.

[52] I. Capek, Hard Template-Directed Synthesis BT - Noble Metal Nanoparticles: Preparation, Composite Nanostructures, Biodecoration and Collective Properties, in: I. Capek (Ed.), Springer Japan, Tokyo, 2017: pp. 415–536. https://doi.org/10.1007/978-4-431-56556-7_5.

[53] H. Ghaedi, M. Zhao, Review on Template Removal Techniques for Synthesis of Mesoporous Silica Materials, Energy & Fuels. 36 (2022) 2424–2446, https://doi.org/10.1021/acs.energyfuels.1c04435.

[54] Y. Lu, H. Fan, A. Stump, T.L. Ward, T. Rieker, C.J. Brinker, Aerosol-assisted self-assembly of mesostructured spherical nanoparticles, Nature. 398 (1999) 223–226, https://doi.org/10.1038/18410.

[55] B.G. Trewyn, I.I. Slowing, S. Giri, H.-T. Chen, V.-S.-Y. Lin, Synthesis and Functionalization of a Mesoporous Silica Nanoparticle Based on the Sol-Gel Process and Applications in Controlled Release, Acc. Chem. Res. 40 (2007) 846–853, https://doi.org/10.1021/ar600032u.

[56] J.G. Croissant, K.S. Butler, J.I. Zink, C.J. Brinker, Synthetic Amorphous Silica Nanoparticles : Toxicity and Biomedical and Environmental Implications, (n.d.).

[57] R.M. Sábio, A.B. Meneguin, T.C. Ribeiro, R.R. Silva, M. Chorilli, New insights towards mesoporous silica nanoparticles as a technological platform for chemotherapeutic drugs delivery, Int. J. Pharm. 564 (2019) 379–409, https://doi.org/10.1016/j.ijpharm.2019.04.067.

[58] X. Du, S.Z. Qiao, Dendritic silica particles with center-radial pore channels: promising platforms for catalysis and biomedical applications, Small. 11 (2015) 392–413, https://doi.org/10.1002/smll.201401201.

[59] C. Xu, C. Lei, Y. Wang, C. Yu, Dendritic Mesoporous Nanoparticles: Structure, Synthesis and Properties, Angew. Chemie Int. Ed. 61 (2022) e202112752, https://doi.org/10.1002/anie.202112752.

[60] S. Malekmohammadi, R.U.R. Mohammed, H. Samadian, A. Zarebkohan, A. García-Fernández, G.R. Kokil, F. Sharifi, J. Esmaeili, M. Bhia, M. Razavi, M. Bodaghi, T. Kumeria, R. Martínez-Máñez, Nonordered dendritic mesoporous silica nanoparticles as promising platforms for advanced methods of diagnosis and therapies, Mater. Today Chem. 26 (2022), 101144, https://doi.org/10.1016/j.mtchem.2022.101144.

[61] W. Wang, P. Wang, X. Tang, A.A. Elzatahry, S. Wang, D. Al-Dahyan, M. Zhao, C. Yao, C.-T. Hung, X. Zhu, T. Zhao, X. Li, F. Zhang, D. Zhao, Facile Synthesis of Uniform Virus-like Mesoporous Silica Nanoparticles for Enhanced Cellular Internalization, ACS Cent. Sci. 3 (2017) 839–846, https://doi.org/10.1021/acscentsci.7b00257.

[62] M. Liu, Y. Zhao, Z. Shi, J.I. Zink, Q. Yu, Virus-like Magnetic Mesoporous Silica Particles as a Universal Vaccination Platform against Pathogenic Infections, ACS Nano. 17 (2023) 6899–6911, https://doi.org/10.1021/acsnano.3c00644.

[63] S.M. Häffner, E. Parra-Ortiz, K.L. Browning, E. Jørgensen, M.W.A. Skoda, C. Montis, X. Li, D. Berti, D. Zhao, M. Malmsten, Membrane Interactions of Virus-like Mesoporous Silica Nanoparticles, ACS Nano. 15 (2021) 6787–6800, https://doi.org/10.1021/acsnano.0c10378.

[64] A.J. Paula, C.P. Silveira, D.S.T. Martinez, A.G. Souza Filho, F.V. Romero, L. C. Fonseca, L. Tasic, O.L. Alves, N. Durán, Topography-driven bionano-interactions on colloidal silica nanoparticles, ACS Appl. Mater. Interfaces. 6 (2014) 3437–3447, https://doi.org/10.1021/am405594q.

[65] Y.-S. Lin, K.R. Hurley, C.L. Haynes, Critical Considerations in the Biomedical Use of Mesoporous Silica Nanoparticles, J. Phys. Chem. Lett. 3 (2012) 364–374, https://doi.org/10.1021/jz2013837.

[66] A. da C. Schneid, C.P. Silveira, F.E. Galdino, L.F. Ferreira, K. Bouchmella, M.B. Cardoso, Colloidal Stability and Redispersibility of Mesoporous Silica Nanoparticles in Biological Media, Langmuir. 36 (2020) 11442–11449. https://doi.org/10.1021/acs.langmuir.0c01571.

[67] R. Mohammadpour, M.A. Dobrovolskaia, D.L. Cheney, K.F. Greish, H. Ghandehari, Subchronic and chronic toxicity evaluation of inorganic nanoparticles for delivery applications, Adv. Drug Deliv. Rev. 144 (2019) 112–132, https://doi.org/10.1016/j.addr.2019.07.006.

[68] K. Greish, G. Thiagarajan, H. Ghandehari, In Vivo Methods of Nanotoxicology, Methods Mol. Biol. 926 (2012) 235–253, https://doi.org/10.1007/978-1-62703-002-1_17.
[69] H. Nehoff, N.N. Parayath, S. Taurin, K. Greish, In Vivo Evaluation of Acute and Chronic Nanotoxicity, Handb. Nanotoxicology, Nanomedicine Stem Cell Use Toxicol. (2014) 65–86. https://doi.org/10.1002/9781118856017.CH3.
[70] J.L. Weaver, G.A. Tobin, T. Ingle, S. Bancos, D. Stevens, R. Rouse, K.E. Howard, D. Goodwin, A. Knapton, X. Li, K. Shea, S. Stewart, L. Xu, P.L. Goering, Q. Zhang, P.C. Howard, J. Collins, S. Khan, K. Sung, K.M. Tyner, Evaluating the potential of gold, silver, and silica nanoparticles to saturate mononuclear phagocytic system tissues under repeat dosing conditions, Part. Fibre Toxicol. 14 (2017), https://doi.org/10.1186/S12989-017-0206-4.
[71] M. Yazdimamaghani, P.J. Moos, M.A. Dobrovolskaia, H. Ghandehari, Genotoxicity of amorphous silica nanoparticles: Status and prospects, Nanomedicine Nanotechnology, Biol. Med. 16 (2019) 106–125, https://doi.org/10.1016/J.NANO.2018.11.013.
[72] T. Yu, K. Greish, L.D. McGill, A. Ray, H. Ghandehari, Influence of Geometry, Porosity, and Surface Characteristics of Silica Nanoparticles on Acute Toxicity: Their Vasculature Effect and Tolerance Threshold, ACS Nano. 6 (2012) 2289–2301, https://doi.org/10.1021/nn2043803.
[73] R. Mohammadpour, M. Yazdimamaghani, D.L. Cheney, J. Jedrzkiewicz, H. Ghandehari, Subchronic toxicity of silica nanoparticles as a function of size and porosity, J. Control. Release. 304 (2019) 216–232, https://doi.org/10.1016/J.JCONREL.2019.04.041.
[74] H. Nishimori, M. Kondoh, K. Isoda, S. ichi Tsunoda, Y. Tsutsumi, K. Yagi, Histological analysis of 70-nm silica particles-induced chronic toxicity in mice, Eur. J. Pharm. Biopharm. 72 (2009) 626–629. https://doi.org/10.1016/J.EJPB.2009.03.007.
[75] R. Mohammadpour, D.L. Cheney, J.W. Grunberger, M. Yazdimamaghani, J. Jedrzkiewicz, K.J. Isaacson, M.A. Dobrovolskaia, H. Ghandehari, One-year chronic toxicity evaluation of single dose intravenously administered silica nanoparticles in mice and their Ex vivo human hemocompatibility, J. Control. Release. 324 (2020) 471–481, https://doi.org/10.1016/j.jconrel.2020.05.027.
[76] M. Van der Zande, R.J. Vandebriel, M.J. Groot, E. Kramer, Z.E. Herrera Rivera, K. Rasmussen, J.S. Ossenkoppele, P. Tromp, E.R. Gremmer, R.J.B. Peters, P. J. Hendriksen, H.J.P. Marvin, R.L.A.P. Hoogenboom, A.A.C.M. Peijnenburg, H. Bouwmeester, Sub-chronic toxicity study in rats orally exposed to nanostructured silica, Part. Fibre Toxicol. 11 (2014) 1–19, https://doi.org/10.1186/1743-8977-11-8/FIGURES/8.
[77] S.W. Lee, P.F. Markham, M.J.C. Coppo, A.R. Legione, N.K. Shil, J.A. Quinteros, A. H. Noormohammadi, G.F. Browning, C.A. Hartley, J.M. Devlin, Cross-Protective Immune Responses Between Genotypically Distinct Lineages of Infectious Laryngotracheitis Viruses, Https://Doi.Org/10.1637/10508-013113-ResNote.1. 58 (2013) 147–152. https://doi.org/10.1637/10508-013113-RESNOTE.1.
[78] K.M. de la Harpe, P.P.D. Kondiah, Y.E. Choonara, T. Marimuthu, L.C. du Toit, V. Pillay, The Hemocompatibility of Nanoparticles: A Review of Cell–Nanoparticle Interactions and Hemostasis, Cells 2019, Vol. 8, Page 1209. 8 (2019) 1209. https://doi.org/10.3390/CELLS8101209.
[79] I.I. Slowing, C. Wu, J.L. Vivero-escoto, V.S. Lin, Mesoporous Silica Nanoparticles for Reducing Hemolytic Activity Towards Mammalian Red Blood Cells **, (2009) 57–62. https://doi.org/10.1002/smll.200800926.
[80] A. Yildirim, E. Ozgur, M. Bayindir, Impact of mesoporous silica nanoparticle surface functionality on hemolytic activity, thrombogenicity and non-specific protein adsorption, J. Mater. Chem. B. 1 (2013) 1909–1920, https://doi.org/10.1039/C3TB20139B.
[81] Y.S. Lin, C.L. Haynes, Impacts of mesoporous silica nanoparticle size, pore ordering, and pore integrity on hemolytic activity, J. Am. Chem. Soc. 132 (2010) 4834–4842, https://doi.org/10.1021/ja910846q.
[82] Y. Zhao, X. Sun, G. Zhang, B.G. Trewyn, I.I. Slowing, V. S-Y Lin, Interaction of Mesoporous Silica Nanoparticles with Human Red Blood Cell Membranes: Size and Surface Effects, (2011). https://doi.org/10.1021/nn103077k.
[83] C. Urata, H. Yamada, R. Wakabayashi, Y. Aoyama, S. Hirosawa, S. Arai, S. Takeoka, Y. Yamauchi, K. Kuroda, Aqueous Colloidal Mesoporous Nanoparticles with, (2011) 8102–8105. https://doi.org/10.1021/ja201779d.
[84] B.S. Zolnik, Á. González-Fernández, N. Sadrieh, M.A. Dobrovolskaia, Minireview: Nanoparticles and the Immune System, Endocrinology. 151 (2010) 458–465, https://doi.org/10.1210/EN.2009-1082.
[85] S. Heidegger, D. Gößl, A. Schmidt, S. Niedermayer, C. Argyo, S. Endres, T. Bein, C. Bourquin, Nanoscale silica nanoparticles for targeted drug delivery †, (2016) 938–948. https://doi.org/10.1039/c5nr06122a.
[86] T.L. Nguyen, Y. Choi, J. Kim, Mesoporous Silica as a Versatile Platform for Cancer Immunotherapy, Adv. Mater. 31 (2019) 1803953, https://doi.org/10.1002/adma.201803953.
[87] S. Hosseinpour, L.J. Walsh, C. Xu, Modulating Osteoimmune Responses by Mesoporous Silica Nanoparticles, ACS Biomater. Sci. Eng. (2021), https://doi.org/10.1021/ACSBIOMATERIALS.1C00899.
[88] M. Vallet-Regí, M. Colilla, I. Izquierdo-Barba, M. Manzano, Mesoporous silica nanoparticles for drug delivery: Current insights, Molecules. 23 (2018) 1–19, https://doi.org/10.3390/molecules23010047.
[89] S. Hosseinpour, L.J. Walsh, C. Xu, Biomedical application of mesoporous silica nanoparticles as delivery systems: a biological safety perspective, J. Mater. Chem. B. (2020), https://doi.org/10.1039/d0tb01868f.
[90] L. Li, H. Liu, Biodegradable inorganic nanoparticles: an opportunity for improved cancer therapy? Nanomedicine (Lond). 12 (2017) 959–961, https://doi.org/10.2217/nnm-2017-0057.
[91] R. Jugdaohsingh, Silicon and bone health, J. Nutr. Health Aging. 11 (2007) 99.
[92] X. Li, F. Gao, Y. Dong, X. Li, Strategies to Regulate the Degradability of Mesoporous Silica-based Nanoparticles for Biomedical Applications, Nano. 14 (2019), https://doi.org/10.1142/S1793292019300081.
[93] V. Poscher, Y. Salinas, Trends in Degradable Mesoporous Organosilica-Based Nanomaterials for Controlling Drug Delivery: A Mini Review., Mater. (Basel, Switzerland). 13 (2020). https://doi.org/10.3390/ma13173668.
[94] J.G. Croissant, C.J. Brinker, Biodegradable Silica-Based Nanoparticles : Dissolution Kinetics and Selective Bond Cleavage, 1st ed., Elsevier Inc., 2018. https://doi.org/10.1016/bs.enz.2018.07.008.
[95] Q. He, J. Shi, M. Zhu, Y. Chen, F. Chen, The three-stage in vitro degradation behavior of mesoporous silica in simulated body fluid, Microporous Mesoporous Mater. 131 (2010) 314–320, https://doi.org/10.1016/j.micromeso.2010.01.009.
[96] I. Izquierdo-Barba, M. Colilla, M. Manzano, M. Vallet-Regí, In vitro stability of SBA-15 under physiological conditions, Microporous Mesoporous Mater. 132 (2010) 442–452, https://doi.org/10.1016/j.micromeso.2010.03.025.
[97] K. Braun, A. Pochert, M. Beck, R. Fiedler, J. Gruber, M. Lindén, Dissolution kinetics of mesoporous silica nanoparticles in different simulated body fluids, J. Sol-Gel Sci. Technol. 79 (2016) 319–327, https://doi.org/10.1007/s10971-016-4053-9.
[98] E. Bindini, Z. Chehadi, M. Faustini, P.A. Albouy, D. Grosso, A. Cattoni, C. Chanéac, O. Azzaroni, C. Sanchez, C. Boissière, Following in Situ the Degradation of Mesoporous Silica in Biorelevant Conditions: At Last, a Good Comprehension of the Structure Influence, ACS Appl. Mater. Interfaces. 12 (2020) 13598–13612, https://doi.org/10.1021/acsami.9b19956.
[99] N. Hao, H. Liu, L. Li, D. Chen, L. Li, F. Tang, In vitro degradation behavior of silica nanoparticles under physiological conditions, J. Nanosci. Nanotechnol. 12 (2012) 6346–6354, https://doi.org/10.1166/jnn.2012.6199.
[100] H. Yamada, C. Urata, Y. Aoyama, S. Osada, Y. Yamauchi, K. Kuroda, Preparation of Colloidal Mesoporous Silica Nanoparticles with Different Diameters and Their Unique Degradation Behavior in Static Aqueous Systems, Chem. Mater. 24 (2012) 1462–1471, https://doi.org/10.1021/cm3001688.
[101] J.G. Croissant, Y. Fatieiev, N.M. Khashab, Degradability and Clearance of Silicon, Organosilica, Silsesquioxane, Silica Mixed Oxide, and Mesoporous Silica Nanoparticles, Adv. Mater. 29 (2017) 1604634, https://doi.org/10.1002/adma.201604634.
[102] D. Shen, J. Yang, X. Li, L. Zhou, R. Zhang, W. Li, L. Chen, R. Wang, F. Zhang, D. Zhao, Biphase stratification approach to three-dimensional dendritic biodegradable mesoporous silica nanospheres, Nano Lett. 14 (2014) 923–932, https://doi.org/10.1021/nl404316v.
[103] G. Chen, Z. Teng, X. Su, Y. Liu, G. Lu, Unique Biological Degradation Behavior of Stöber Mesoporous Silica Nanoparticles from Their Interiors to Their Exteriors, J. Biomed. Nanotechnol. 11 (2015) 722–729, https://doi.org/10.1166/jbn.2015.2072.
[104] E. Choi, S. Kim, How Can Doxorubicin Loading Orchestrate in Vitro Degradation Behaviors of Mesoporous Silica Nanoparticles under a Physiological Condition? Langmuir. 33 (2017) 4974–4980, https://doi.org/10.1021/acs.langmuir.7b00332.
[105] E. Choi, S. Kim, Surface pH buffering to promote degradation of mesoporous silica nanoparticles under a physiological condition, J. Colloid Interface Sci. 533 (2019) 463–470, https://doi.org/10.1016/j.jcis.2018.08.088.
[106] V. Cauda, C. Argyo, T. Bein, Impact of different PEGylation patterns on the long-term bio-stability of colloidal mesoporous silica nanoparticles †, (2010) 8693–8699. https://doi.org/10.1039/c0jm01390k.
[107] V. Cauda, A. Schlossbauer, T. Bein, Bio-degradation study of colloidal mesoporous silica nanoparticles: Effect of surface functionalization with organo-silanes and poly(ethylene glycol), Microporous Mesoporous Mater. 132 (2010) 60–71, https://doi.org/10.1016/J.MICROMESO.2009.11.015.
[108] S. Seré, B. De Roo, M. Vervaele, S. Van Gool, S. Jacobs, J.W. Seo, J.-P. Locquet, Altering the Biodegradation of Mesoporous Silica Nanoparticles by Means of Experimental Parameters and Surface Functionalization, J. Nanomater. 2018 (2018) 7390618, https://doi.org/10.1155/2018/7390618.
[109] W. Ratirotjanakul, T. Suteewong, D. Polpanich, P. Tangboriboonrat, Amino acid as a biodegradation accelerator of mesoporous silica nanoparticles, Microporous Mesoporous Mater. 282 (2019) 243–251, https://doi.org/10.1016/J.MICROMESO.2019.02.033.
[110] Y. Yang, A. Wang, Q. Wei, C. Schlesener, R. Haag, Q. Li, J. Li, Hyperbranched Polyglycerol-Induced Porous Silica Nanoparticles as Drug Carriers for Cancer Therapy In Vitro and In Vivo, ChemistryOpen. 6 (2016) 1–9, https://doi.org/10.1002/open.201600072.
[111] L. Yu, Y. Chen, M. Wu, X. Cai, H. Yao, L. Zhang, H. Chen, J. Shi, Manganese Extraction" Strategy Enables Tumor-Sensitive Biodegradability and Theranostics of Nanoparticles, J. Am. Chem. Soc. 138 (2016) 9881–9894, https://doi.org/10.1021/jacs.6b04299.
[112] X. Li, L. Zhang, X. Dong, J. Liang, J. Shi, Preparation of mesoporous calcium doped silica spheres with narrow size dispersion and their drug loading and degradation behavior, Microporous Mesoporous Mater. 102 (2007) 151–158, https://doi.org/10.1016/j.micromeso.2006.12.048.
[113] X. Hao, X. Hu, C. Zhang, S. Chen, Z. Li, X. Yang, H. Liu, G. Jia, D. Liu, K. Ge, X.-J. Liang, J. Zhang, Hybrid Mesoporous Silica-Based Drug Carrier Nanostructures with Improved Degradability by Hydroxyapatite, ACS Nano. 9 (2015) 9614–9625, https://doi.org/10.1021/nn507485j.
[114] Y. He, B. Zeng, S. Liang, M. Long, H. Xu, Synthesis of pH-Responsive Biodegradable Mesoporous Silica– Calcium Phosphate Hybrid Nanoparticles as a High Potential Drug Carrier, (2017). https://doi.org/10.1021/acsami.7b16787.
[115] L. Wang, M. Huo, Y. Chen, J. Shi, Iron-engineered mesoporous silica nanocatalyst with biodegradable and catalytic framework for tumor-specific therapy,

Biomaterials. 163 (2018) 1–13, https://doi.org/10.1016/j.biomaterials.2018.02.018.
[116] H. Omar, J.G. Croissant, K. Alamoudi, S. Alsaiari, I. Alradwan, M.A. Majrashi, D. H. Anjum, P. Martins, R. Laamarti, J. Eppinger, B. Moosa, A. Almalik, N. M. Khashab, Biodegradable Magnetic Silica@Iron Oxide Nanovectors with Ultra-Large Mesopores for High Protein Loading, Magnetothermal Release, and Delivery, J. Control. Release. 259 (2017) 187–194, https://doi.org/10.1016/j.jconrel.2016.11.032.
[117] W. Wu, L. Yu, Q. Jiang, M. Huo, H. Lin, L. Wang, Y. Chen, J. Shi, Enhanced Tumor-Specific Disulfiram Chemotherapy by in Situ Cu2+ Chelation-Initiated Nontoxicity-to-Toxicity Transition, J. Am. Chem. Soc. 141 (2019) 11531–11539, https://doi.org/10.1021/jacs.9b03503.
[118] T. Fontecave, C. Sanchez, T. Azaïs, C. Boissiére, Chemical modification as a versatile tool for tuning stability of silica based mesoporous carriers in biologically relevant conditions, Chem. Mater. 24 (2012) 4326–4336, https://doi.org/10.1021/CM302142K/SUPPL_FILE/CM302142K_SI_001.PDF.
[119] C.-G. Liu, Y.-H. Han, J.-T. Zhang, R.K. Kankala, S.-B. Wang, A.-Z. Chen, Rerouting engineered metal-dependent shapes of mesoporous silica nanocontainers to biodegradable Janus-type (sphero-ellipsoid) nanoreactors for chemodynamic therapy, Chem. Eng. J. 370 (2019) 1188–1199, https://doi.org/10.1016/j.cej.2019.03.272.
[120] P. Huang, X. Qian, Y. Chen, L. Yu, H. Lin, L. Wang, Y. Zhu, J. Shi, Metalloporphyrin-encapsulated biodegradable nanosystems for highly efficient magnetic resonance imaging-guided sonodynamic cancer therapy, J. Am. Chem. Soc. 139 (2017) 1275–1284, https://doi.org/10.1021/JACS.6B11846/SUPPL_FILE/JA6B11846_SI_001.PDF.
[121] P. Huang, Y. Chen, H. Lin, L. Yu, L. Zhang, L. Wang, Y. Zhu, J. Shi, Molecularly organic/inorganic hybrid hollow mesoporous organosilica nanocapsules with tumor-specific biodegradability and enhanced chemotherapeutic functionality, Biomaterials. 125 (2017) 23–37, https://doi.org/10.1016/J.BIOMATERIALS.2017.02.018.
[122] Q. Zhang, C. Shen, N. Zhao, F.J. Xu, Redox-Responsive and Drug-Embedded Silica Nanoparticles with Unique Self-Destruction Features for Efficient Gene/Drug Codelivery, Adv. Funct. Mater. 27 (2017) 1606229, https://doi.org/10.1002/ADFM.201606229.
[123] J.-L. Li, Y.-J. Cheng, C. Zhang, H. Cheng, J. Feng, R.-X. Zhuo, X. Zeng, X.-Z. Zhang, Dual Drug Delivery System Based on Biodegradable Organosilica Core−Shell Architectures, (2018). https://doi.org/10.1021/acsami.7b17949.
[124] W. Fan, N. Lu, Z. Shen, W. Tang, B. Shen, Z. Cui, L. Shan, Z. Yang, Z. Wang, O. Jacobson, Z. Zhou, Y. Liu, P. Hu, W. Yang, J. Song, Y. Zhang, L. Zhang, N. M. Khashab, M.A. Aronova, G. Lu, X. Chen, Generic synthesis of small-sized hollow mesoporous organosilica nanoparticles for oxygen-independent X-ray-activated synergistic therapy, Nat. Commun. 10 (2019), https://doi.org/10.1038/S41467-019-09158-1.
[125] Y. Lu, Y. Yang, Z. Gu, J. Zhang, H. Song, G. Xiang, C. Yu, Glutathione-depletion mesoporous organosilica nanoparticles as a self-adjuvant and Co-delivery platform for enhanced cancer immunotherapy, Biomaterials. 175 (2018) 82–92, https://doi.org/10.1016/j.biomaterials.2018.05.025.
[126] D. Shao, M. Li, Z. Wang, X. Zheng, Y.H. Lao, Z. Chang, F. Zhang, M. Lu, J. Yue, H. Hu, H. Yan, L. Chen, W. fei Dong, K.W. Leong, Bioinspired Diselenide-Bridged Mesoporous Silica Nanoparticles for Dual-Responsive Protein Delivery, Adv. Mater. 30 (2018) 1–8, https://doi.org/10.1002/adma.201801198.
[127] Y. Fatieiev, J.G. Croissant, K. Julfakyan, L. Deng, D.H. Anjum, A. Gurinov, N. M. Khashab, Enzymatically degradable hybrid organic–inorganic bridged silsesquioxane nanoparticles for in vitro imaging, Nanoscale. 7 (2015) 15046–15050, https://doi.org/10.1039/C5NR03065J.
[128] J.G. Croissant, Y. Fatieiev, K. Julfakyan, J. Lu, A.-H. Emwas, D.H. Anjum, H. Omar, F. Tamanoi, J.I. Zink, N.M. Khashab, Biodegradable Oxamide-Phenylene-Based Mesoporous Organosilica Nanoparticles with Unprecedented Drug Payloads for Delivery in Cells, Chemistry. 22 (2016) 14806–14811, https://doi.org/10.1002/chem.201601714.
[129] Y. Yang, J. Wan, Y. Niu, Z. Gu, J. Zhang, M. Yu, C. Yu, Structure-Dependent and Glutathione-Responsive Biodegradable Dendritic Mesoporous Organosilica Nanoparticles for Safe Protein Delivery, Chem. Mater. 28 (2016) 9008–9016, https://doi.org/10.1021/acs.chemmater.6b03896.
[130] L. Yu, Y. Chen, H. Lin, W. Du, H. Chen, J. Shi, Ultrasmall mesoporous organosilica nanoparticles: Morphology modulations and redox-responsive biodegradability for tumor-specific drug delivery, Biomaterials. 161 (2018) 292–305, https://doi.org/10.1016/j.biomaterials.2018.01.046.
[131] M. Qian, L. Chen, Y. Du, H. Jiang, T. Huo, Y. Yang, W. Guo, Y. Wang, R. Huang, Biodegradable Mesoporous Silica Achieved via Carbon Nanodots-Incorporated Framework Swelling for Debris-Mediated Photothermal Synergistic Immunotherapy, Nano Lett. 19 (2019) 8409–8417, https://doi.org/10.1021/acs.nanolett.9b02448.
[132] X. Wang, X. Li, A. Ito, Y. Sogo, Y. Watanabe, N.M. Tsuji, T. Ohno, Biodegradable Metal Ion-Doped Mesoporous Silica Nanospheres Stimulate Anticancer Th1 Immune Response in Vivo, ACS Appl. Mater. Interfaces. 9 (2017) 43538–43544, https://doi.org/10.1021/acsami.7b16118.
[133] Y. Choi, J.E. Lee, J.H. Lee, J.H. Jeong, J. Kim, A Biodegradation Study of SBA-15 Microparticles in Simulated Body Fluid and in Vivo, Langmuir. 31 (2015) 6457–6462, https://doi.org/10.1021/acs.langmuir.5b01316.
[134] D. Bhavsar, V. Patel, K. Sawant, Systematic investigation of in vitro and in vivo safety, toxicity and degradation of mesoporous silica nanoparticles synthesized using commercial sodium silicate, Microporous Mesoporous Mater. 284 (2019) 343–352, https://doi.org/10.1016/j.micromeso.2019.04.050.
[135] Y. Chen, W. Yang, B. Chang, H. Hu, X. Fang, X. Sha, In vivo distribution and antitumor activity of doxorubicin-loaded N-isopropylacrylamide-co-methacrylic acid coated mesoporous silica nanoparticles and safety evaluation, Eur. J. Pharm. Biopharm. 85 (2013) 406–412, https://doi.org/10.1016/j.ejpb.2013.06.015.
[136] T. Wu, M. Tang, Review of the effects of manufactured nanoparticles on mammalian target organs, J. Appl. Toxicol. 38 (2018) 25–40, https://doi.org/10.1002/jat.3499.
[137] J. Lazarovits, Y.Y. Chen, E.A. Sykes, W.C.W. Chan, Nanoparticle-blood interactions: The implications on solid tumour targeting, Chem. Commun. 51 (2015) 2756–2767, https://doi.org/10.1039/c4cc07644c.
[138] M.A. Dobrovolskaia, P. Aggarwal, J.B. Hall, S.E. McNeil, Preclinical studies to understand nanoparticle interaction with the immune system and its potential effects on nanoparticle biodistribution, in: Mol. Pharm., Mol Pharm, 2008: pp. 487–495. https://doi.org/10.1021/mp800032f.
[139] T.S.P. Grandhi, K. Rege, Design, synthesis, and functionalization of nanomaterials for therapeutic drug delivery, Adv. Exp. Med. Biol. 811 (2014) 157–182, https://doi.org/10.1007/978-94-017-8739-0_9.
[140] F. Danhier, O. Feron, V. Préat, To exploit the tumor microenvironment: Passive and active tumor targeting of nanocarriers for anti-cancer drug delivery, J. Control. Release. 148 (2010) 135–146, https://doi.org/10.1016/J.JCONREL.2010.08.027.
[141] I. Garrido-Cano, V. Candela-Noguera, G. Herrera, J.M. Cejalvo, A. Lluch, M. D. Marcos, F. Sancenon, P. Eroles, R. Martínez-Máñez, Biocompatibility and internalization assessment of bare and functionalised mesoporous silica nanoparticles, Microporous Mesoporous Mater. 310 (2021), 110593, https://doi.org/10.1016/j.micromeso.2020.110593.
[142] Y. Matsumura, H. Maeda, A new concept for macromolecular therapeutics in cancer chemotherapy: mechanism of tumoritropic accumulation of proteins and the antitumor agent smancs, Cancer Res. 46 (1986) 6387–6392.
[143] Q. Wei, Y. Chen, X. Ma, J. Ji, Y. Qiao, B. Zhou, F. Ma, D. Ling, H. Zhang, M. Tian, J. Tian, M. Zhou, High-Efficient Clearable Nanoparticles for Multi-Modal Imaging and Image-Guided Cancer Therapy, Adv. Funct. Mater. 28 (2018) 1–12, https://doi.org/10.1002/adfm.201704634.
[144] D. Wang, S.R. Goldring, The bone, the joints and the balm of gilead, Mol. Pharm. 8 (2011) 991–993, https://doi.org/10.1021/mp200328t.
[145] F. Yuan, R.K. Nelson, D.E. Tabor, Y. Zhang, M.P. Akhter, K.A. Gould, D. Wang, Dexamethasone prodrug treatment prevents nephritis in lupus-prone (NZB × NZW)F1 mice without causing systemic side effects, Arthritis Rheum. 64 (2012) 4029–4039, https://doi.org/10.1002/ART.34667.
[146] J.M. Van Den Hoven, S.R. Van Tomme, J.M. Metselaar, B. Nuijen, J.H. Beijnen, G. Storm, Liposomal Drug Formulations in the Treatment of Rheumatoid Arthritis, Mol. Pharm. 8 (2011) 1002–1015, https://doi.org/10.1021/MP2000742.
[147] F. Yuan, L. Quan, L. Cui, S.R. Goldring, D. Wang, Development of macromolecular prodrug for rheumatoid arthritis, Adv. Drug Deliv. Rev. 64 (2012) 1205–1219, https://doi.org/10.1016/j.addr.2012.03.006.
[148] A. García-Fernández, G. García-Laínez, M.L. Ferrándiz, E. Aznar, F. Sancenón, M. J. Alcaraz, J.R. Murguía, M.D. Marcos, R. Martínez-Máñez, A.M. Costero, M. Orzáez, Targeting inflammasome by the inhibition of caspase-1 activity using capped mesoporous silica nanoparticles, J. Control. Release. 248 (2017) 60–70, https://doi.org/10.1016/j.jconrel.2017.01.002.
[149] A. García-Fernández, M. Sancho, V. Bisbal, P. Amorós, M.D. Marcos, M. Orzáez, F. Sancenón, R. Martínez-Máñez, Targeted-lung delivery of dexamethasone using gated mesoporous silica nanoparticles. A new therapeutic approach for acute lung injury treatment, J. Control. Release. 337 (2021) 14–26, https://doi.org/10.1016/j.jconrel.2021.07.010.
[150] M.H. Chan, H.M. Lin, Preparation and identification of multifunctional mesoporous silica nanoparticles for invitro and invivo dual-mode imaging, theranostics, and targeted tracking, Biomaterials. 46 (2015) 149–158, https://doi.org/10.1016/j.biomaterials.2014.12.034.
[151] F. Chen, H. Hong, S. Shi, S. Goel, H.F. Valdovinos, R. Hernandez, C.P. Theuer, T. E. Barnhart, W. Cai, Engineering of hollow mesoporous silica nanoparticles for remarkably enhanced tumor active targeting efficacy, Sci. Rep. 4 (2014) 1–10, https://doi.org/10.1038/srep05080.
[152] G.F. Luo, W.H. Chen, Y. Liu, Q. Lei, R.X. Zhuo, X.Z. Zhang, Multifunctional enveloped mesoporous silica nanoparticles for subcellular co-delivery of drug and therapeutic peptide, Sci. Rep. 4 (2014), https://doi.org/10.1038/srep06064.
[153] L. Pascual, C. Cerqueira-Coutinho, A. García-Fernández, B. de Luis, E. S. Bernardes, M.S. Albernaz, S. Missailidis, R. Martínez-Máñez, R. Santos-Oliveira, M. Orzaez, F. Sancenón, MUC1 aptamer-capped mesoporous silica nanoparticles for controlled drug delivery and radio-imaging applications, Nanomedicine Nanotechnology, Biol. Med. 13 (2017) 2495–2505, https://doi.org/10.1016/j.nano.2017.08.006.
[154] A. Agostini, L. Mondragón, A. Bernardos, R. Martínez-Máñez, M. Dolores Marcos, F. Sancenõn, J. Soto, A. Costero, C. Manguan-García, R. Perona, M. Moreno-Torres, R. Aparicio-Sanchis, J.R. Murguía, L. Mondragon, A. Bernardos, R. Martinez-Mañez, M. Dolores Marcos, F. Sancenon, J. Soto, A. Costero, C. Manguan-Garcia, R. Perona, M. Moreno-Torres, R. Aparicio-Sanchis, J. R. Murguia, Targeted cargo delivery in senescent cells using capped mesoporous silica nanoparticles, Angew. Chemie - Int. Ed. 51 (2012) 10556–10560, https://doi.org/10.1002/anie.201204663.
[155] Y. Zhou, G. Quan, Q. Wu, X. Zhang, B. Niu, B. Wu, Y. Huang, X. Pan, C. Wu, Mesoporous silica nanoparticles for drug and gene delivery, Acta Pharm. Sin. B. 8 (2018) 165–177, https://doi.org/10.1016/j.apsb.2018.01.007.
[156] S. Goel, F. Chen, S. Luan, H.F. Valdovinos, S. Shi, S.A. Graves, F. Ai, T.E. Barnhart, C.P. Theuer, W. Cai, Engineering Intrinsically Zirconium-89 Radiolabeled Self-

Destructing Mesoporous Silica Nanostructures for In Vivo Biodistribution and Tumor Targeting Studies, Adv. Sci. 3 (2016) 1600122, https://doi.org/10.1002/advs.201600122.
[157] I. Galiana, B. Lozano-Torres, M. Sancho, M. Alfonso, A. Bernardos, V. Bisbal, M. Serrano, R. Martínez-Máñez, M. Orzáez, Preclinical antitumor efficacy of senescence-inducing chemotherapy combined with a nanoSenolytic, J. Control. Release. 323 (2020) 624–634, https://doi.org/10.1016/j.jconrel.2020.04.045.
[158] B. Lozano-Torres, J.F. Blandez, I. Galiana, A. García-Fernández, M. Alfonso, M. D. Marcos, M. Orzáez, F. Sancenón, R. Martínez-Máñez, Real-Time In Vivo Detection of Cellular Senescence through the Controlled Release of the NIR Fluorescent Dye Nile Blue, Angew. Chemie Int. Ed. 59 (2020) 15152–15156.
[159] Q. He, Z. Zhang, F. Gao, Y. Li, J. Shi, In vivo biodistribution and urinary excretion of mesoporous silica nanoparticles: Effects of particle size and PEGylation, Small. 7 (2011) 271–280, https://doi.org/10.1002/smll.201001459.
[160] P. Dogra, N.L. Adolphi, Z. Wang, Y.S. Lin, K.S. Butler, P.N. Durfee, J.G. Croissant, A. Noureddine, E.N. Coker, E.L. Bearer, V. Cristini, C.J. Brinker, Establishing the effects of mesoporous silica nanoparticle properties on in vivo disposition using imaging-based pharmacokinetics, Nat. Commun. 9 (2018) 1–14, https://doi.org/10.1038/s41467-018-06730-z.
[161] X. Huang, L. Li, T. Liu, N. Hao, H. Liu, D. Chen, F. Tang, The Shape Effect of Mesoporous Silica Nanoparticles on Biodistribution, Clearance, and Biocompatibility in Vivo, ACS Nano. 5 (2011) 5390–5399, https://doi.org/10.1021/nn200365a.
[162] D. Westmeier, R.H. Stauber, D. Docter, The concept of bio-corona in modulating the toxicity of engineered nanomaterials (ENM), Toxicol. Appl. Pharmacol. 299 (2016) 53–57, https://doi.org/10.1016/j.taap.2015.11.008.
[163] K.E. Wheeler, A.J. Chetwynd, K.M. Fahy, B.S. Hong, J.A. Tochihuitl, L.A. Foster, I. Lynch, Environmental dimensions of the protein corona, Nat. Nanotechnol. 2021 166. 16 (2021) 617–629. https://doi.org/10.1038/s41565-021-00924-1.
[164] M.P. Monopoli, D. Walczyk, A. Campbell, G. Elia, I. Lynch, F. Baldelli Bombelli, K. A. Dawson, Physical-Chemical aspects of protein corona: Relevance to in vitro and in vivo biological impacts of nanoparticles, J. Am. Chem. Soc. 133 (2011) 2525–2534, https://doi.org/10.1021/ja107583h.
[165] E. Rascol, M. Daurat, A. Da Silva, M. Maynadier, C. Dorandeu, C. Charnay, M. Garcia, J. Lai-Kee-Him, P. Bron, M. Auffan, W. Liu, B. Angeletti, J. M. Devoisselle, Y. Guari, M. Gary-Bobo, J. Chopineau, Biological fate of Fe3O4 core-shell mesoporous silica nanoparticles depending on particle surface chemistry, Nanomaterials. 7 (2017) 1–15, https://doi.org/10.3390/nano7070162.
[166] M. Laprise-Pelletier, M. Bouchoucha, J. Lagueux, P. Chevallier, R. Lecomte, Y. Gossuin, F. Kleitz, M.A. Fortin, Metal chelate grafting at the surface of mesoporous silica nanoparticles (MSNs): Physico-chemical and biomedical imaging assessment, J. Mater. Chem. B. 3 (2015) 748–758, https://doi.org/10.1039/c4tb01423e.
[167] S.H. Wu, Y.S. Lin, Y. Hung, Y.H. Chou, Y.H. Hsu, C. Chang, C.Y. Mou, Multifunctional mesoporous silica nanoparticles for intracellular labeling and animal magnetic resonance imaging studies, ChemBioChem. 9 (2008) 53–57, https://doi.org/10.1002/cbic.200700509.
[168] C.-H.-H. Lee, S.-H.-H. Cheng, Y.-J.-J. Wang, Y.-C.-C. Chen, N.-T.-T. Chen, J. Souris, C.-T.-T. Chen, C.-Y.-Y. Mou, C.-S.-S. Yang, L.-W.-W. Lo, Near-infrared mesoporous silica nanoparticles for optical imaging: Characterization and in vivo biodistribution, Adv. Funct. Mater. 19 (2009) 215–222, https://doi.org/10.1002/adfm.200800753.
[169] C. Guo, J. Hu, L. Kao, D. Pan, K. Luo, N. Li, Z. Gu, Pepetide Dendron-Functionalized Mesoporous Silica Nanoparticle-Based Nanohybrid: Biocompatibility and Its Potential as Imaging Probe, ACS Biomater. Sci. Eng. 2 (2016) 860–870, https://doi.org/10.1021/acsbiomaterials.6b00093.
[170] S. Rojas, J.D. Gispert, C. Menchón, H.G. Baldoví, M. Buaki-Sogo, M. Rocha, S. Abad, V.M. Victor, H. García, J.R. Herance, Novel methodology for labelling mesoporous silica nanoparticles using the 18F isotope and their in vivo biodistribution by positron emission tomography, J. Nanoparticle Res. 17 (2015) 131, https://doi.org/10.1007/s11051-015-2938-0.
[171] M. Xuan, J. Shao, J. Zhao, Q. Li, L. Dai, J. Li, Magnetic Mesoporous Silica Nanoparticles Cloaked by Red Blood Cell Membranes: Applications in Cancer Therapy, Angew. Chemie - Int. Ed. 57 (2018) 6049–6053, https://doi.org/10.1002/anie.201712996.
[172] J.G. Croissant, D. Zhang, S. Alsaiari, J. Lu, L. Deng, F. Tamanoi, A.M. Almalik, J. I. Zink, N.M. Khashab, Protein-gold clusters-capped mesoporous silica nanoparticles for high drug loading, autonomous gemcitabine/doxorubicin co-delivery, and in-vivo tumor imaging, J. Control. Release. 229 (2016) 183–191, https://doi.org/10.1016/j.jconrel.2016.03.030.
[173] K. Chaudhary, S. Haddadin, R. Nistala, C. Papageorgio, Intraperitoneal drug therapy: an advantage, Curr. Clin. Pharmacol. 5 (2010) 82–88, https://doi.org/10.2174/157488410791110779.
[174] W. Ceelen, H. Braet, G. van Ramshorst, W. Willaert, K. Remaut, Intraperitoneal chemotherapy for peritoneal metastases: an expert opinion, Expert Opin. Drug Deliv. 17 (2020) 511–522, https://doi.org/10.1080/17425247.2020.1736551.
[175] A. Al Shoyaib, S.R. Archie, V.T. Karamyan, Intraperitoneal Route of Drug Administration: Should it Be Used in Experimental Animal Studies? Pharm. Res. 37 (2019) 12, https://doi.org/10.1007/S11095-019-2745-X.
[176] Y. Zhao, Y. Wang, F. Ran, Y. Cui, C. Liu, Q. Zhao, Y. Gao, D. Wang, S. Wang, A comparison between sphere and rod nanoparticles regarding their in vivo biological behavior and pharmacokinetics, Sci. Rep. 7 (2017) 4131, https://doi.org/10.1038/s41598-017-03834-2.
[177] L. Li, T. Liu, C. Fu, L. Tan, X. Meng, H. Liu, Biodistribution, excretion, and toxicity of mesoporous silica nanoparticles after oral administration depend on their shape, Nanomedicine Nanotechnology, Biol. Med. 11 (2015) 1915–1924, https://doi.org/10.1016/j.nano.2015.07.004.
[178] L.W. Moreland, ed., Reticuloendothelial system, in: Rheumatol. Immunol. Ther., Springer Berlin Heidelberg, Berlin, Heidelberg, 2004: p. 759. https://doi.org/10.1007/3-540-29662-X_2327.
[179] M. González-Alvarez, C. Coll, I. Gonzalez-Alvarez, C. Giménez, E. Aznar, M. C. Martínez-Bisbal, I. Lozoya-Agulló, M. Bermejo, R. Martínez-Máñez, F. Sancenón, Gated Mesoporous Silica Nanocarriers for a "two-Step" Targeted System to Colonic Tissue, Mol. Pharm. 14 (2017) 4442–4453, https://doi.org/10.1021/acs.molpharmaceut.7b00565.
[180] A.H. Teruel, É. Pérez-Esteve, I. González-Álvarez, M. González-Álvarez, A. M. Costero, D. Ferri, M. Parra, P. Gaviña, V. Merino, R. Martínez-Mañez, F. Sancenón, Smart gated magnetic silica mesoporous particles for targeted colon drug delivery: New approaches for inflammatory bowel diseases treatment, J. Control. Release. 281 (2018) 58–69.
[181] A.H. Teruel, É. Pérez-Esteve, I. González-Álvarez, M. González-Álvarez, A. M. Costero, D. Ferri, P. Gaviña, V. Merino, R. Martínez-Máñez, F. Sancenón, Double Drug Delivery Using Capped Mesoporous Silica Microparticles for the Effective Treatment of Inflammatory Bowel Disease, Mol. Pharm. 16 (2019) 2418–2429, https://doi.org/10.1021/acs.molpharmaceut.9b00041.
[182] D. Desai, N. Prabhakar, V. Mamaeva, D.Ş. Karaman, I.A.K. Lähdeniemi, C. Sahlgren, J.M. Rosenholm, D.M. Toivola, Targeted modulation of cell differentiation in distinct regions of the gastrointestinal tract via oral administration of differently PEG-PEI functionalized mesoporous silica nanoparticles, Int. J. Nanomedicine. 11 (2016) 299–313, https://doi.org/10.2147/IJN.S94013.
[183] G. Zhang, W. Han, P. Zhao, Z. Wang, M. Li, X. Sui, Y. Liu, B. Tian, Z. He, Q. Fu, Programmed pH-responsive core–shell nanoparticles for precisely targeted therapy of ulcerative colitis, Nanoscale. 15 (2023) 1937–1946, https://doi.org/10.1039/D2NR04968F.
[184] S.H. van Rijt, D.A. Bölükbas, C. Argyo, K. Wipplinger, M. Naureen, S. Datz, O. Eickelberg, S. Meiners, T. Bein, O. Schmid, T. Stoeger, Applicability of avidin protein coated mesoporous silica nanoparticles as drug carriers in the lung, Nanoscale. 8 (2016) 8058–8069, https://doi.org/10.1039/C5NR04119H.
[185] O. Taratula, O.B. Garbuzenko, A.M. Chen, T. Minko, Innovative strategy for treatment of lung cancer: targeted nanotechnology-based inhalation co-delivery of anticancer drugs and siRNA, J. Drug Target. 19 (2011) 900–914, https://doi.org/10.3109/1061186X.2011.622404.
[186] E. Tenland, A. Pochert, N. Krishnan, K. Umashankar Rao, S. Kalsum, K. Braun, I. Glegola-Madejska, M. Lerm, B.D. Robertson, M. Lindén, G. Godaly, Effective delivery of the anti-mycobacterial peptide NZX in mesoporous silica nanoparticles, PLoS One. 14 (2019) e0212858.
[187] Y. Inoue, S. Kiryu, M. Watanabe, N. Oyaizu, K. Ohtomo, Fluorescence lymph node mapping in living mice using quantum dots and a compression technique, J. Fluoresc. 20 (2010) 599–606, https://doi.org/10.1007/s10895-009-0593-5.
[188] S. Ku, F. Yan, Y. Wang, Y. Sun, N. Yang, L. Ye, The blood-brain barrier penetration and distribution of PEGylated fluorescein-doped magnetic silica nanoparticles in rat brain, Biochem. Biophys. Res. Commun. 394 (2010) 871–876, https://doi.org/10.1016/j.bbrc.2010.03.006.
[189] Y. Wang, Q. Zhao, N. Han, L. Bai, J. Li, J. Liu, E. Che, L. Hu, Q. Zhang, T. Jiang, S. Wang, Mesoporous silica nanoparticles in drug delivery and biomedical applications, Nanomedicine Nanotechnology, Biol. Med. 11 (2015) 313–327, https://doi.org/10.1016/j.nano.2014.09.014.
[190] L. Nam, C. Coll, L.C.S. Erthal, C. de la Torre, D. Serrano, R. Martínez-Máñez, M.J. Santos-Martínez, E. Ruiz-Hernández, Drug Delivery Nanosystems for the Localized Treatment of Glioblastoma Multiforme., Mater. (Basel, Switzerland). 11 (2018). https://doi.org/10.3390/ma11050779.
[191] P. Calvo, B. Gouritin, H. Chacun, D. Desmaile, J. D'Angelo, J.P. Noel, D. Georgin, E. Fattal, J.P. Andreux, P. Couvreur, Long-circulating pegylated polycyanoacrylate nanoparticles as new drug carrier for brain delivery, Pharm. Res. 18 (2001) 1157–1166, https://doi.org/10.1023/A:1010931127745.
[192] S. Mendiratta, M. Hussein, H.A. Nasser, A.A.A. Ali, Multidisciplinary Role of Mesoporous Silica Nanoparticles in Brain Regeneration and Cancers: From Crossing the Blood-Brain Barrier to Treatment, Part. Part. Syst. Charact. 36 (2019), https://doi.org/10.1002/ppsc.201900195.
[193] H. Li, X. Wu, B. Yang, J. Li, L. Xu, H. Liu, S. Li, J. Xu, M. Yang, M. Wei, Evaluation of biomimetically synthesized mesoporous silica nanoparticles as drug carriers: Structure, wettability, degradation, biocompatibility and brain distribution, Mater. Sci. Eng. C. 94 (2019) 453–464, https://doi.org/10.1016/j.msec.2018.09.053.
[194] M. Bouchoucha, E. Beliveau, F. Kleitz, F. Calon, M.-A. Fortin, Antibody-conjugated mesoporous silica nanoparticles for brain microvessel endothelial cell targeting., J. Mater. Chem. B Mater, Biol. Med. 5 (2017) 7721–7735, https://doi.org/10.1039/C7TB01385J.
[195] H.M. Fahmy, M.M. Ahmed, A.S. Mohamed, E. Shams-Eldin, T.M. Abd El-Daim, A. S. El-Feky, A.B. Mustafa, M.W. Abd Alrahman, F.F. Mohammed, M.M. Fathy, Novel lipid-coated mesoporous silica nanoparticles loaded with thymoquinone formulation to increase its bioavailability in the brain and organs of Wistar rats, BMC, Pharmacol. Toxicol. 23 (2022) 1–13, https://doi.org/10.1186/s40360-022-00616-z.
[196] T.I. Janjua, A. Ahmed-Cox, A.K. Meka, F.M. Mansfeld, H. Forgham, R.M. C. Ignacio, Y. Cao, J.A. McCarroll, R. Mazzieri, M. Kavallaris, A. Popat, Facile synthesis of lactoferrin conjugated ultra small large pore silica nanoparticles for the treatment of glioblastoma, Nanoscale. 13 (2021) 16909–16922, https://doi.org/10.1039/d1nr03553c.

[197] T.I. Janjua, Y. Cao, A. Ahmed-Cox, A. Raza, M. Moniruzzaman, D.T. Akhter, N. L. Fletcher, M. Kavallaris, K.J. Thurecht, A. Popat, Efficient delivery of Temozolomide using ultrasmall large-pore silica nanoparticles for glioblastoma, J. Control. Release. 357 (2023) 161–174, https://doi.org/10.1016/j.jconrel.2023.03.040.
[198] S. Shen, Y. Wu, Y. Liu, D. Wu, High drug-loading nanomedicines: progress, current status, and prospects, Int. J. Nanomedicine. 12 (2017) 4085–4109, https://doi.org/10.2147/IJN.S132780.
[199] W. Feng, W. Nie, C. He, X. Zhou, L. Chen, K. Qiu, W. Wang, Z. Yin, Effect of pH-responsive alginate/chitosan multilayers coating on delivery efficiency, cellular uptake and biodistribution of mesoporous silica nanoparticles based nanocarriers, ACS Appl. Mater. Interfaces. 6 (2014) 8447–8460, https://doi.org/10.1021/am501337s.
[200] W. Feng, X. Zhou, C. He, K. Qiu, W. Nie, L. Chen, H. Wang, X. Mo, Y. Zhang, Polyelectrolyte multilayer functionalized mesoporous silica nanoparticles for pH-responsive drug delivery: Layer thickness-dependent release profiles and biocompatibility, J. Mater. Chem. B. 1 (2013) 5886–5898, https://doi.org/10.1039/c3tb21193b.
[201] J. Zhou, M. Wang, H. Ying, D. Su, H. Zhang, G. Lu, J. Chen, Extracellular Matrix Component Shelled Nanoparticles as Dual Enzyme-Responsive Drug Delivery Vehicles for Cancer Therapy, ACS Biomater. Sci. Eng. 4 (2018) 2404–2411, https://doi.org/10.1021/acsbiomaterials.8b00327.
[202] A.C. Eifler, C. Shad Thaxton, Nanoparticle therapeutics: FDA approval, clinical trials, regulatory pathways, and case study, in: S.J. Hurst (Ed.), Methods Mol. Biol., Humana Press, Totowa, NJ, 2011: pp. 325–338. https://doi.org/10.1007/978-1-61779-052-2_21.
[203] S. Tinkle, S.E. McNeil, S. Mühlebach, R. Bawa, G. Borchard, Y. (Chezy) Barenholz, L. Tamarkin, N. Desai, Nanomedicines: addressing the scientific and regulatory gap, Ann. N. Y. Acad. Sci. 1313 (2014) 35–56. https://doi.org/https://doi.org/10.1111/nyas.12403.
[204] M. Yu, J. Zheng, Clearance Pathways and Tumor Targeting of Imaging Nanoparticles, ACS Nano. 9 (2015) 6655–6674, https://doi.org/10.1021/acsnano.5b01320.
[205] E.B. Ehlerding, F. Chen, W. Cai, Biodegradable and Renal Clearable Inorganic Nanoparticles, Adv. Sci. (Weinheim, Baden-Wurttemberg, Ger. 3 (2016) 1500223. https://doi.org/10.1002/advs.201500223.
[206] J.F. Popplewell, S.J. King, J.P. Day, P. Ackrill, L.K. Fifield, R.G. Cresswell, M.L. di Tada, K. Liu, Kinetics of uptake and elimination of silicic acid by a human subject: A novel application of 32Si and accelerator mass spectrometry, J. Inorg. Biochem. 69 (1998) 177–180, https://doi.org/10.1016/S0162-0134(97)10016-2.
[207] H. Ehrlich, K.D. Demadis, O.S. Pokrovsky, P.G. Koutsoukos, Modern views on desilicification: Biosilica and abiotic silica dissolution in natural and artificial environments, Chem. Rev. 110 (2010) 4656–4689, https://doi.org/10.1021/cr900334y.
[208] J.-H. Park, L. Gu, G. von Maltzahn, E. Ruoslahti, S.N. Bhatia, M.J. Sailor, Biodegradable luminescent porous silicon nanoparticles for in vivo applications, Nat. Mater. 8 (2009) 331–336, https://doi.org/10.1038/nmat2398.
[209] Z. Liu, C. Davis, W. Cai, L. He, X. Chen, H. Dai, Circulation and long-term fate of functionalized, biocompatible single-walled carbon nanotubes in mice probed by Raman spectroscopy, Proc. Natl. Acad. Sci. 105 (2008), https://doi.org/10.1073/pnas.0707654105.
[210] D. Kim, S. Park, J.H. Lee, Y.Y. Jeong, S. Jon, Antibiofouling Polymer-Coated Gold Nanoparticles as a Contrast Agent for in Vivo X-ray Computed Tomography Imaging, J. Am. Chem. Soc. 129 (2007) 7661–7665, https://doi.org/10.1021/ja071471p.
[211] J.L. Vivero-Escoto, K.M.L. Taylor-Pashow, R.C. Huxford, J. Della Rocca, C. Okoruwa, H. An, W. Lin, W. Lin, Multifunctional mesoporous silica nanospheres with cleavable Gd(III) chelates as MRI contrast agents: synthesis, characterization, target-specificity, and renal clearance, Small. 7 (2011) 3519–3528, https://doi.org/10.1002/smll.201100521.
[212] W. Lu, Z.Y. Xie, Y. Tang, L.B. Yao, C. Fu, G. Ma, Photoluminescent mesoporous silicon nanoparticles with siCCR2 improve the effects of mesenchymal stromal cell transplantation after acute myocardial infarction, Theranostics. 5 (2015) 1068–1082, https://doi.org/10.7150/thno.11517.
[213] J. Lu, Z. Li, J.I. Zink, F. Tamanoi, In vivo tumor suppression efficacy of mesoporous silica nanoparticles-based drug-delivery system: enhanced efficacy by folate modification, Nanomedicine Nanotechnology, Biol. Med. 8 (2012) 212–220, https://doi.org/10.1016/j.nano.2011.06.002.
[214] R. Roggers, S. Kanvinde, S. Boonsith, D. Oupický, The practicality of mesoporous silica nanoparticles as drug delivery devices and progress toward this goal, AAPS PharmSciTech. 15 (2014) 1163–1171, https://doi.org/10.1208/s12249-014-0142-7.
[215] S. Toyokuni, K. Okamoto, J. Yodoi, H. Hiai, Persistent oxidative stress in cancer, FEBS Lett. 358 (1995) 1–3, https://doi.org/10.1016/0014-5793(94)01368-B.
[216] S.H. Lee, M.K. Gupta, J.B. Bang, H. Bae, H.-J. Sung, Current Progress in Reactive Oxygen Species (ROS)-Responsive Materials for Biomedical Applications, Adv. Healthc. Mater. 2 (2013) 908–915, https://doi.org/10.1002/adhm.201200423.
[217] Y.-N. Zhang, W. Poon, A.J. Tavares, I.D. McGilvray, W.C.W. Chan, Nanoparticle–liver interactions: Cellular uptake and hepatobiliary elimination, J. Control. Release. 240 (2016) 332–348, https://doi.org/10.1016/j.jconrel.2016.01.020.
[218] S.H. Cheng, F.C. Li, J.S. Souris, C.S. Yang, F.G. Tseng, H.S. Lee, C.T. Chen, C. Y. Dong, L.W. Lo, Visualizing dynamics of sub-hepatic distribution of nanoparticles using intravital multiphoton fluorescence microscopy, ACS Nano. 6 (2012) 4122–4131, https://doi.org/10.1021/nn300558p.
[219] H. Li, K. Li, Y. Dai, X. Xu, X. Cao, Q. Zeng, H. He, L. Pang, J. Liang, X. Chen, Y. Zhan, In vivo near infrared fluorescence imaging and dynamic quantification of pancreatic metastatic tumors using folic acid conjugated biodegradable mesoporous silica nanoparticles, Nanomedicine Nanotechnology, Biol. Med. 14 (2018) 1867–1877, https://doi.org/10.1016/j.nano.2018.04.018.
[220] J.S. Souris, C.H. Lee, S.H. Cheng, C.T. Chen, C.S. Yang, J. an A. Ho, C.Y. Mou, L. W. Lo, Surface charge-mediated rapid hepatobiliary excretion of mesoporous silica nanoparticles, Biomaterials. 31 (2010) 5564–5574. https://doi.org/10.1016/j.biomaterials.2010.03.048.
[221] T.I. Janjua, Y. Cao, C. Yu, A. Popat, Clinical translation of silica nanoparticles, Nat. Rev. Mater. 6 (2021) 1072–1074, https://doi.org/10.1038/s41578-021-00385-x.
[222] A.C. Anselmo, Samir Mitragotri, S. Paulson, J.A. Mitragotri, Nanoparticles in the clinic: An update post COVID-19 vaccines, Bioeng. Transl. Med. 6 (2021), https://doi.org/10.1002/BTM2.10246.
[223] K. Bukara, L. Schueller, J. Rosier, M.A. Martens, T. Daems, L. Verheyden, S. Eelen, M. Van Speybroeck, C. Libanati, J.A. Martens, G. Van Den Mooter, F. Frérart, K. Jolling, M. De Gieter, B. Bugarski, F. Kiekens, Ordered mesoporous silica to enhance the bioavailability of poorly water-soluble drugs: Proof of concept in man, Eur. J. Pharm. Biopharm. 108 (2016) 220–225, https://doi.org/10.1016/j.ejpb.2016.08.020.
[224] A. Tan, N.G. Eskandar, S. Rao, C.A. Prestidge, First in man bioavailability and tolerability studies of a silica-lipid hybrid (Lipoceramic) formulation: A Phase I study with ibuprofen, Drug Deliv, Transl. Res. 4 (2014) 212–221, https://doi.org/10.1007/s13346-013-0172-9.
[225] T.R. Meola, A.Y. Abuhelwa, P. Joyce, P. Clifton, C.A. Prestidge, A safety, tolerability, and pharmacokinetic study of a novel simvastatin silica-lipid hybrid formulation in healthy male participants, Drug Deliv Transl. Res. 11 (2021) 1261–1272, https://doi.org/10.1007/s13346-020-00853-x.
[226] A.N. Kharlamov, A.E. Tyurnina, V.S. Veselova, O.P. Kovtun, V.Y. Shur, J. L. Gabinsky, Silica-gold nanoparticles for atheroprotective management of plaques: Results of the NANOM-FIM trial, Nanoscale. 7 (2015) 8003–8015, https://doi.org/10.1039/c5nr01050k.
[227] A.N. Kharlamov, J.A. Feinstein, J.A. Cramer, J.A. Boothroyd, E.V. Shishkina, V. Shur, Plasmonic photothermal therapy of atherosclerosis with nanoparticles: Long-term outcomes and safety in NANOM-FIM trial, Future Cardiol. 13 (2017) 345–363, https://doi.org/10.2217/fca-2017-0009.
[228] E. Phillips, O. Penate-Medina, P.B. Zanzonico, R.D. Carvajal, P. Mohan, Y. Ye, J. Humm, M. Gönen, H. Kalaigian, H. Schöder, H.W. Strauss, S.M. Larson, U. Wiesner, M.S. Bradbury, Clinical translation of an ultrasmall inorganic optical-PET imaging nanoparticle probe, Sci. Transl. Med. 6 (2014), https://doi.org/10.1126/scitranslmed.3009524.
[229] D.K. Zanoni, H.E. Stambuk, B. Madajewski, P.H. Montero, D. Matsuura, K. J. Busam, K. Ma, M.Z. Turker, S. Sequeira, M. Gonen, P. Zanzonico, U. Wiesner, M.S. Bradbury, S.G. Patel, Use of Ultrasmall Core-Shell Fluorescent Silica Nanoparticles for Image-Guided Sentinel Lymph Node Biopsy in Head and Neck Melanoma: A Nonrandomized Clinical Trial, JAMA Netw. Open. 4 (2021) 1–14, https://doi.org/10.1001/jamanetworkopen.2021.1936.
[230] F. Chen, K. Ma, M. Benezra, L. Zhang, S.M. Cheal, E. Phillips, B. Yoo, M. Pauliah, M. Overholtzer, P. Zanzonico, S. Sequeira, M. Gonen, T. Quinn, U. Wiesner, M. S. Bradbury, Cancer-Targeting Ultrasmall Silica Nanoparticles for Clinical Translation: Physicochemical Structure and Biological Property Correlations, Chem. Mater. 29 (2017) 8766–8779, https://doi.org/10.1021/acs.chemmater.7b03033.
[231] A.R. Rastinehad, H. Anastos, E. Wajswol, J.S. Winoker, J.P. Sfakianos, S. K. Doppalapudi, M.R. Carrick, C.J. Knauer, B. Taouli, S.C. Lewis, A.K. Tewari, J. A. Schwartz, S.E. Canfield, A.K. George, J.L. West, N.J. Halas, Gold nanoshell-localized photothermal ablation of prostate tumors in a clinical pilot device study, Proc. Natl. Acad. Sci. U. S. A. 116 (2019) 18590–18596, https://doi.org/10.1073/pnas.1906929116.
[232] I. Melero, E. Castanon, M. Alvarez, S. Champiat, A. Marabelle, Intratumoural administration and tumour tissue targeting of cancer immunotherapies, Nat. Rev. Clin. Oncol. 18 (2021) 558–576, https://doi.org/10.1038/S41571-021-00507-Y.
[233] J.S. Patton, P.R. Byron, Inhaling medicines: delivering drugs to the body through the lungs, Nat. Rev. Drug Discov. 6 (2007) 67–74, https://doi.org/10.1038/nrd2153.
[234] P. Muralidharan, M. Malapit, E. Mallory, D. Hayes, H.M. Mansour, Inhalable nanoparticulate powders for respiratory delivery, Nanomedicine Nanotechnology, Biol. Med. 11 (2015) 1189–1199, https://doi.org/10.1016/j.nano.2015.01.007.
[235] F. Rodriguez-Otormin, A. Duro-Castano, I. Conejos-Sánchez, M.J. Vicent, Envisioning the future of polymer therapeutics for brain disorders, Wiley Interdiscip. Rev. Nanomedicine Nanobiotechnology. 11 (2019), https://doi.org/10.1002/WNAN.1532.
[236] A. Misra, G. Kher, Drug delivery systems from nose to brain, Curr. Pharm. Biotechnol. 13 (2012) 2355–2379, https://doi.org/10.2174/138920112803341752.
[237] L. Illum, Is nose-to-brain transport of drugs in man a reality? J. Pharm. Pharmacol. 56 (2010) 3–17, https://doi.org/10.1211/0022357022539.
[238] X. Li, B. Wang, S. Zhou, W. Chen, H. Chen, S. Liang, L. Zheng, H. Yu, R. Chu, M. Wang, Z. Chai, W. Feng, Surface chemistry governs the sub-organ transfer, clearance and toxicity of functional gold nanoparticles in the liver and kidney, J. Nanobiotechnology. 18 (2020) 45, https://doi.org/10.1186/s12951-020-00599-1.

[239] D. Yuan, H. He, Y. Wu, J. Fan, Y. Cao, Physiologically Based Pharmacokinetic Modeling of Nanoparticles, J. Pharm. Sci. 108 (2019) 58–72, https://doi.org/10.1016/j.xphs.2018.10.037.
[240] S.M. Moghimi, A.C. Hunter, J.C. Murray, Long-Circulating and Target-Specific Nanoparticles: Theory to Practice, Pharmacol. Rev. 53 (2001) 283 LP – 318. http://pharmrev.aspetjournals.org/content/53/2/283.abstract.
[241] J.A. Damasco, S. Ravi, J.D. Perez, D.E. Hagaman, M.P. Melancon, Understanding nanoparticle toxicity to direct a safe-by-design approach in cancer nanomedicine, Nanomater 10 (2020), https://doi.org/10.3390/nano10112186.
[242] S. Mühlebach, Regulatory challenges of nanomedicines and their follow-on versions: A generic or similar approach? Adv. Drug Deliv. Rev. 131 (2018) 122–131, https://doi.org/10.1016/J.ADDR.2018.06.024.
[243] S. Đorđević, M.M. Gonzalez, I. Conejos-Sánchez, B. Carreira, S. Pozzi, R.C. Acúrcio, R. Satchi-Fainaro, H.F. Florindo, M.J. Vicent, Current hurdles to the translation of nanomedicines from bench to the clinic, Drug Deliv. Transl. Res. 2021 123. 12 (2021) 500–525. Doi: 10.1007/S13346-021-01024-2.
[244] F. Farjadian, A. Ghasemi, O. Gohari, A. Roointan, M. Karimi, M.R. Hamblin, Nanopharmaceuticals and nanomedicines currently on the market: Challenges and opportunities, Nanomedicine. 14 (2019) 93–126, https://doi.org/10.2217/nnm-2018-0120.
[245] A.M. Vargason, A.C. Anselmo, S. Mitragotri, The evolution of commercial drug delivery technologies, Nat. Biomed. Eng. 5 (2021) 951–967, https://doi.org/10.1038/s41551-021-00698-w.
[246] D. Bowman, A. Marino, D.S.-M.R. Archives, undefined 2017, The patent landscape of nanomedicines, Esmed.Org. (n.d.).